2007-03-02

One-Dimensional Performance Modeling of Centrifugal Flow Vaned Diffusers

Jamin J. Bitter
Brigham Young University - Provo

ONE-DIMENSIONAL PERFORMANCE MODELING

OF CENTRIFUGAL FLOW VANED DIFFUSERS

by

Jamin J. Bitter

A thesis submitted to the faculty of

Brigham Young University

in partial fulfillment of the requirements for the degree of

Master of Science

Department of Mechanical Engineering

Brigham Young University

April 2007

BRIGHAM YOUNG UNIVERSITY

GRADUATE COMMITTEE APPROVAL

of a thesis submitted by

Jamin J. Bitter

This dissertation has been read by each member of the following graduate committee and by majority vote has been found satisfactory.

_____ _____
Date R. Daniel Maynes, Chair

_____ _____
Date Jeffrey P. Bons

_____ _____
Date Scott L. Thomson

BRIGHAM YOUNG UNIVERSITY

As chair of the candidate's graduate committee, I have read the thesis of Jamin J. Bitter in its final form and have found that (1) its format, citations, and bibliographical style are consistent and acceptable and fulfill university and department style requirements; (2) its illustrative materials including figures, tables, and charts are in place; and (3) the final manuscript is satisfactory to the graduate committee and is ready for submission to the university library.

_____ _____
Date   R. Daniel Maynes
             Chair, Graduate Committee

Accepted for the Department

             _____
             Matthew R. Jones
             Graduate Coordinator

Accepted for the College

             _____
             Alan R. Parkinson
             Dean, Ira A. Fulton College of Engineering and
             Technology

ABSTRACT

ONE-DIMENSIONAL PERFORMANCE MODELING

OF CENTRIFUGAL FLOW VANED DIFFUSERS

Jamin J. Bitter

Department of Mechanical Engineering

Master of Science

The Two Element in Series (TEIS) and Two Zone models stand out as powerful tools that enable deeper understanding of compressor stage designs after they have been tested. The insights gained from these investigations have aided in improving new stage designs. Up to now, it has only been possible to use the TEIS and Two Zone models for analysis of test data due to the inability to predict the four required input parameters for untested machines.

Empirical models for the TEIS and Two Zone model input parameters, η_{a5}, η_{b5}, χ_5, and δ_{5p}, for two different types of vaned diffusers, channel and cascade, are proposed. These models were developed with frozen impeller modeling. This is the first time that modeling the TEIS and Two Zone input parameters has been attempted for vaned diffusers and impeller-diffuser coupling was not considered in this initial investigation. The centrifugal compressor experimental data used in the model building was obtained

from Concepts NREC, an industry sponsor. Each dataset provided was evaluated for quality and reliability and only the data deemed reliable were used in the model building databases. The empirical models presented are built solely on this higher quality data.

Seven models are proposed for use in predicting the TEIS and Two Zone model input parameters η_{a5}, η_{b5}, χ_5, and δ_{5p}. Models for η_{a5}, η_{b5}, and δ_{5p} are specific to the type of vane present in the diffuser, while the model for χ_5 is common to both diffuser types. These are the first models ever built for the TEIS and Two Zone model inputs applied to channel and cascade diffusers and become a benchmark for future studies. The work with these models is not complete, however. The databases are not of a size that data could be withheld from empirical model building for the express purpose of validation. Instead the model performance is evaluated by applying all of the models, simultaneously, to the database from which they were built. The determination of the effectiveness of the combined modeling is based on the average error across the entire speedline. The models proved to be effective and a contributing step to employing such models for use in future compressor design.

ACKNOWLEDGMENTS

TABLE OF CONTENTS

LIST OF TABLES

LIST OF FIGURES

LIST OF SYMBOLS

Roman Symbols

Symbol	Unit	Definition
a_{11}	-	Coefficient in χ_5 Model
a_{12}	-	Coefficient in χ_5 Model
a_{21}	-	Coefficient in χ_5 Model
a_{22}	-	Coefficient in χ_5 Model
A	m^2	Area
AR_a	-	Area Ratio a
AR_b	-	Area Ratio b
AR_{45}	-	Area Ratio Station 4 to 5
AS_2	-	Impeller Exit Aspect Ratio $\left(\dfrac{B_2}{W_2}\right)$
B	m	Vane Height
b	-	Solidity Exponent
b_k	-	Diffuser Passage Blockage $\left(\dfrac{\delta_1}{W}\right)$
b_1	-	Coefficient in χ_5 Model
b_2	-	Coefficient in χ_5 Model
C_∞	m/s	Boundary Layer Edge Velocity
C_τ	m/s	Shear Velocity $\left(\sqrt{\dfrac{\tau_w}{\rho}}\right)$
C	m/s	Fluid Velocity
C_f	-	Coefficient of Friction
Clr	m	Impeller Exit Tip Clearance
CP_{23}	-	Pressure Recovery Coefficient 2-3 $\left(\dfrac{P_3 - P_2}{\frac{1}{2}\rho u_2{}^2}\right)$
CPI_{23}	-	Ideal Pressure Recovery 2-3
CPI_{45}	-	Ideal Pressure Recovery 4-5
DR_{2I}	-	Ideal Diffusion Ratio 1-2 $\left(\dfrac{u_1}{u_{2,ideal}}\right)$

xxx

DR5I	-	Ideal Diffusion Ratio 4-5 $\left(\dfrac{u_3}{u_{5,ideal}}\right)$
E	-	Area Flow Fraction $\left(\dfrac{A_{\sec}}{A_{tot}}\right)_2$
g	m/s^2	Gravity Constant 9.81
ΔH	m	Head Rise
H	-	Shape Factor $\left(\dfrac{\delta_1}{\delta_2}\right)$
h	-	Shape Factor $\left(\dfrac{\delta_1-\delta_2}{\delta_1}\right)$
h_0	kJ/kg	Fluid Total Enthalpy
J	-	Coefficient in χ_5 Model
L	m	Diffuser Blade Length
LC	-	Loss Coefficient
M	-	Mach Number
m	-	Solidity Exponent in Deviation Model
m_{sec}	kg/s	Secondary Mass Flow Rate
m_{tot}	kg/s	Total Mass Flow Rate
N	rpm	Impeller Rotational Speed
NS	-	Stage Specific Speed $\left(\dfrac{2\pi N\sqrt{Q}}{60(g\Delta H)^{3/4}}\right)$
P	Pa	Static Pressure
P_0	Pa	Total Pressure
PR_{tt}	-	Stage Pressure Ratio
Q	m^3/s	Volume Flow Rate
r	m	Radius
$Re_{\delta 1}$	-	Displacement Thickness Reynolds Number
Re_{23}	-	Vaneless Reynolds Number
Ro_{CA}	-	Rossby Number (C,A) $\left(\dfrac{u_{m1}+u_{m2}}{2}\dfrac{60}{N*rcr_{rms}}\right)$
rcr_{rms}	m	Radius of Curvature
V_T	-	Non-dimensional Shear Velocity $\left(\dfrac{U_\tau}{\kappa U_\infty}\right)$
W	m	Vane Spacing Width
W_{ex}	m	Diffuser Passage Exit Width
Z_D	-	Number of Diffuser Blades
Z_R	-	Number of Impeller Blades

Greek Symbols

Symbol	Unit	Definition
α	deg	Fluid Flow Angle
α_b	deg	Diffuser Blade Angle
β_b	deg	Impeller Blade Angle
χ	-	Exit Mass Fraction $\left(\dfrac{m_{sec}}{m_{tot}} \right)$
δ_0	deg	Zero Camber Deviation Angle
δ_p	deg	Flow Deviation from Blade
δ	m	Boundary Layer Thickness
δ_1	m	Boundary Layer Displacement Thickness $\left(\int_0^\infty \left(1 - \dfrac{u}{U}\right) dy \right)$
δ_2	m	Boundary Layer Momentum Thickness $\left(\int_0^\infty \dfrac{u}{U}\left(1 - \dfrac{u}{U}\right) dy \right)$
ϕ	-	Standard Deviation
γ_2	-	Impeller Slip Factor $\left(1 - \dfrac{\sqrt{\cos \beta_{2b}}}{Z_R^{0.7}} \right)$
φ	deg	Blade Turning Angle $\left(\alpha_{3b} - \alpha_{5b} \right)$
κ	-	Von Karman Constant
η_a	-	Inlet Effectiveness
η_b	-	Passage Effectiveness
η_{tt}	-	Stage Total-to-Total Efficiency
μ	-	Mean Value
θ	deg	Diffuser Vane Divergence Angle
ρ	Kg/m^3	Fluid Density
σ	-	Cascade Solidity
τ_w	N/m^2	Wall Shear Stress
τ_{max}	N/m^2	Maximum Shear Stress in the Boundary layer
ξ	-	Constant
Λ	-	Boundary Layer Blockage Fraction $\left(\dfrac{\delta_1}{\delta} \right)$

Station Locations and Subscripts

Symbol	Station Location
0	Inlet Condition
1	Impeller Inlet or "eye"
2	Impeller Blade Exit
3	Diffuser Leading Edge
4	Wedge Diffuser Throat; Cascade diffuser exit
5	Diffuser Exit
m	Mixed Primary and Secondary Flow

.

1 Introduction

1.1 Introduction to Turbomachinery

The turbomachinery field represents a class of machines that are responsible for energy transfer between a rotor, the rotating piece in the turbomachine, and the fluid. There are two main types of turbomachines, axial and radial—often referred to as a centrifugal machine. In both of these categories are further divisions. Turbomachines can be a pump, compressor, or turbine. While pumps and compressors are responsible for transferring energy from a rotor to a fluid, turbines transfer energy from the fluid to the rotor. Axial turbomachines are primarily used in the aviation and power generation industries and will not be discussed here. The research described here focuses on the centrifugal compressor.

A typical centrifugal compressor (see Figure 1-1) contains a number of distinct elements: an impeller, diffuser, and a volute or collector at the exit. Each element is specially designed to perform specific tasks. The centrifugal impeller is responsible for transferring energy from the rotating shaft to the fluid and to collect some of the energy in the form of pressure. The diffuser is designed to re cover some of the kinetic energy not recovered by the impeller and then the flow is collected in either a volute or collector for use downstream. Separate models for predicting thermodynamic and kinetic

flowquantities are used for each element of the stage. This study is concerned with the

models used for predicting energy recovery in vaned diffusers.
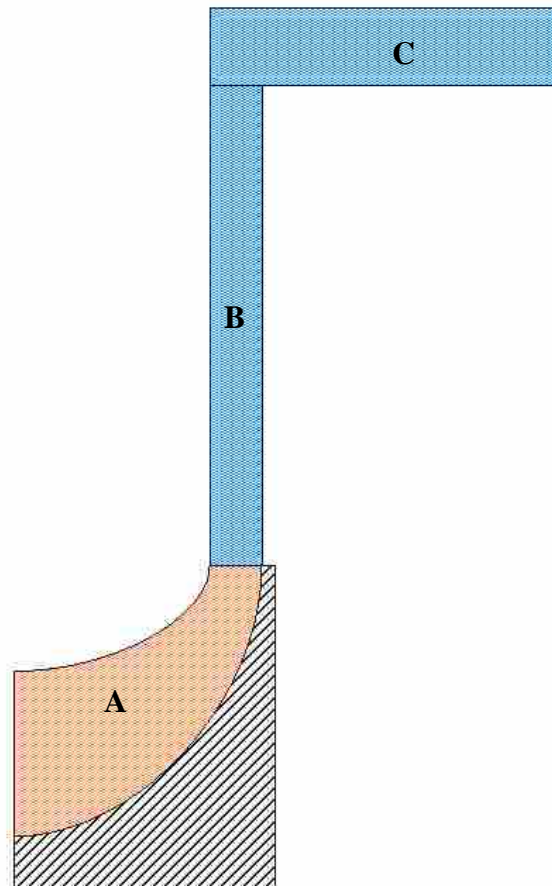
Figure 1-1 A schematic of a typical compressor stage with (A) impeller, (B) vaneless diffuser, and (C) collector.

The kinetic energy recovery is essential to the performance of a stage and is

accomplished by two principles of conversion: 1) increasing the flow passage area to

diffuse the average velocity and thereby raise the static pressure and 2) through

conservation of angular momentum principle, $rC_\theta \approx constant$ where r is the radius and C_θ

is the angular velocity. The latter states that as the flow path radius increases the angular

velocity decreases which results in a recovery of pressure in similar fashion to increasing the flow passage area. Each diffuser is specifically designed to, in principle, give the maximum pressure recovery for the given flow conditions present in the stage. All advanced compressor stages utilize at least one type of diffuser to ensure efficient pressure recovery by one or both of the aforementioned conservation methods [1]. Because the energy recovery in the diffuser is significant to the stage efficiency, the analytical model used in diffuser design is extremely important. Diffusing flows by nature occur in adverse pressure gradients and are liable to boundary layer separation. Extreme care must be taken in diffuser design because considerable performance may be lost if the rate of diffusion is too great or if the models used for predicting boundary layer quantities are not sufficiently accurate [1, 2].

There are two main types of diffusers, vaneless and those with vanes. Each type has its own advantages and disadvantages. A vaneless diffuser is used for many applications where a wide operating range and low cost is required, such as in automotive turbochargers. However, when size constraints or high pressure ratio requirements exist, it is often necessary to use a diffuser with vanes. Vaned diffusers achieve a better pressure recovery when compared to the larger vaneless diffuser option and also allow for flow angle control. However, because of more complex geometry, they do cost more to design and manufacture. The use of vaned diffusers is often a balance between stage requirements and manufacturing cost. Vaneless diffusers will not be discussed further. The focus here will be on models used to predict vaned diffuser performance.

This study includes two types of vaned diffusers: a wedge diffuser and a cascade diffuser. The names for these diffusers come from the vane shapes. In the wedge, or

3

channel, type of diffuser, wedge shaped vanes are placed radially outward from the centrifugal impeller as shown in Figure 1-2. The typical wedge diffuser has straight walls that deviate from the inlet width by an amount designated by a divergence angle. The divergence angle and length of the diffuser are calculated to provide the maximum pressure recovery without boundary layer separation.

Figure 1-2. Picture of a wedge diffuser build with the shroud removed to show the impeller and diffuser. A short vaneless diffuser, or vaneless space, is located just after the impeller exit [3].

The cascade diffuser consists of one or two rows of airfoil section vanes positioned radially around the rotor. Most of the diffuser designs are based on the NACA database, a large database of airfoil cascade data taken between 1940 and 1960. This database gives the designer all of the information needed for a first order design, from turning angle to stall margin [4].

When discussing turbomachinery it is useful to distinguish certain stations where fluid properties and flow quantities are calculated. This thesis will follow the station numbering as set out by Japikse [4]. The numbering is as follows for the wedge diffuser stage: station 1 is at the impeller inlet, station 2 is at the impeller exit, station 3 is at the vaned diffuser inlet, station 4 is at the throat—or minimum area of the vaned diffuser—and station 5 is at the exit of the vaned diffuser. The station numbering for a cascade diffuser build varies only slightly. The exit of the vane is station 4 and the stage exit is station 5. Schematics illustrating the location are given in Figure 1-3.
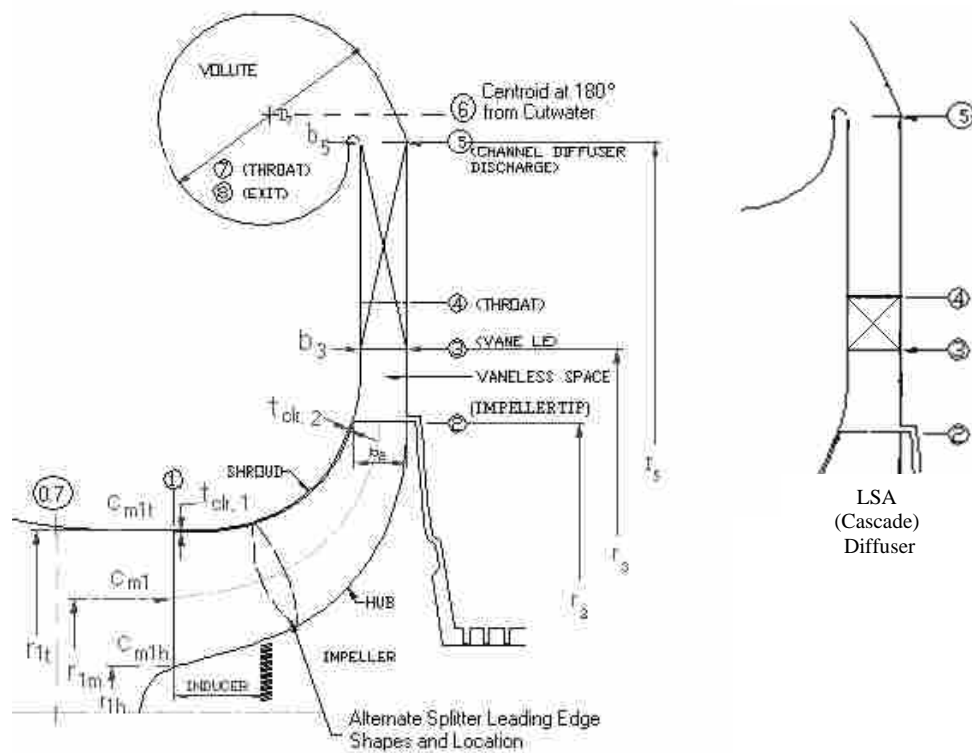
Figure 1-3 Illustration of station numbering for a wedge (left) and cascade (right) diffuser builds [4].

5

1.2 Motivation and Definition of Problem

Centrifugal compressors are found in many different industries. Their use has become widespread in the aviation, automotive, refrigeration, and chemical processing industries. With this widespread use comes a greater demand for improved performance and increasingly smaller stages. This demand fuels the need to create improved design techniques which can deliver advanced stages that meet these high efficiency requirements. To find out where efficiency gains might be made, the design process must be examined.

In the overall design process, the greatest potential for enhancing stage design is in making improvement to the meanline models. The term "meanline" refers to the point on the blades that geometric and fluid dynamic quantities are determined, usually calculated as a mean or average of the tip and hub values. This may not be intuitive in a world where 3-D viscous solvers or CFD codes are available and widely used. A closer look at the design process shows the very important role meanline models play in compressor design. The design process will be explained in further detail in a subsequent section. In short, it is through meanline models that the inputs to CFD solvers are determined. These quantities are rarely, if ever changed, after CFD runs. Hence, a poor meanline design will not get any better through the use of CFD [5].

The emphasis of this thesis is on improving the one-dimensional or meanline models for use in diffuser design. One set of advanced meanline models stand out as powerful tools that enable deeper understanding of stage designs after they have been tested. These are the Two Element in Series (TEIS) and Two Zone models. These models have been used by engineers as analysis tools to aid in understanding physical

phenomena from historical stages. The insights gained from these investigations have aided in improving new stage designs. Up to now, it has only been possible to use the TEIS and Two Zone models for analysis of test data due to the inability to predict the four required input parameters for untested machines. These input parameters are needed to close the equations and make designing with these tools possible. If these input parameters could be specified for new designs the TEIS and Two Zone models would have the potential to meet the demand for increased stage modeling and design enhancement ability.

Turbomachinery is very widely used in industry. The size of this large industrial market was described by Japikse; "Turbomachinery represents a $400 billion market (possibly much more) with enormous worldwide growth at this time. It is estimated that industrial centrifugal pumps alone consume 5% of all energy produced in the USA." [6]. If relatively small gains in efficiency were made due to improved accuracy in compressor modeling the monetary and energy savings across this grand scale would be staggering. The importance of the TEIS and Two Zone models is illustrated in Figure 1-4. The meanline equations typically output idealized flow curves for a turbomachine. The TEIS and Two Zone models approximate the losses due to flow friction and shocks. When used in conjunction with recirculation and disk friction models, the TEIS and Two Zone equations yield the actual stage efficiency curve. The ability to predict flow at this level would increase modeling accuracy and enable the monetary and energy savings described above.
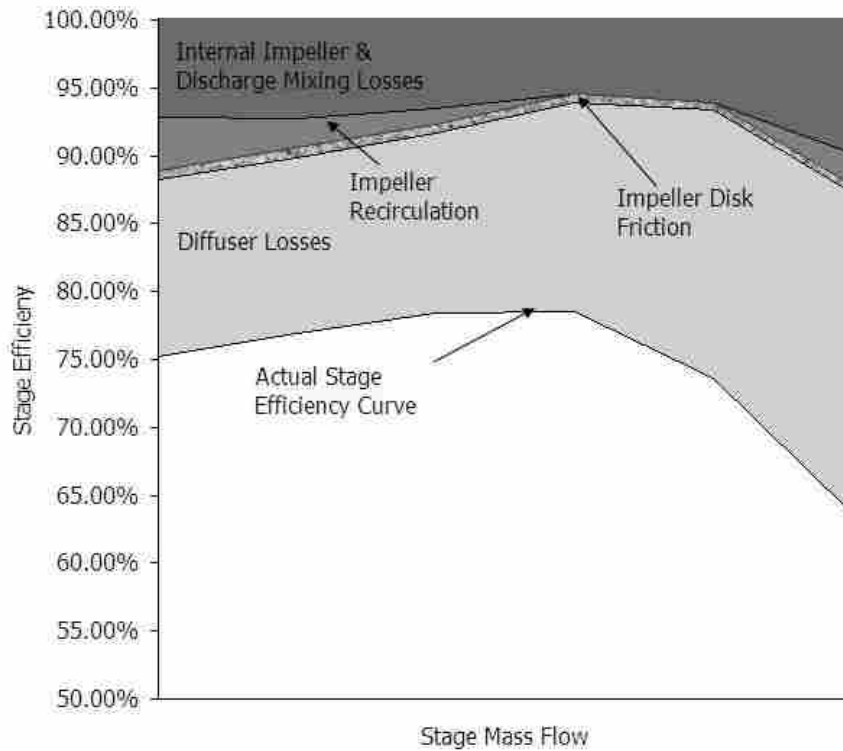
Figure 1-4. Meanline equation efficiency output for a channel diffuser build. The TEIS and Two Zone models approximate the losses experienced in the impeller and diffuser.

1.3 Literature Review

The TEIS and Two Zone models require two inputs each. It has not been possible for analytical models to be built for these input parameters. The reasons for this will become evident as each of the inputs is defined. Because the inputs can not be modeled analytically, empirical models are the logical next step in making the TEIS and Two Zone equations effective design tools. Initial work in building empirical models for the TEIS and Two Zone input parameters has been done prior to this study [7]. Some of the attempts were performed under business contracts with Concepts NREC. Early attempts were performed with small amounts of data and limited resources yielding results that

8

were indicative of these restrictions on empirical model building. Recent work, that has been most successful to date, is that performed by Pelton [7]. All previous attempts (including that of Pelton) at developing models of sufficient resolution to enable their use in the design process have focused primarily on the centrifugal impeller and vaneless diffuser. No previous attempts have been made to develop models for application to vaned diffusers. The work done by Pelton [7] aided in the creation of data processing algorithms and computer programs that are used in this current study. Pelton is currently in the final stages of completing his work and his results will soon be published.

Japikse has authored or coauthored numerous papers and other literature on the development of the TEIS and Two Zone models and their approach to becoming viable design tools [2, 4, 8]. Prior to discussing the TEIS and Two Zone models it is helpful to understand where they fit in the design process.

The design of a compressor is an involved process that may require many different stages of modeling. The approach taken in designing a compressor stage varies depending on the level of design needed to meet the requirements. This section gives an overview of the steps one would take for a number of different design scenarios.

The initial stage design is performed using one-dimensional—sometimes called meanline or station-by-station—analysis and models [4]. These models call for relatively few inputs; namely the required flow rate, rotational speed, inlet flow conditions, desired pressure ratio, and any size constraints for the given application of the compressor. Through the use of 1-D meanline analysis several geometric and flow quantities are determined. Such quantities include inlet and exit impeller blade and flow angles,

impeller inlet and exit radii, diffuser radii, and diffuser blade (if applicable), flow angles, etc.

The 1-D design of a turbomachine can have three different levels of rigor. It is advantageous for designers to use the simplest design level to meet stage requirements. The simpler the method the faster it can be accomplished and the less it will cost. Each of the three levels of design should be discussed.

A Level-One design analysis utilizes the laws of similitude. This level of design takes stages that are already in existence, whose performance is known, and scales them using affinity rules to meet the design requirements of the current problem. Care does need to be taken in order to ensure that the scaling is done correctly. Examples of how to correctly apply the similitude scaling laws are given by Whitfield & Baines [9], Dixon [1] and Japikse & Baines [2]. If a stage can not be found that, when scaled, is suitable for the desired application then it is appropriate to perform a higher level of analysis.

A Level-Two design uses correlations for component performance, such as impeller or diffuser efficiency, created from prior test experience which is combined to predict overall stage performance. Designs created in this manner have the ability to form new stages for flow conditions already experienced. This is done through a mix of previously designed components to match design parameters at the different stations. For example, by correlating rotor efficiency, rotor slip factor, and diffuser performance on an element by element basis the elements from different stages may be combined to create new stage designs. Again, this must be done properly to achieve the desired results. This type of design allows for increased ability to satisfy new stage requirements but falls short of many design needs.

A Level-Three analysis is the most detailed of the three design methods. It uses a set of models developed to represent the internal flow physics and predict output conditions at each of the different stations in a compressor build. This is fundamentally different than the other two design levels and allows for designs to be developed that deviate from past experience. This level of design is required for many new applications dealing with various fluids, multiphase flow, or high efficiency design requirements.

Once the one-dimensional analysis has been performed one can then determine the blade angle and thickness distributions. Japikse discusses several geometric techniques available to determine blade shapes for the given requirements [4]. After the initial blade shapes are determined they can then be fed into inviscid quasi-three-dimensional codes and fully three-dimensional viscous CFD solvers for further refinement.

This study focuses on the development of the TEIS and Two-Zone models, which are a Level-Three analysis tool, into a viable means for diffuser design. The ability to use these models in design will increase accuracy over previous design procedures while using a flow model that is computationally easy to solve.

1.3.1 Two Zone Flow Model

In 1975, Ekardt [10] published the results of meticulous flow measurements that confirmed the belief that the flow exiting the impeller of a centrifugal flow turbomachine is divided into two regions. The two regimes are commonly referred to as the jet and wake. After the existence of this impeller exit phenomenon was experimentally proven, a Jet-Wake model was proposed by Dean [11] to model these observed flow physics. In

this model, separate calculations are performed for both the primary (jet) and secondary (wake) flow regimes.

The Jet-Wake model was later improved by Japikse [8] and renamed the Two-Zone model, referring to primary and secondary flow zones. In this Two-Zone model the primary zone, or jet, is considered isentropic and the secondary zone, or wake, adopts all of the losses. Japikse also showed that the Two-Zone model outperforms previous techniques used in impeller exit flow predictions [8]. To calculate the change in fluid properties, the Two-Zone model requires that two additional quantities be defined. First, the ratio of mass flow in the secondary zone to the total mass flow, χ, must be specified. Second, the exit deviation, δ_p, must also be defined, which is the angular difference between the exit primary flow direction and the blade angle.

The Two-Zone model was developed initially for flow through an impeller (at station 2 making the inputs χ_2 and δ_{2p}). There is nothing in the model development, however, that would restrict it from being applied across a diffuser stage as well (at station 5 making the inputs χ_5 and δ_{5p}). The non-isentropic flow at the diffuser exit is located along the walls of the diffuser primarily due to boundary layer growth. This is in contrast to flow through the impeller where boundary layer growth exists in addition to secondary flows induced by the large curvature effects and Coriolis forces acting on the fluid.

The Two-Zone model has proven to be an accurate method to predict thermodynamic state change through a radial impeller and has the same potential for the diffuser. However, the flow kinematics must also be calculated to fully specify the

thermodynamic state. The TEIS model fills this knowledge gap and allows the thermodynamic state of the fluid to be calculated.

1.3.2 TEIS Model

The TEIS (Two Element in Series) model was originally developed for impeller flow physics. The TEIS model breaks up a bladed passage into two elements in series as the illustration in Figure 1-5 shows. The flow in these elements could be accelerating or decelerating, depending on the actual geometry in question. Element "a" models the inlet portion and Element "b" models the passage portion. In Element "a", the throat area, A_{th}, (Figure 1-6) is fixed by the blade spacing, but the inlet area, A_{in}, is not constant and changes with flow rate. This fictitious area represents a variable geometry diffuser that
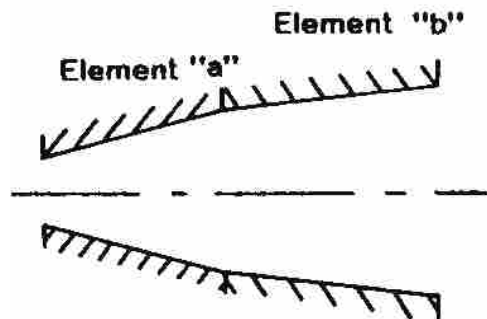
Figure 1-5 A conceptual representation of the TEIS model showing the arrangement of "Element a" and "Element b" as given by Japikse [2].

changes with incidence. This inlet area is a maximum at high flow rates and a minimum at low flow rates. At high flows the inlet element accelerates the fluid and the element acts as a nozzle while at low flows the inlet diffuses the flow. Element "b" models the passage portion (the bladed passage) as a fixed geometry diffuser. The TEIS model

13

requires the specification of two constants, η_a and η_b, which represent the inlet and passage effectiveness respectively.

These quantities are defined similar to typical diffuser or nozzle effectiveness widely used in industry. The definition for η_a is given by Japikse [2] in Equation 1-1.

$$\eta_a = \frac{C_{pa}}{C_{pa,i}}$$

(1-1)

In this equation C_p is the pressure recovery coefficient for Element "a" and is equal to the change in static pressure across the element over the dynamic head defined as $\frac{1}{2}\rho C_3^2$, where ρ is the density and C_3 is the velocity at the vaned diffuser inlet. For uniform entrance and exit flows and no frictional losses, the ideal pressure recovery coefficient is defined as [4]

$$C_{pa,i} = 1 - \frac{1}{AR_a^2}$$

(1-2)

where AR_a is the area ratio for Element "a".

Figure 1-6 shows the geometric areas for Element "a". Upon inspection it is immediately evident that the inlet area is not constant but changes with flow conditions and the area ratio needs defining. Japikse [4] defines AR_a is as

$$AR_a = \frac{A_{th}}{A_{in}} = 1 - \left(\frac{\cos\alpha_3}{\cos\alpha_{3b}} \right)^2$$

(1-3)

14

where α_3 and α_{3b} are the inlet flow and blade angles at the diffuser inlet.
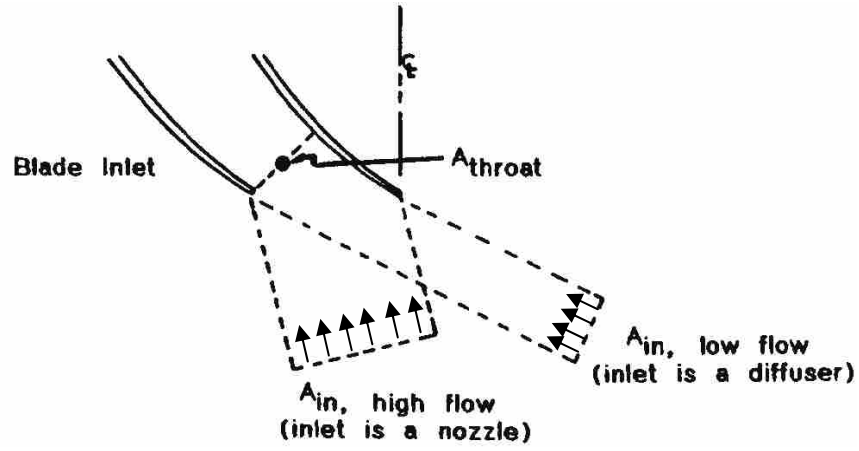
Figure 1-6 TEIS model inlet portion (Element "a") showing variable geometry characteristic of the model [4].

The definition of η_b is similar to that of η_a,

$$\eta_b = \frac{C_{pb}}{C_{pb,i}}$$

(1-4)

where $C_{pb,i}$ is given by the following, assuming uniform entrance and exit flows and no frictional losses [4]:

$$C_{pb,i} = \frac{1}{AR_b^2}$$

(1-5)

where AR_b is defined as

$$AR_b = \frac{A_e}{A_{th}} \tag{1-6}$$

In this equation, A_{th} is the throat area and A_e is the exit area as defined by the diffuser blade geometry. To complete the TEIS model it is necessary to define the overall diffusion ratio, or decrease in velocity, through the vaned passage. The diffusion ratio is defined as:

$$DR = \frac{C_{in}}{C_{exit}} \tag{1-7}$$

where C_{exit} is the velocity of the primary flow zone at the passage exit and C_{in} is the fluid velocity at the passage inlet. The TEIS model, as described above, does not extend into the range where stall is encountered. A modification to the model, however, allows for the approximation of this phenomenon. Stall can be approximated by the use of a constant denoted, DR_{stall}. The difficulty of setting this parameter in design is that the onset of stall is not easy to predict and can only be set by one who knows the diffusion or pressure loss characteristics of the diffuser in question.

Japikse derived a relationship for DR^2 that relates the performance model to the thermodynamic state at the exit of the bladed passage:

$$DR^2 = \left(\frac{1}{1 - \eta_a C_{pa,i}} \right) \left(\frac{1}{1 - \eta_b C_{pb,i}} \right) \tag{1-8}$$

16

Using this equation in combination with equation (1-6), the change in fluid velocity through any bladed passage can be predicted. Consequently the complete state of any bladed passage can now be calculated by combining the TEIS and Two-Zone models, provided that η_a, η_b, χ, and δ_p are known.

The TEIS and Two-Zone models have been applied to the impeller with great success in matching data trends but have not been applicable, as of yet, as a design tool. As can be seen from equation (1-1), η_a and η_b cannot be known before a stage is tested; neither can χ or δ_p for the Two-Zone model. However, research aimed at developing empirical models to predict these inputs for the impeller (station 2), coupled with a vaneless diffuser is nearly complete [7]. The initial testing of these TEIS and Two-Zone input parameter models as design tools has shown great promise for their use in future impeller design. The next step in developing the TEIS and Two-Zone models as a viable design tool is creating empirical input parameter models for the vaned diffuser, η_{a5}, η_{b5}, χ_5, and δ_{5p}.

1.4 Contribution of this Work

The scope of this thesis is to develop predictive models for the TEIS and Two Zone input parameters, namely η_{a5}, η_{b5}, χ_5, δ_{5p}, for two the vaned diffuser types described: a wedge diffuser and a cascade diffuser. There will also be code developed which will enable the models to be applied in the proprietary design software of Concepts NREC.

Early estimates and previous models built for impeller input parameters show that these quantities are difficult to predict. Japikse postulated that the models for η_{a5} and η_{b5}

would be highly nonlinear functions of numerous variables some of which may not have been recorded in the test data [4].

It is intended that this thesis will add to the turbomachinery field in two ways. First, by making historical diffuser designs available in an accessible electronic database format to aid in the general understanding of the current technology level. And second, by making the TEIS and Two Zone models effective design tools, it will allow for systematic design optimization to aid in advancing the technology base.

2 Methodology

2.1 COMPAL

Concepts NREC provided two software tools required to build empirical models for the TEIS and Two-Zone input parameters. The first of these programs is called COMPAL. COMPAL aids in the meanline (1-D control volume analysis) design of new centrifugal or mixed flow compressor stages as well as the meanline data reduction of previously tested designs. It is a software tool that Concepts NREC makes commercially available. COMPAL can be operated in three different modes: design mode, analysis mode and data reduction mode. The modes that are used in this study are analysis and data reduction modes. There is a distinct difference in these two modes of the program. Analysis mode performs the meanline calculations with user defined model inputs. For the TEIS and Two Zone models the inputs are η_{a5}, η_{b5}, χ_5, and δ_{5p}. Data reduction performs the meanline calculations as well; however, the modeling inputs are no longer needed because of user supplied experimental data. In data reduction, the data is used to remove the need for the modeling inputs by forcing the meanline model results to match the measurements at each station location where they are provided. After solving the meanline equations important stage parameter results are plotted for easy viewing, although access to numerical results in tabular form is also available.

This use of analysis and data reduction modes is ideal for this type of study. It provides the ability to determine the settings needed for the analysis to match the data. This is achieved by overlaying plots generated by the two approaches and varying the modeling inputs in analysis mode until the speedlines generated from analysis and data reduction modes lie on top of each other as shown in Figure 2-1. The figure shows two stage parameters, stage efficiency and stage pressure ratio plotted against the mass flow through the machine, where the data reduction matches the analysis. The data reduction results are denoted with the dashed lines and the analysis results are denoted with the solid lines. This program has proven invaluable in matching the data reduction with the analysis to determine the TEIS and Two-Zone input parameter values.
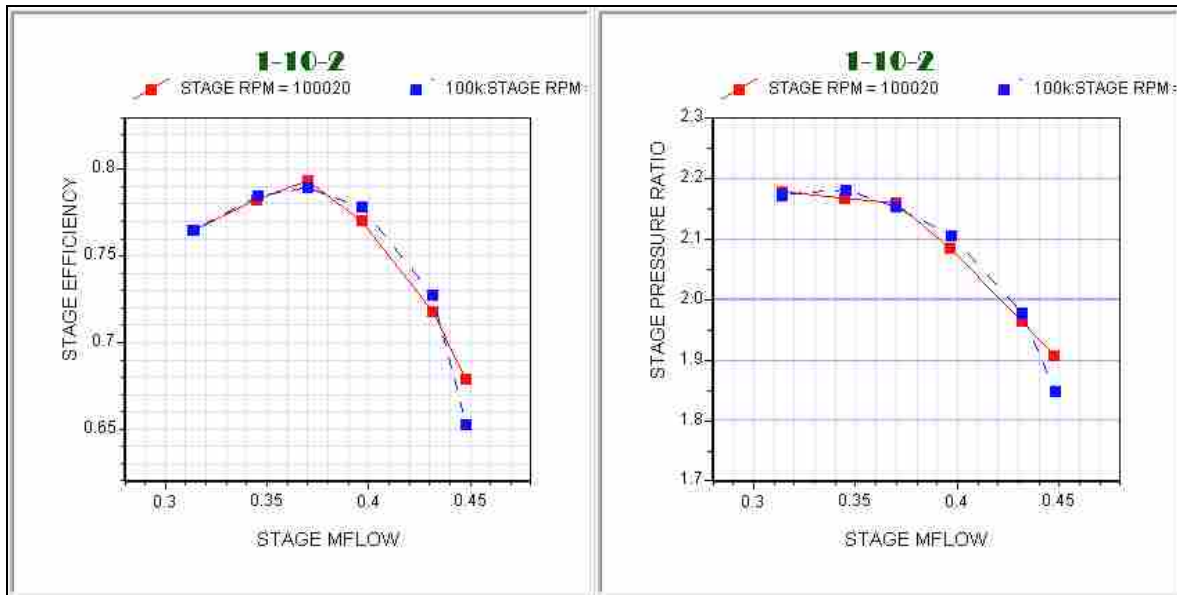
Figure 2-1. In this example of a match between the data reduction and the analysis of a speedline, the solid line is the analysis and the dashed the data. The data is matched well on plots of stage efficiency vs. mass flow (left) and stage pressure ratio vs. mass flow rate (right).

20

2.2 Modeling Descriptions for All Elements

Every stage considered in this study consists of an impeller followed by a vaneless space with a subsequent channel or airfoil diffuser. There are models used in each of these elements to predict static pressure rise and total pressure loss. The accuracy of these models is essential to the deduced values of η_{a5}, η_{b5}, χ_5, and δ_{5p} used in empirical model building. A description of the model used in each element is provided below.

2.2.1 Impeller Modeling

The centrifugal impeller is modeled with the TEIS and Two Zone approach, the same models which are used for the vaned diffuser and described in the Literature Review. The models are in a slightly different form than those presented earlier (Eqs 1-1—1-8). Modification is made to account for the rotating frame of reference. To see a derivation of the changes and the equations used for the impeller see the work of Japikse [4]. Empirical models of the user input parameters applicable to the impeller have been created by Pelton [7]. These empirical models are in the validation process and were not used in this study.

2.2.2 Vaneless Diffuser Modeling

Every stage used in this study consists of an impeller followed by a vaneless space before the channel or airfoil diffuser. As previously stated, the static pressure rise in this vaneless space needs to be modeled. For this study the model used was extremely important due to a lack of measured pressures at the vane inlet. The model used was the

Time Cyclic (TC) model, an advanced vaneless diffuser model developed by Dubitsky and Japikse [12]. The flow exiting the impeller has two distinct regions, a jet and wake. A previous vaneless model in COMPAL assumed that these two flow regions were mixed throughout the entire vaneless diffuser—usually the flow is assumed mixed at the impeller exit plane. The TC model allows for the primary and secondary flow regimes to mix as the flow progresses through the vaneless space. The model uses the linear and angular momentum equations, continuity, energy equation, and a density relation which are then solved using Runge-Kutta integration. The mixing is controlled by a wake mixing coefficient, which for this study was fixed at 0.005.

2.2.3   Vaned Diffuser Modeling

The vaned diffuser modeling has been described in the Literature Review (section 1.3). The TEIS and Two-Zone models are applied to the channel and cascade diffusers. For these models to be effective as a design tool the modeling inputs η_{a5}, η_{b5}, χ_5, and δ_{5p} need to be specified. Differences exist between the two types of vaned diffusers that are discussed below.

2.2.3.1   Channel Diffuser

The channel diffuser typically has long vanes preceded by a very short vaneless space (see Figure 1-2). The model used in this vaneless space is the TC vaneless model previously described. Subsequently the TEIS and Two Zone models are employed in the diffuser passage. This modeling requires some geometric inputs; the throat (or minimum area) width and height, vane number, and inlet and exit blade angles. The channel

22

diffuser exits directly to the collector and TEIS and Two Zone models are used up to this point.

2.2.3.2 Cascade Diffusers

Cascade diffusers are also preceded by a vaneless space; however, here this space is typically much larger than that characteristic of channel diffusers. This vaneless space is again modeled with the TC vaneless diffuser model. The cascade diffuser performance is modeled with the TEIS and Two Zone models similar to the channel diffusers, although the vaned space for the cascade diffusers is typically much shorter. Up to the exit of the diffuser the modeling of the two vaned diffuser builds is performed in an identical fashion. At the exit of the vaned diffuser, however, the cascade modeling differs from that of the channel diffusers. Whereas the channel diffuser at this point exits to a collector, the cascade diffuser is followed by another vaneless space prior to exiting the stage. This second vaneless space is modeled here with a modified Stanitz Vaneless Diffuser model [4]. This is performed using the linear and angular momentum equations, continuity, energy equation, and a density relation which are solved with a Runge-Kutta algorithm.

2.3 Data Matching

In order to determine the TEIS and Two-Zone model input parameters for channel and cascade diffusers, the stage analysis (models predicting stage performance) is forced to match the data reduction (inputting known data quantities for tested machines) by varying η_{a5}, η_{b5}, χ_5, and δ_{5p}. To do this by hand can be a very time consuming process. The test

data is used in COMPAL to perform the data reduction for one speedline, effectively eliminating the user inputs to the models as stated earlier. This is then compared to the analysis mode where user inputs are used to model the machine behavior. The user inputs in analysis mode are then varied until the results of the analysis match those of the data reduction. Subsequently, the values of the user inputs are recorded and the file outputs saved. An example of how one would determine values of varying η_{a5} and η_{b5} for a speedline is shown in Figure 2-2. In matching the data, varying η_{a5} largely controls the initial slope of the speedline and η_{b5} controls the magnitude. By changing these two inputs one can match the diffusion ratio of the data.
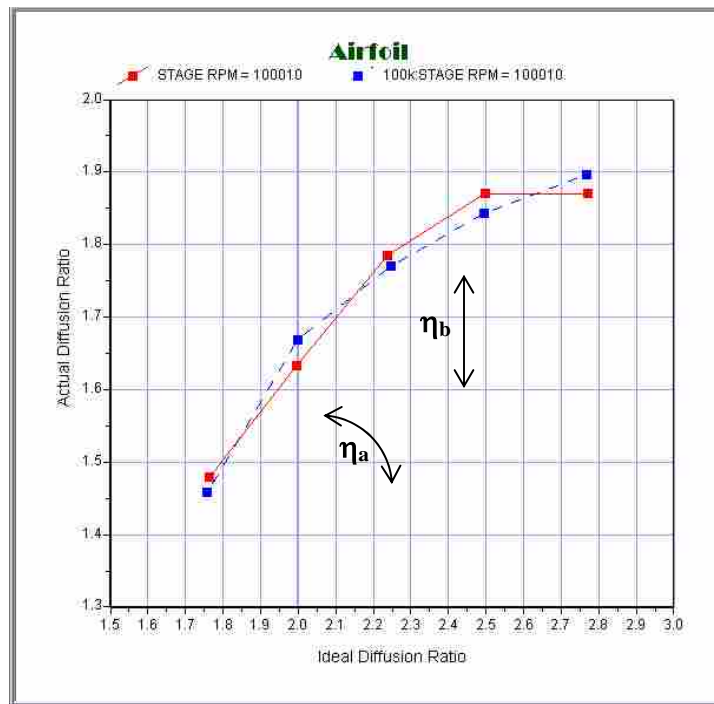
Figure 2-2. The values of η_{a5} and η_{b5} are determined while matching the diffusion ratio data— dashed—and the analysis—solid. In the matching process η_{a5} controls the slope and η_{b5} the level of the analysis diffusion ratio.

24

The same type of matching process with the diffuser loss coefficient and coefficient of pressure recovery is needed to determine values of χ_5, and δ_{5p}. the loss coefficient, LC, and coefficient of pressure recovery, CP, are defined as

$$LC = \frac{\Delta P_0}{\frac{1}{2}\rho_3 C_3^{\,2}}$$ (2-1)

$$CP = \frac{\Delta P}{\frac{1}{2}\rho_3 C_3^{\,2}}$$ (2-2)

where ΔP_0 is change in total pressure and ΔP is the change in pressure across the vaned diffuser.

For an experienced engineer to accomplish the above process by hand takes, on average, 20-30 minutes for the impeller alone. The diffuser requires a similar amount of time if there are measured pressures at the inlet and the exit of the diffuser vanes. To do this for the entire database, approximately 230 machines, would be time consuming but possible. This process becomes much more involved, however, when a vaned exit static pressure is not present in the data. Without the exit pressure specified the user defined inputs are needed to determine this essential pressure and complete the meanline equations. This lack of data makes it necessary to use the values of η_{a5}, η_{b5}, χ_5, and δ_{5p} in the data reduction as well as the analysis modes in COMPAL. Once initial values for the input parameters have been specified, it is necessary to iterate between data reduction and analysis modes in COMPAL, comparing the solutions each time and varying the input

parameter values until the two COMPAL modes converge to a single solution. The ideal scenario would be to have static and total pressure measurements at the inlet and exit of the vanes available for each diffuser build. In practice this is very uncommon because of the difficulty, and enormous cost, of instrumenting and testing each build.

2.4 Data Processing

The research conducted involved creating a large database of compressors with cascade and channel diffusers. All of the data used in the study was provided by the company sponsor, Concepts NREC. This data had been collected over a period of time exceeding three decades with the intent to improve fundamental compressor modeling. It is the largest collection of radial compressor data ever used for this type of study. Many different organizations have contributed to this rather large accumulation of compressor designs. The full collected database contained 148 channel diffuser and 427 cascade diffuser speedlines.

The amount of data necessary for this project requires a standardized and systematic way of processing the data. The data was initially contained in historical reports describing stage design and performance and needed to be entered into the computer. For each case, a computer file was generated through the use of the commercially available meanline compressor design program COMPAL. To do this required certain geometric knowledge about the stage, such as diffuser inlet and exit radii, blade angles and thicknesses, as well as numbers of blades, etc. This information was extracted from the historical files.

Once the stage geometric values, design mass flow, and rotational speed are specified the meanline calculations can be performed. All of the meanline or one-dimensional equation solving was performed in COMPAL. The test data is entered in the COMPAL interface where a test data file is created containing all of the measurement information. The test data is identified by a station location number as identified earlier in Figure 1-3. All of the stages used in this study have the following test data: mass flow, rotational speed, inlet total pressure, P_{00}, inlet total temperature, T_{00}, static pressure at the impeller exit, P_2, static pressure at the diffuser exit, P_5, and the temperature in the collector, T_{COLL}.

The pressure measurements for the test data were taken with the use of static wall pressure taps. Much of the data provided were taken by Concepts NREC employees. Therefore, the instruments used and the accuracy of the measurements are recorded in the historical reports with the test data. However, less is known for some parts of the database and there exists greater uncertainty as to the measurement devices used, the location of the measurements, or the accuracy of the data. Because of the disparity in the measurement techniques and procedures a data classification system is necessary.

2.4.1   Data Classification

The data provided by Concepts NREC came from many different sources with qualities ranging from highly detailed test consortia to publicly available datasets that have only flange-to-flange measurements, meaning only inlet and exit pressures were acquired with no intermediary data. Because the data does not all come from one consistent source there is additional error due to the changes in measurement conditions (change in location, operator, technique, etc). This error influences the determination of

the TEIS and Two-Zone parameters. To categorize the different quality of datasets a classification procedure was utilized. The data classification procedure outlined by Japikse [4] was used to organize all of the data used in this study and is reproduced in Table 2-1.

Table 2-1 A list of the criteria used for determining data classification as outlined by Japikse [4].

	Data Classification
	Data Classification
1	Internal data with traverses, plus overall pressures and temperatures a. Full pressure data including traverses in and out of each element, work input to 1% or better b. Partial traverses, full static pressures, work input to 1% or better c. Occasional traverses, work input to 2% or better
2	Internal data without traverses, plus overall data a. Full station static pressure, work input to 1% or better b. Impeller tip static pressures, work input to 2% or better c. Impeller tip static pressures, work input to 3% or better
3	Overall data only a. Overall pressure and temperature rise, work input to 1% or better b. Overall pressure and temperature rise, work input to 2% or better c. Overall pressure and temperature rise, work input to 3% or better
4	Overall pressure, flow rate, and impeller speed only

Table 2-1 details how this data classification is determined for each dataset based on both the quality and quantity of measurements taken for each dataset. The highest level of data in Table 2-1 typically comes from an advanced research study where sufficient resources were available to conduct detailed flow surveys, or traverses, from which detailed information on all surfaces of an impeller or diffuser control volume can be determined. Such data sets are rare and none were found for inclusion in this study. By contrast, Level 4 is the least accurate data and includes only the overall pressure ratio for

a compressor and no indication of input power for the stage. Level 2 data can be just as valuable as Level 1 for broad model development, especially if it is Level 2a or Level 2b, which has sufficient accuracy to determine many of the key parameters of a stage. Level 3 data is not as desirable as either Levels 1 or 2, but meaningful trends can still be derived. All of the data used in this study was of Level 2b quality.

2.4.2 Data Concerns

It was understood that some of the data provided might not be useable in the model building process. The data not of a sufficient quality to be included (Levels 3 and 4) or those data sets determined unreliable after unrealistic data reduction results were obtained were removed form the model building databases. Nearly half of the assembled database came from a separate entity that was acquired by Concepts NREC. The data acquired by this company proved to be problematic on further inspection. The difficulty with the historical cases from this company was due to one main reason: the measurements acquired are not at traditional station locations. This makes it necessary to correct the pressure measurement values to bring them in line with the correct station locations if the data is to be used. This is a delicate process that must be done correctly to ensure accurate results. Several months of the project focused on this so that all of the data possible could be utilized for model building.

Taking data measurements in a turbomachine is not an easy task. The flow in the passage is very three dimensional and distorted. It is, therefore, prudent to have multiple pressure taps at station locations so that a numerical average may be used to give better representation of average flow conditions. If done correctly, each of these pressure taps should be located at a different pitch location [13]. At times it is advantageous to look at

a single blade passage in the centrifugal compressor. A common, and reasonably good assumption, is that the flow physics are approximately the same for each bladed passage. A diffuser pitch is the radial extent of one single diffuser blade passage. The rest of the machine can be collapsed, or laid on top of the single diffuser pitch. An example of tap locations used in several compressor builds from which hundreds of speedlines of data were taken is shown in Figure 2-3. In this example the diffuser pitch encompasses 24 degrees. The pressure measurement values for a single mass flow point on a speedline have been plotted by pitch location in Figure 2-4

PressureTap Locations

75% Impeller Shroud Distance

◆ Impeller Shroud Taps

■ Impeller Discharge

△ Suction Side and Pressure Side Vaned Diffuser Passage Taps

△ Diffuser Discharge

■ Diffuser Discharge Total Pressure

95% Impeller Shroud Distance

107% Impeller Shroud Distance
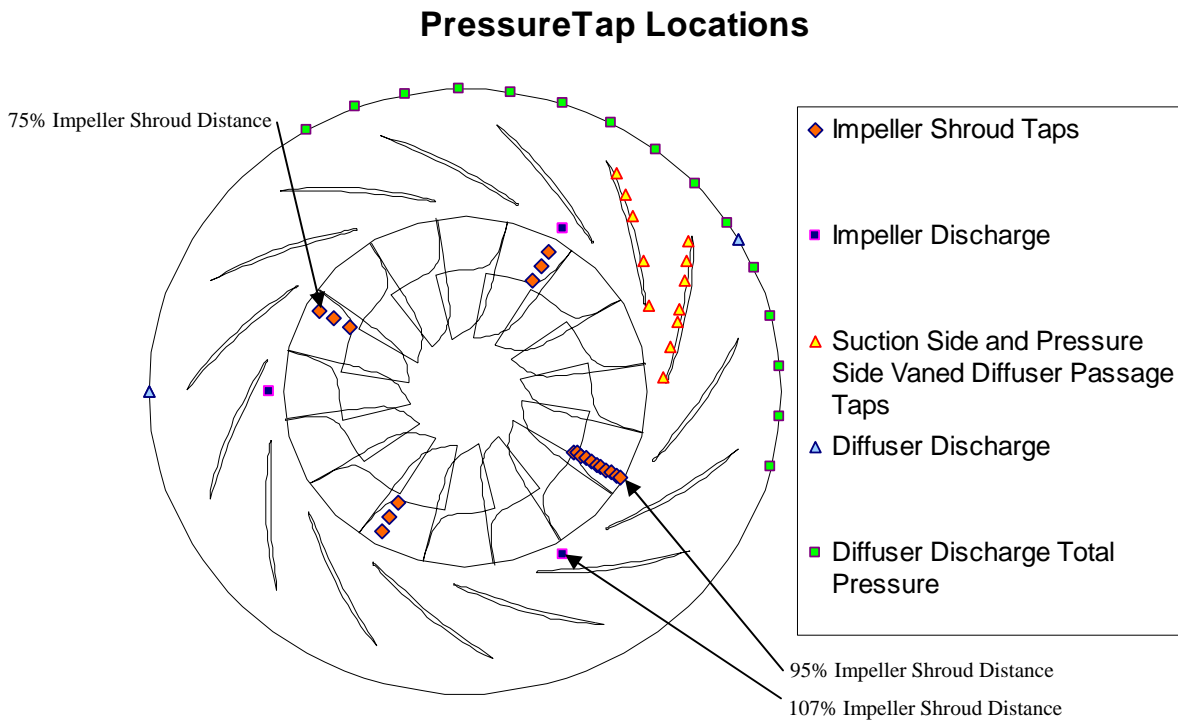
Figure 2-3. A view of pressure tap locations for case 00I2VD11 superimposed on impeller and cascade diffuser geometry. Many of the pressure taps, at a single radial location, are at identical pitch locations, as illustrated in next figure, making pressure interpolation difficult.

As is shown in the Figure 2-3, there were no pressure taps located directly at the impeller exit—the closest one to the impeller exit was at 95% of the distance from the

impeller shroud inlet to the impeller shroud exit. This impeller exit pressure is one of the most critical measurements needed for a high level of confidence in the database. Because there were no pressure taps at the impeller exit an attempt was made to interpolate the pressure measurements to that point. This interpolation was made difficult because the pressure measurements at a single radial location were located only at a single pitch position.
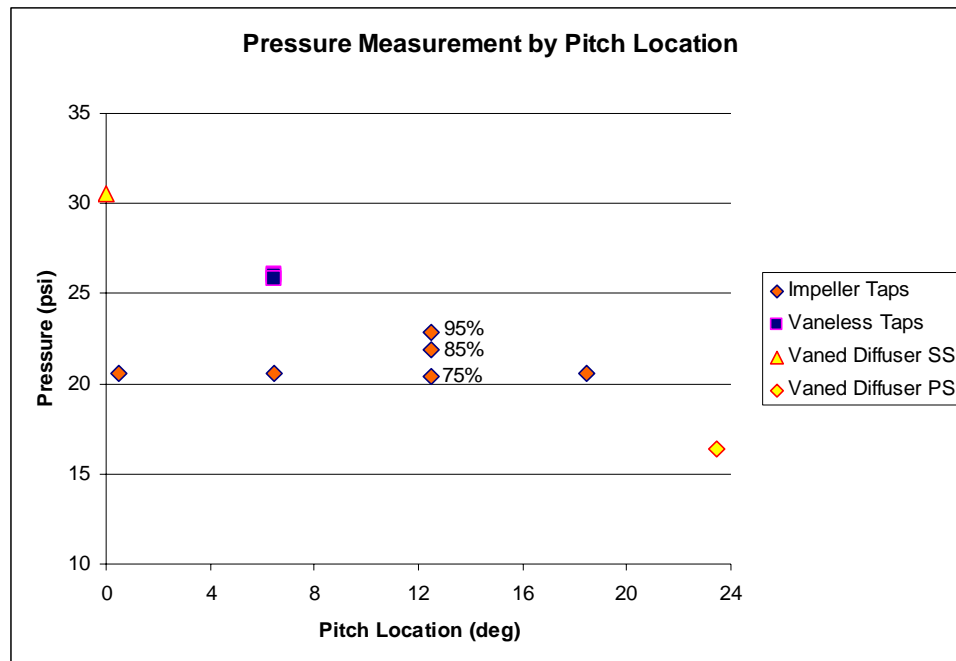
Figure 2-4. The pressure values for five different radial locations from one mass flow point in case 00I2VD11 are presented in the plot. The impeller taps have four different radial locations: 1) at 75% (total of 4 taps), 2) at 85%, and 3) 95 % of the distance along the impeller shroud. The three vaneless taps are at the same pitch location.

In order to create a better understanding of how the static pressure increases in the compressor, measurement locations and values were plotted on a pitch-wise basis to create a pressure mapping along the pitch. The pressure surface, shown in Figure 2-5 , was created using a linear interpolation routine in MATLAB. The pressure at the

31

impeller exit was then integrated across the pitch. The interpolated pressure values were then used in the meanline data reduction of the stage. An example of the integrated pressure in comparison to the pressure measurements is shown in Figure 2-6. In this
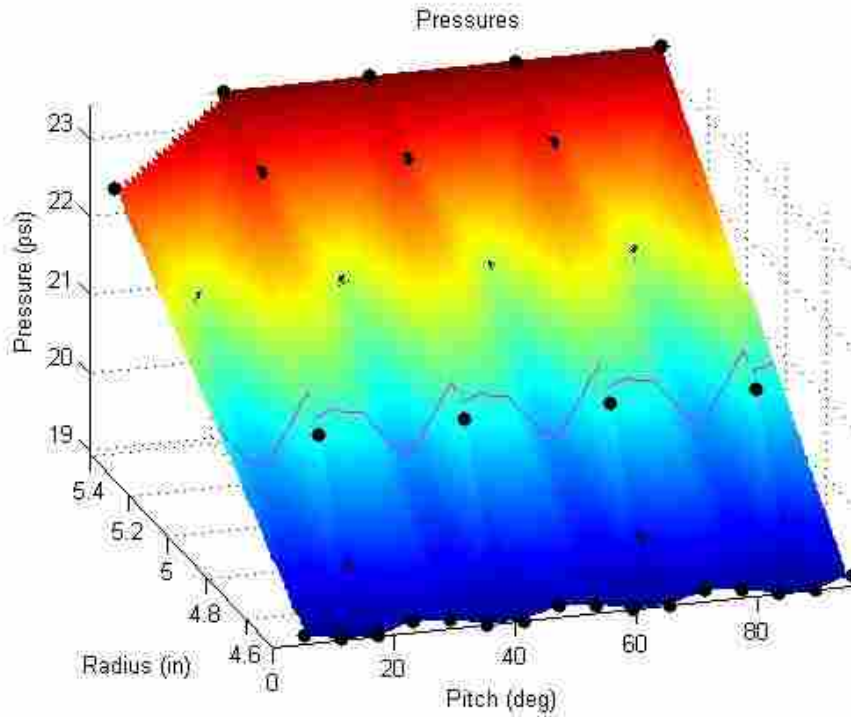
Figure 2-5. The surface represents a pressure interpolation across one pitch. The line indicates the impeller exit location where an integrated pressure was calculated. A total of four pitches are shown.

figure the integrated pressure is illustrated by the dotted line. This yielded reasonable data reduction results for many of the data points, such as is illustrated in the figure, but not for all. Some of the results were unrealistic due to uncertainty and error in the interpolated pressure measurement, posing a problem. To take each pressure interpolation value on a case-by-case basis would take a considerable amount of time. But more importantly, changing the interpolation process for each measurement would add user error and would be similar to choosing the impeller exit pressure by what was "felt" to be

32

a reasonable value. This could bias the resulting models, minimizing the usefulness of the research.
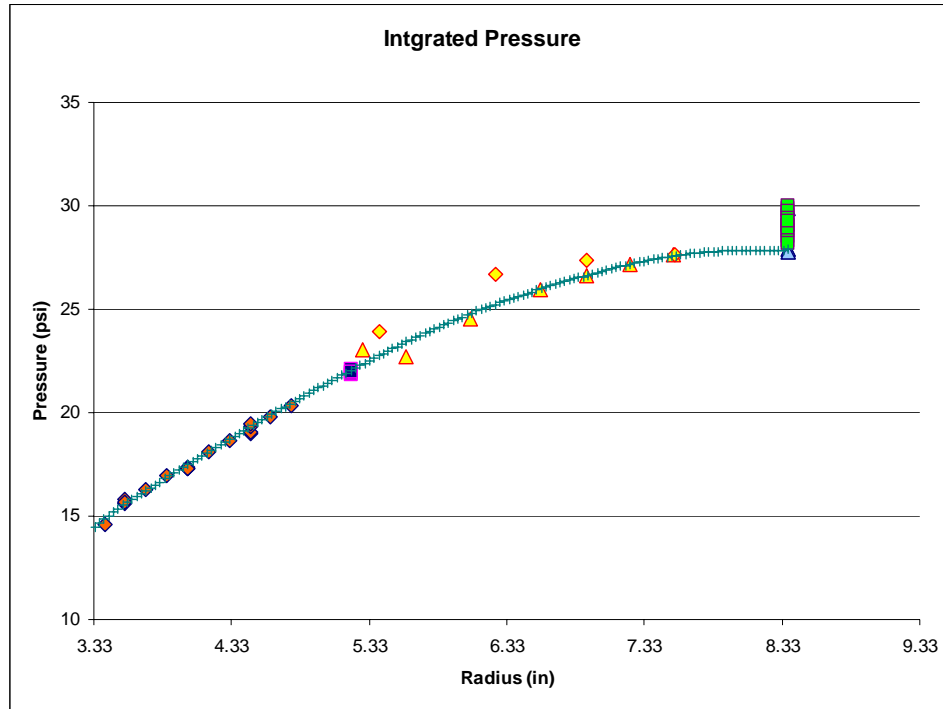
Figure 2-6. Plot of the pressure magnitude at corresponding radial locations. The pressure surface integrated across the pitch is shown by the dotted line.

Another difficulty with this data was measurement point density inside the boundaries of choke and stall. There were usually 5 data points taken along a speedline: one in choke, one in stall, and three in between choke and stall. Having few data points in between choke and stall makes it difficult to determine accurate values for η_{a5}, and η_{b5}. After many involved attempts it was determined that all of these cases had to be discarded due to the untrustworthy nature of the measured data. Doing this enhances the integrity of the models built because the data they are built from is of a higher quality.

33

In order to hold constant the diffusion ratio curve using data reduction mode (eliminating the TEIS inputs in the meanline models) and determine the actual values for η_{a5} and η_{b5}, there must be pressure measurements at the inlet and exit of the vaned element. These measurements are not available in the cascade diffuser database, or for any other cascade database that is publicly known or available. This may introduce some error into the analysis process. The quantity of this error cannot be determined until such data is found and analyzed. To determine the values for η_{a5} and η_{b5} one needs to iterate between the data reduction model and the analysis mode, changing η_{a5}, η_{b5}, χ_5, and δ_{5p} values and comparing the solutions each time, until the two modes converge to a solution.

The current databases are much smaller than those originally assembled. Some of the speedlines could not be used because they were taken too close to stall and TEIS and Two Zone input parameters could not be clearly identified. The channel database has 100 speedlines and the cascade database has 130 speedlines. This is reduced from the original collected numbers by one third for the channel database and two thirds for the cascade database—mostly due to not having clear pressure measurements at the impeller exit, P_2, for many cases in the database. This loss of large amounts of data could be perceived as detrimental to the eventual models that were built. While it is true that fewer speedlines were used in model building, the confidence in the model building data is enhanced by ensuring only the highest quality of data available was included.

2.5   Automated Data Matching Using Easy Control

The manual matching of analysis to data reduction in COMPAL is a slow process. Also it is prone to user bias since two engineers will not choose the same exact values of

η_{a5}, η_{b5}, χ_5, and δ_{5p} in matching speedline data. User bias is evident as each match is evaluated. To remove this bias an analysis tool was developed to analyze the data in a systematic, unbiased manner. This tool, provided by Concepts NREC, is called Easy Control. Easy Control utilizes the COMPAL solver to perform all meanline equation calculations.

Table 2-2. A listing of the different weights applied in the objective function in Easy Control. An additional multiplier is used if an impeller exit static pressure, P_2, is given in the data reduction.

Objective Plots			
X-axis	Y-axis	Weighting	P_2 Multiplier
Mass Flow	Stage Efficiency TT	5	1
Mass Flow	Stage Power	5	1
Mass Flow	Impeller Recirculation Loss	0.1	1
Mass Flow	Rotor Efficiency	1	2
Mass Flow	Stage Pressure Ratio TT	5	1
Mass Flow	P_{02}/P_{00}	0.5	2
Mass Flow	MR_2	1	2
Mass Flow	Total Dynamic Head	5	1
Mass Flow	$P_{02}-P_{00}$	0.5	2
Mass Flow	DR_2	1	2
Mass Flow	CP	1	2
Mass Flow	LC	1	2

Easy Control is used to determine values of η_{a5}, η_{b5}, χ_5, and δ_{5p} for each speedline by minimizing a specific function. The objective function is a combination of the least squares fit error of the data reduction and analysis results across a speedline for many key values such as overall stage power, stage efficiency, rotor efficiency, stage pressure ratio, and diffusion ratio. There are additional penalties that are applied so that un-realistic results cannot be obtained. There is also a weighting in the objective function applied to different stage quantities. For instance, the weighting on rotor efficiency is greater than the weighting for coefficient of pressure recovery in the vaneless diffuser. The weightings used were determined by industry leading compressor design engineers and

are given in Table 2-2 [7]. There is allowance for the user to change the weighting on the quantities in the objective function, however, this is not recommended and was not done in this work. As illustrated in the table, there is an additional weighting (multiplier) added if an impeller exit pressure, P_2, is present in data reduction mode. This multiplier is employed because there is greater confidence in the results when the impeller exit pressure, P_2, is measured. All of the data used in this study includes this key measurement.

Easy Control was originally developed for Pelton's [7] work of creating models for the TEIS and Two-Zone input parameters applicable to the impeller. The functionality of the program was expanded to allow for data matching with the TEIS and Two Zone models applied to the diffuser. Easy Control was used to optimize the TEIS and Two Zone model input parameters for the impeller. The values found through Easy Control were used to model the impeller even though the diffuser values were not yet fixed, thus making the impeller modeling frozen. The work described here does not take into account any impeller-diffuser interaction in the TEIS and Two-Zone input parameters. Interaction is expected and will be the subject of future research.

 Not only can Easy Control be used as an optimization program, but it also has database management capabilities. Upon completion of the data matching it stores the tabulated results of the meanline modeling equations for each data point on a speedline. The Easy Control tool also has the ability to output a file of these calculated meanline quantities at any point along a speedline, such as maximum rotor or stage efficiency. Thus it allows for the compilation and interpolation of flow and geometric quantities that are necessary in making empirical models.

3 Procedure

3.1   Database Organization

The approach followed to develop the empirical models has already partially been described. The first step was to enter data and geometry into a computer database. The data and stage geometric information were recorded in historical company reports which describe performance characteristics of the tested compressors. A COMPAL computer file was created for each build tested and the meanline models were run in data reduction mode. The stage efficiency and stage pressure ratio results from data reduction were compared to the historical reports to ensure accurate stage information entry. Two databases of these files were created, channel and cascade—one for each type of vaned diffuser. Each COMPAL file was organized in one of these two databases depending on the type of vaned diffuser present in the build. The COMPAL files were prepared for automated data matching through Easy Control by certifying that identical settings were used for each COMPAL file. This ensured that each file would be treated the same way in Easy Control.

3.2   Easy Control

The two assembled databases were analyzed in Easy Control with the automatic data reduction matching routine described previously. The data match of each speedline was evaluated and the speedlines that were found to be in stall were removed from the model building sets. Stall was determined from the diffusion ratio curve—the actual diffusion ratio plotted against the ideal diffusion ratio, determined with a frictionless analysis, for each point on the speedline. Figure 3-1 shows how this is accomplished. The figure shows the diffusion ratio curve for two different speedlines of the same compressor build. The speedline on the left is in full stall. This is determined by the negative slope of the curve. The curve on the right has only a single point in stall—the right most data point—and the speedline is still useable.
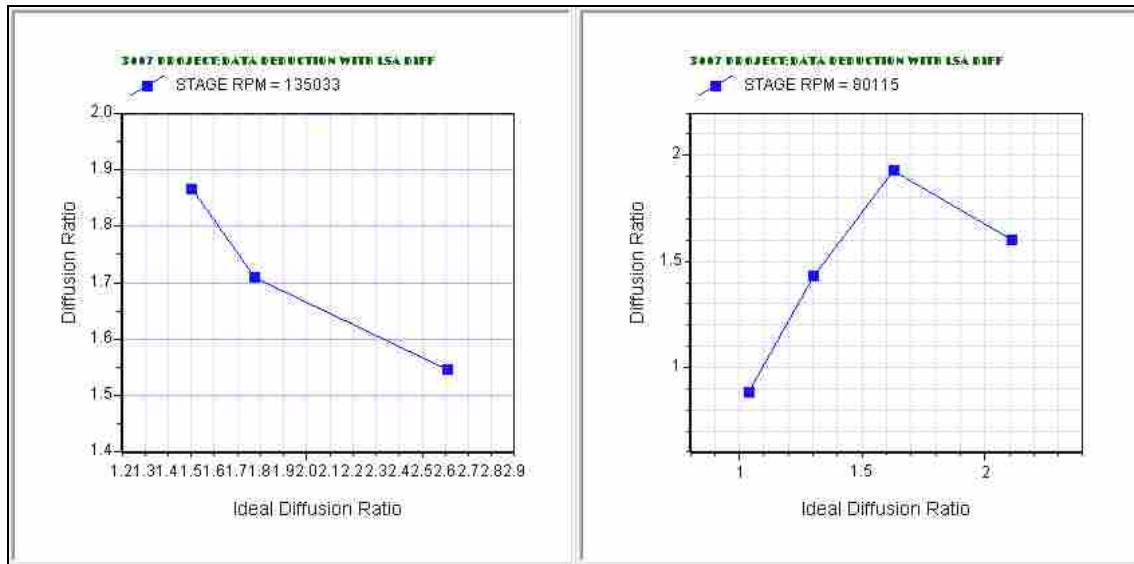
Figure 3-1. The figure shows the diffusion ratio curves—actual diffusion versus ideal diffusion—for two different speedlines of the same machine. The speedline on the left is in full stall, determined by the negative slope of the curve, while for the case on the right only the right most point is in stall conditions.

Some of the speedlines had numerous data points that were in choke. The amount of mass that can be put through a compressor is limited by the smallest passage area in the machine. This minimum area or 'throat' can be located in either the impeller or the diffuser. When the maximum amount of mass the throat can accept is put through the compressor passage it is said to be choked. This occurs when the velocity through the minimum area is equal to a Mach number of one. An example of this is shown in Figure 3-2. The figure shows three speedlines of data that all have points in choke. The data that is near vertical on the plot is choked; no more mass flow can be ingested by the compressor at that rotational speed. The data points that are in choke pose a problem for
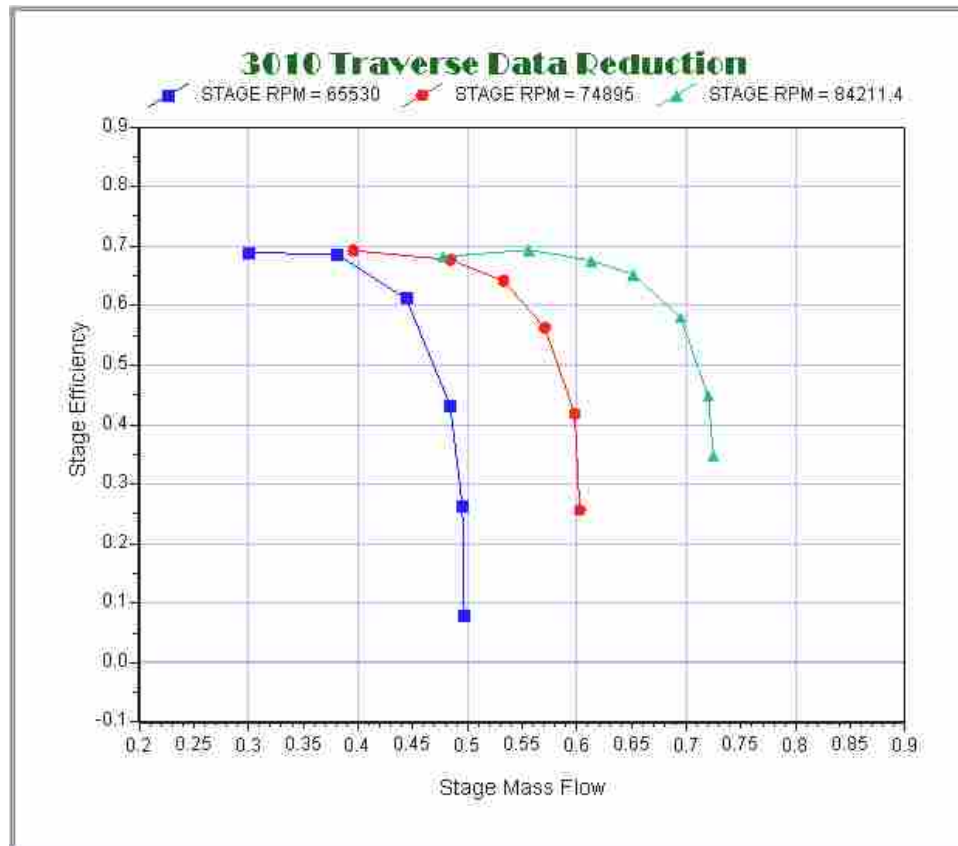
Figure 3-2. Stage efficiency plotted vs. mass flow through the compressor illustrating choke for three different speedlines. The points that are in choke are on the right of each speedline and form near vertical lines on the plot.

automatic data reduction. Points in choke tend to drive the matched value of η_{a5} to the un-choked upper limit since the slope on the diffusion ratio curve with chokes points is very steep. Such points must be removed from the data file to ensure the η_{a5} and η_{b5} values determined in Easy Control are accurate for the speedline. After the choked points are removed from the data file, the case is evaluated again in Easy Control to obtain new values of η_{a5} and η_{b5}.

Once the speedlines that were determined to be in stall and the data points in choke were removed, and the data reduction matching has been performed, Easy Control is used to output a single point database file. This is a collection of geometric and flow variables that are calculated at a single, identifiable point on a speedline and saved to a file for use in empirical model building or as a design aid. This database file can be output at any arbitrary point along a speedline—such as the maximum rotor efficiency or the minimum flow incidence at the rotor inlet. A critical decision made was the specific location on a speedline that would be specified as representative and where the empirical models would be generated. There are two items to be considered when determining at what point this would be done; 1) the model performance at that point and 2) the ability to apply the model at the same point on the speedline after it had been built. Empirical models were developed at a number of different points with the best success at the maximum total-to-total stage efficiency point. The consistent location chosen where the final empirical models would be developed is this maximum total-to-total efficiency for the stage. This is defined as

$$\eta_{tt} = \frac{h_{05s} - h_{01}}{h_{05} - h_{01}} \tag{3-1}$$

where h_{01} is the inlet total enthalpy, h_{05} is the exit total enthalpy and h_{05s} is the exit total enthalpy calculated as if the process were isentropic.

3.3   Variable Scaling

The single point database file is contained within a single computer file. This file consists of multiple columns of data, each with a header that lists the variable name followed by all the variable values for the cases in the database. Two files were created; one for the channel diffuser builds containing 100 speedlines and one for the cascade diffuser builds containing 130 speedlines.

Once the single point database file is output from Easy Control the data was centered with the standard normal variable normalization prior to model building [14]. It was found that using this normalization yielded superior models. All of the variables used were scaled as shown in Equation (3-2).

$$\overline{X} = \frac{X - \mu}{\phi} \qquad \text{(3-2)}$$

In this equation X is the variable of interest, μ is the mean of the variable in the database and ϕ is the standard deviation of the variable. This normalization is the standard approach in statistical modeling and can give sufficient spread to the data in addition to centering it [14]. The scaled variables have both positive and negative values centered at zero.

3.4 Model Building Process

When building statistical empirical models it is essential to have a large database that encompasses great variation in machine design parameters. This enables greater opportunity for the models to capture the variation in the data without being heavily influenced by the noise in the data. The database provided by Concepts NREC is the largest collection of compressor data ever compiled for this type of study and, therefore, provides a sound foundation for the initial building of these empirical models.

Empirical models can be built in a variety of ways. The method chosen in this study was to create relatively simple models using a stepwise linear regression approach [14, 15, and 16]. Linear regression is a method of fitting a straight line through a set of data points using a goodness-of-fit criterion. In this case the goodness of fit criterion is the mean square error or MSE. This is defined as

$$MSE = \frac{\sum_{i=1}^{k}(D_i - M_i)^2}{k} \tag{3-3}$$

where D_i is the database value for the parameter of interest (i.e. η_{a5}) M_i is the model value for the same parameter, and k is the size of the database. Other statistical quantities were also calculated and compared to aid in understanding the effectiveness of the model such as the classical R^2 defined by the following equations:

$$ss_{xx} = \sum_{i=1}^{k}(D_i - \overline{D})^2 \tag{3-4}$$

$$ss_{yy} = \sum_{i=1}^{k} \left(M_i - \overline{M} \right)^2 \tag{3-5}$$

$$ss_{xy} = \sum_{i=1}^{k} \left(D_i - \overline{D} \right)\left(M_i - \overline{M} \right) \tag{3-6}$$

$$R^2 = \frac{ss^2_{xy}}{ss_{xx} ss_{yy}} \tag{3-7}$$

Where $\overline{D}$ indicates the mean database value and $\overline{M}$ is the mean modeling value. The linear regression approach was determined to be an efficient model building method, while ensuring an acceptable performance level and still having control over the final form of the equation.

The parameters being modeled (η_{a5}, η_{b5}, χ_5, and δ_{5p}) have previously been thought to depend on flow and machine variables in both linear and nonlinear coupled forms [4]. Variable transformations were performed to elicit coupled and nonlinear effects in the model building. A variable can be transformed from one mathematical space to another by performing an operation on the variable. For example a variable can be transformed to log-space by taking the logarithm of the variable. At times a transformation such as this can prove advantageous to model building. Data that is not well correlated with any independent variables may exhibit much stronger correlation upon transformation. However, difficulties in transforming the final result back can be problematic. This exists because model performance may be compromised in the return transformation.

There are over 90 variables that could be used in the empirical model building process. Determining which of these variables were important in the modeling was critical, requiring time and fundamental flow physics understanding. Variables were chosen based on possible importance to the parameter being modeled. Subsequently they were made non-dimensional by forming dimensionless products or dimensionless groups with other variables deemed important. Sixty variables remained after making the original set non-dimensional. These non-dimensional variables were then normalized as discussed in Equation (3-2). The correlation coefficient between the normalized, non-dimensional variables and the parameter of interest was computed. The correlation coefficient is a measure of how linearly dependant the parameter of interest is on this variable. An example of the correlation coefficient is shown in Table 3-1. In this table the parameters η_{a5} and η_{b5} are correlated with eight different variables: area ratio for impeller element "b", AR_b, aspect ratio at the impeller exit, AS_2, impeller exit blade angle, β_{2b}, tip clearance over impeller exit height, Clr/B_2, ideal pressure recovery for element "a" in the impeller, CpA_{Ideal}, ideal pressure recovery for element "b" in the impeller, CpB_{Ideal} and the ideal diffusion ratio at the impeller exit, DR_{2I}. The magnitude, or absolute value, of the correlation coefficient indicates the linear importance the variable has on the parameter of interest, a coefficient value of 1 indicating the two are perfectly correlated and a value of 0 means there is no correlation. In the selected sample shown, the variable of greatest importance to modeling η_{b5} is the impeller exit blade angle, β_{2b}, with a correlation coefficient value of 0.51. Following this approach all important variables exerting first order linear dependence on the parameter of interest were identified.

Table 3-1. An example of the correlation performed for select variables.

Variable Name	η_{a5} Correlation Coefficient	η_{b5} Correlation Coefficient
η_{a5}	--	
η_{b5}	-0.171	--
AR_b	-0.131	0.339
AS_2	-0.132	0.077
β_{2b}	-0.235	0.513
Clr/B_2	0.151	-0.386
CpA_{Ideal}	-0.159	-0.187
CpB_{Ideal}	-0.066	0.409
DR_{2I}	-0.057	0.352

This process was performed again if the variables were to be transformed or changed from their linear state (i.e if they were raised to a power). Another way that the variables were changed was to create interaction or coupled terms. The product of any two variables could also be a term of interest. When considering all of the interaction terms that may exert an influence, large arrays of variables resulted. These arrays were then evaluated for potential modeling importance. All of the independent variables were therefore formed into products to create all possible interaction terms. The correlation between those interaction terms and the parameter of interest was then computed. Including all of the possible interaction terms, there were well over 3400 potentially important terms that were evaluated in the model building process. One phenomenon that is anticipated to be captured in this type of coupled term is an impeller-diffuser interaction. It has long been observed that this interaction occurs and has significant influence on the performance of a compressor [17, 18]. This interaction may be captured in a term involving both the impeller blade number and diffuser blade number. It might also be captured in fluid dynamic and geometric variables such as impeller exit flow

angles and diffuser blade angles. Terms such as these cannot be left out in the modeling process.

With so many potential variables, models could be created that were quite accurate but which were not physically possible. There needed to be a limit to the number of variables that could be included in each model. It was determined that each of the models built could have no more variables then one tenth of the number of points in the databases. This meant that the channel models could include no more than 10 variables and the cascade models no more than 13. This limit would help ensure that the models created did not become too large and begin to model noise in the database and not the variation due to physics present in the data.

In summary, the models were built by performing linear correlations on the non-dimensional, normalized variables and using the most statistically important variables in forming an initial model. The products of these terms were then taken and correlated with the parameter of interest as well. The most statistically significant products were used in model creation. In special cases where an infinite series expansion of one of the variables seemed appropriate, higher order terms were also correlated and used if found to aid in the model building.

3.5   Model Performance Evaluation

Prior to their use in design all models must be validated. Validation provides an indication of how well the models will perform when given new inputs (i.e. inputs that the model has never seen before). Care must be taken when building empirical models because there is a danger in pushing the performance—MSE, R^2, etc—of the model to an

artificially high level. The danger is that the model may simply 'learn' the dataset upon which it is built. When this occurs the model loses the ability to predict accurately for cases outside the model building database, although it may yield excellent fit to the database on which it is built.

Originally the models were to be validated with datasets that had not been used to create them; however, this became impractical when many speedlines in the database had to be eliminated because of measurement uncertainty and data acquired during stall. Splitting up the database would make the model building dataset too small to yield sound empirical models. It was thus decided that all of the data would be used to build the empirical models.

The models still need to be validated prior to use in design. Because of the limited datasets on which they are built, the performance evaluation of the models was not carried out with data outside the model building database. The performance was evaluated by calculating the average error across the speedline for each case in the database. This is not meant to be taken as model validation but merely as a modeling performance evaluation.

4   Results and Model Performance

At the outset it was hoped that a single set of empirical models could be developed that would perform well for the entire database, regardless of vaned diffuser type. Such was found futile early on in the model building process. Only one model was found suitable to be used in both databases. This was the model for the secondary mass fraction at the vane exit, or χ_5.

This model for χ_5 will be presented after comments about the automatic data reduction in Easy Control for each database. Following the model for χ_5, the channel and cascade models for η_{a5}, η_{b5} and δ_{p5} will be presented and discussed separately. The evaluation of the full set models for each diffuser database will be presented and their effectiveness evaluated. In the interest of Concepts NREC, some of the constants have been suppressed and replaced with a dummy variable, K_i, where i varies for each term in the model. The models are created for the TEIS input parameters are database specific and would most likely be different for different industries and even different companies within the same industry. The most effective models would presumably be created by individual companies and tailored for their specific design practices.

4.1 Automated Data Reduction

4.1.1 Channel Diffuser Builds

The channel database is the smaller of the two and therefore took less time in Easy Control to perform the data matching. The channel modeling database is made up of a total of 100 speedlines. In these there were some unexpected TEIS values for the impeller that were returned. Specifically, on occasion, the values of η_{a2} (the impeller) were higher than is reasonable and η_{b2} values were lower than is reasonable. To address this issue the vaneless build using the same impeller was consulted. The value of η_{a2} and η_{b2} for the vaneless cases should be close to that for vaned cases, although they will not be exactly the same. This is because there is a coupling effect that is present when a vaned diffuser is placed in series with a centrifugal impeller. The effect that the coupling has on the performance of a machine is still not entirely clear and is an area where more needs to be done to be able to predict this impact. The overall speedline data point density for the vaneless case was greater than that of the vaned cases and there was no difficulty in determining impeller TEIS values. The TEIS values from the vaneless speedlines were then used to guide Easy Control in data matching the impeller for cases where the vaned build did not yield rational results.

4.1.2 Cascade Diffuser Builds

The cascade database consists of 130 speedlines and is larger than that of the channel database. Greater uncertainty exists, however, in the elicited values of η_{a5} and η_{b5}. The greater uncertainty is a result of a lack of measured static pressures at the diffuser vane leading and trailing edges. For the cascade diffuser database the measured

pressures do not include the intermediary pressures P_3 and P_4. It is therefore necessary to model the pressure between the impeller exit pressure, P_2, and the diffuser exit pressure, P_5. The pressures at station 3 and 4 (see Figure 4-1) are modeled by the Time Cyclic vaneless diffuser model and the TEIS model respectively. This fact allows for error to propagate into the calculations for η_{a5} and η_{b5}. The actual amount of the error present in the data reduction is unknown because no set of data with pressure measurements at station 3 is available for error calculations. The impeller and vaneless diffuser models used in this study have been shown to be quite good [4, 7, 12] and yield some confidence in the calculations performed.
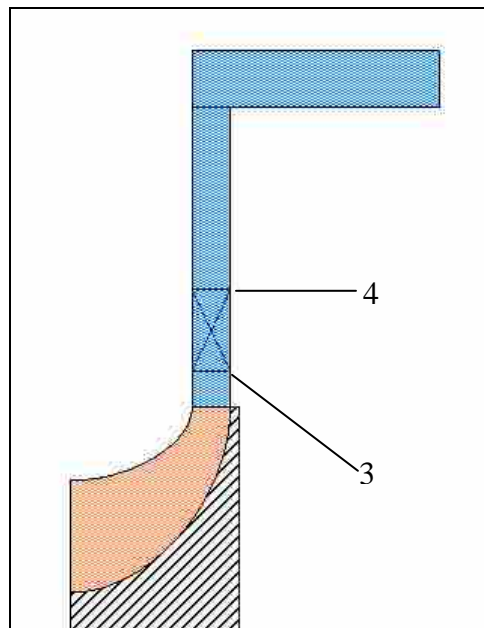
Figure 4-1. The locations of station 3 and station 4 are illustrated on a cascade diffuser build schematic. The X on the schematic illustrates the location of the airfoil cascade diffuser vanes.

4.2 χ_5 Modeling

Initial data matching results for χ_5 were discouraging. Results returned from Easy Control were inconsistent between speedlines for the same machine. Further the χ_5 values were not near expected magnitudes. It was evident from these inconsistent χ_5 values in the data matches that not enough information could be gleaned from the data to determine a unique, sensible χ_5 for each speedline in the database. Upon further examination of the results, it was found that the values were also inconsistent for different speedlines of the same compressor build. One of the more dramatic variations had a range from χ_5=0.05 on the low end to χ_5=0.95 on the high end, all for the same machine. The inconsistency in data matching χ_5 in Easy Control is unphysical and needed to be explained. The inconsistency in χ_5 was found to be an artifact of not having total pressure measurements at the inlet to the vaned diffuser. A relationship was observed to exist between the friction coefficient, C_f, in the short vaneless space and the value of χ_5 found through Easy Control. This relationship is shown in Figure 4-2. The figure was created by fixing all input parameters except for χ_5, or the diffuser χ, and C_f, or the coefficient of friction in the vaneless diffuser just after the impeller, in analysis mode and comparing them to the data reduction results by utilizing Easy Control's objective function. The plot shows a surface fit to the objective function values for each combination of χ_5 and C_f. The figure indicates a valley—or optimal variable combinations—exists for certain χ_5 and C_f values. Any combination of the two could be a match that Easy Control would consider optimal. This relationship is due to not having high quality traverse data wherein an additional constraint on the modeling can be imposed.
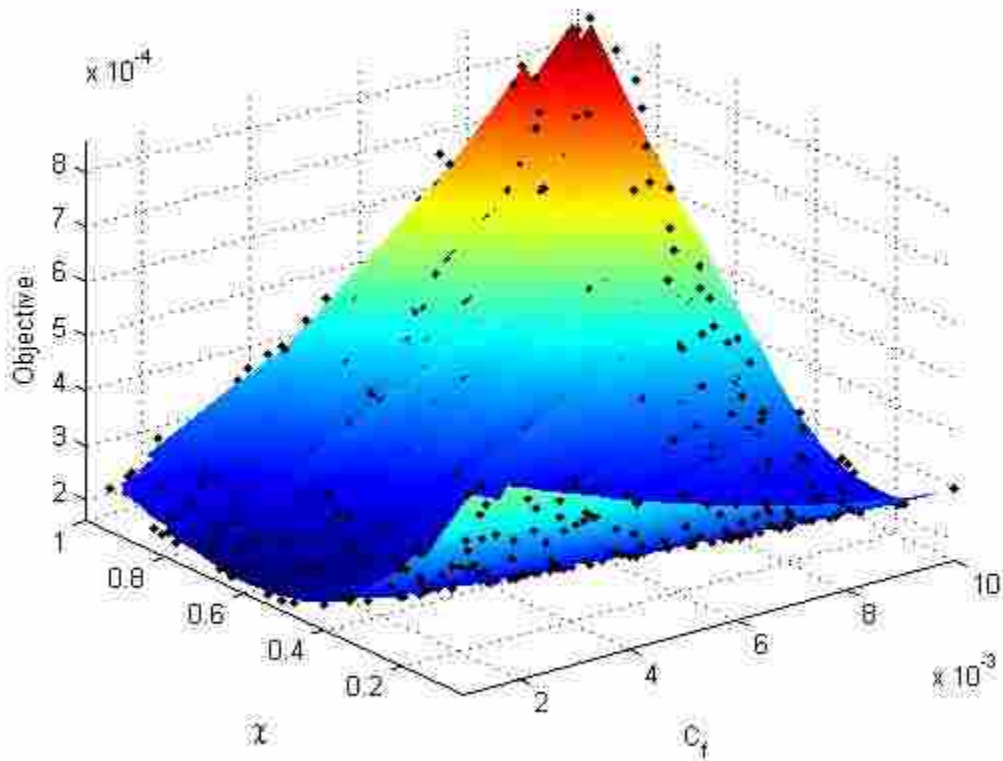
Figure 4-2. The design space for χ_5 and vaneless C_f is shown to have a relationship. A number of combinations can conceivably be used to match the analysis to the data.

To solve the problem and get physical results it is necessary to constrain one of the two parameters, χ_5 and C_f. The average coefficient of friction in the vaneless space, C_f, is a very difficult quantity to measure and was not measured for any cases in the database. It is a quantity that is deduced in data reduction, the value chosen ensures the model calculations match pressure measurements [14]. Therefore, it was necessary to take a different, more classical approach to determining how much secondary flow is present in the passage. To do this the definition of χ_5 is revisited.

$$\chi_5 = \frac{m_{\text{sec}}}{m_{tot}} = \frac{\left(\int \rho C dA\right)_{\text{sec}}}{\left(\int \rho C dA\right)_{tot}}$$

(4-1)

In this equation m_{sec} is the secondary mass flow, all loss laden or non-isentropic flow, and m_{tot} is the total mass flow present in the channel passage. One needs to know the change of density and velocity as functions of area to explicitly calculate the integrals. Assuming ρ is constant across a diffuser cross-section, the secondary mass flow calculation then becomes

$$\left(\rho \int CdA\right)_{sec} = \rho \int_0^{\delta} CdA \qquad \text{(4-2)}$$

where δ is the boundary layer thickness where $C/C_{\infty}=0.99$ where C_{∞} is the velocity at the edge of the boundary layer. This is simplified by using the following relation

$$\int_0^{\delta} CdA = C_{\infty}\left(\delta - \delta_1\right) \qquad \text{(4-3)}$$

where δ_1 is the displacement thickness. Evaluation of the integral above depends on how accurately the boundary layer growth through the passage can be modeled. A representation of what the secondary flow might be like, assuming equal boundary layer growth on all sides of the channel, at a slice along a diffuser passage is shown in Figure 4-3. The figure shows a representation of the flow present in a vaned diffuser with the secondary flow represented as the hatched area and the primary or isentropic flow as the white center. In the figure, B represents the channel height and W represents the channel width.

The results of Equation 4-3 are applied to the diffuser assuming the boundary layer grows at the same rate on all walls in the diffuser. This results in the following equations, again where B is the channel height and W the channel width:

$$\left(\int CdA\right)_{sec} = 2B\int_0^\delta Cdy + 2W\int_0^\delta Cdy - 4\delta\int_0^\delta Cdy \qquad \textbf{(4-4)}$$
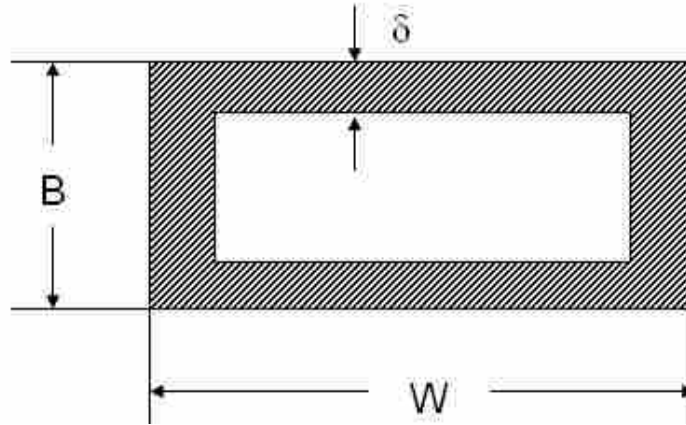
Figure 4-3. A simple representation of boundary layer flow in a single channel diffuser passage. The assumption is made that the boundary layer (δ) grows at the same rate on all sides of the diffuser passage.

$$\left(\int CdA\right)_{sec} = C_\infty(\delta - \delta_1)(2B + 2W - 4\delta) \qquad \textbf{(4-5)}$$

$$\left(\int CdA\right)_{tot} = \left(\int CdA\right)_{sec} + C_\infty(W - 2\delta)(B - 2\delta) \qquad \textbf{(4-6)}$$

The final calculation for χ_5 simplifies to a simple ratio of Equations 4-6 and 4-7 and involves only boundary layer and geometric quantities.

$$\chi_5 = \frac{(\delta - \delta_1)(2B + 2W - 4\delta)}{(\delta - \delta_1)(2B + 2W - 4\delta) + (W - 2\delta)(B - 2\delta)} \qquad \textbf{(4-7)}$$

Determining boundary layer growth in the diffuser is not trivial. The boundary layer is developing in a turbulent flow with an adverse pressure gradient and is susceptible to separation. The calculation of the boundary layer quantities and separation location in diffusing flows has long been a problem of concern [19]. One approach to this calculation stands out because of the accuracy that has been demonstrated. This approach was developed by Bardina [20].

The method presented by Bardina gives accurate prediction of boundary layer growth for three diffuser flow regimes: un-stalled flow, transitory stall, and fully developed stall. Only two of the three would be applicable in this study, there is no attempt in this study to model fully stalled flow. Bardina's work involved more than merely calculating boundary layer quantities but used these calculations to evaluate diffuser performance. Only the boundary layer calculation will be discussed here. The model uses the following non-dimensional coordinates that simplify boundary layer computations.

$$\Lambda = \frac{\delta_1}{\delta} \qquad \text{(4-8)}$$

$$h = \frac{H - \delta_1}{H} = \frac{\delta_1 - \delta_2}{\delta_1} \qquad \text{(4-9)}$$

In these equations Λ is the boundary layer blockage fraction, H is the classical shape factor (δ_1/δ_2) and h is another form of shape factor. Coles [21] demonstrated that there is

a nearly linear relation between these variables that exhibits weak dependant on the Reynolds number as shown in the following equations:

$$\frac{h}{\Lambda} = 1.5 + 0.179\frac{V_T}{\Lambda} + 0.321\left(\frac{V_T}{\Lambda}\right)^2 \qquad \textbf{(4-10)}$$

$$\frac{V_T}{\Lambda} = \frac{1/\Lambda - 2}{0.05 + \ln\left(\kappa\,\text{Re}_{\delta_1}\right) - \ln|V_T/\Lambda|} \qquad \textbf{(4-11)}$$

Where V_T is the non-dimensional shear velocity ($V_T = C_\tau/\kappa C$), $\text{Re}_{\delta 1}$ is the Reynolds number based on the boundary layer displacement thickness, δ_1, and κ is the Von Karman constant with value of 0.41. Bardina's calculations combine these equations 4-10 and 4-11 with conservation of mass, the classical Von Karman momentum integral equation,

$$\frac{W}{\delta_2}\frac{d\delta_2}{dx} + \left(2 + H + \frac{\xi H}{\Lambda}\right)\frac{W}{U_\infty}\frac{dC_\infty}{dx} = \frac{C_f}{2}\frac{H}{b_k} \qquad \textbf{(4-12)}$$

where b_k is a blockage factor, ξ is a constant that has two different values, 0 for attached flows and 0.0015 for detached flows, and x is the diffuser coordinate beginning at the passage throat and ending at length L. The entrainment correlation of Bradshaw [22] is also used to simplify the calculations.

$$\frac{d}{dx}Q = \frac{d}{dx}C_\infty(\delta - \delta_1) = \frac{10\tau_{\text{max}}}{C_\infty} \qquad \textbf{(4-13)}$$

Here dQ/dx is the entrainment and τ_{max} is the maximum shear stress in the boundary layer.

These 5 equations, equations 4-10—4-13 and conservation of mass, are combined to form two ODE's that are solved for two unknowns; the passage blockage, b_k, and the boundary layer blockage fraction, Λ. The two ODE's are:

$$a_{11}\frac{db_k}{dx} + a_{12}\frac{d\Lambda}{dx} = b_1 \tag{4-14}$$

$$a_{21}\frac{db_k}{dx} + a_{22}\frac{d\Lambda}{dx} = b_2 \tag{4-15}$$

where the coefficients a_{11}, a_{12}, a_{21}, a_{22}, b_1, and b_2 are defined below. They are dependent on b_k, Λ, V_T, h, and the constant ξ.

$$a_{11} = \frac{1}{b_k(1-2b_k)}\left[1-h+JV_T+2b_k\left(2-h+\frac{\xi}{\Lambda}\right)\right] \tag{4-16}$$

$$a_{12} = -1.5 + 0.321\frac{V_T^{\,2}}{\Lambda} = J\left(\frac{V_T}{\Lambda}-2\right) \tag{4-17}$$

$$b_1 = \frac{2}{b_k W}\frac{C_f}{2} + \frac{2\theta}{W}\left[2-h+\frac{\xi}{\Lambda}\right] \tag{4-18}$$

58

$$a_{21} = \frac{1}{b_k(1-2b_k)}$$

(4-19)

$$a_{22} = \frac{1}{\Lambda(1-\Lambda)}$$

(4-20)

$$b_2 = \frac{\Lambda}{b_k W(1-\Lambda)} \frac{10\tau_{max}}{\rho C_\infty^2}$$

(4-21)

$$J = \frac{0.642 + 1.79\left(2.005 + \ln\left(\kappa Re_{\delta_1}\right)\right) + \left(0.179 - 0.642\left(0.05 + \ln\left(\kappa Re_{\delta_1}\right)\right)\frac{V_T}{\Lambda}\right)}{\left(1.05 + \ln\left(\kappa Re_{\delta_1}\right)\right)^2}$$

(4-22)

In the above, θ is the divergence angle between the diffuser vanes—the amount the vanes deviate from being parallel to each other.

The inlet blockage, a necessary input to the Bardina model, is calculated using a correlation between the vaneless space pressure recovery coefficient and the blockage at the diffuser throat as shown in Figure 4-4. A correlation was created to fit the data shown in the figure and allow for easy blockage calculation. It would be better to have a more general correlation for diffuser inlet blockage which would account for other effects that impact throat blockage in vaned diffusers, such as inlet blade angle. However, this correlation has been used for decades with workable results and for this study, determining initial correlations for the TEIS and Two Zone input parameters, it was beyond the scope of the project and was left for future study. The throat blockage found from the correlation is the blockage for the entire throat. Bardina's model calculates the

boundary layer values along a single wall. From the throat blockage it is then possible to

calculate the average boundary layer displacement thickness as a function of streamwise
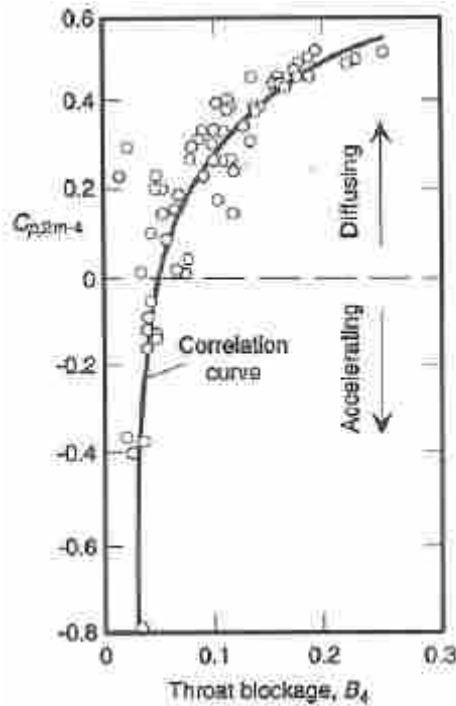
Figure 4-4. Throat blockage, B_4, correlated with pressure recovery coefficient in the vaneless space, C_{p2m-4}. This correlation is used to provide the input blockage for the Bardina model [4].

position in the diffuser for a single wall. This throat blockage is the only flow dependant

input to the Bardina model, the rest of the inputs are geometric and known. With the inlet

conditions known, the system of equations can be solved at the inlet and at each step

through the diffuser. This closes the equations and allows for χ_5 to be calculated. This is

currently done outside of COMPAL in a user defined program and fed into COMPAL

through an external link. The code written to accomplish this is included in Appendix A.
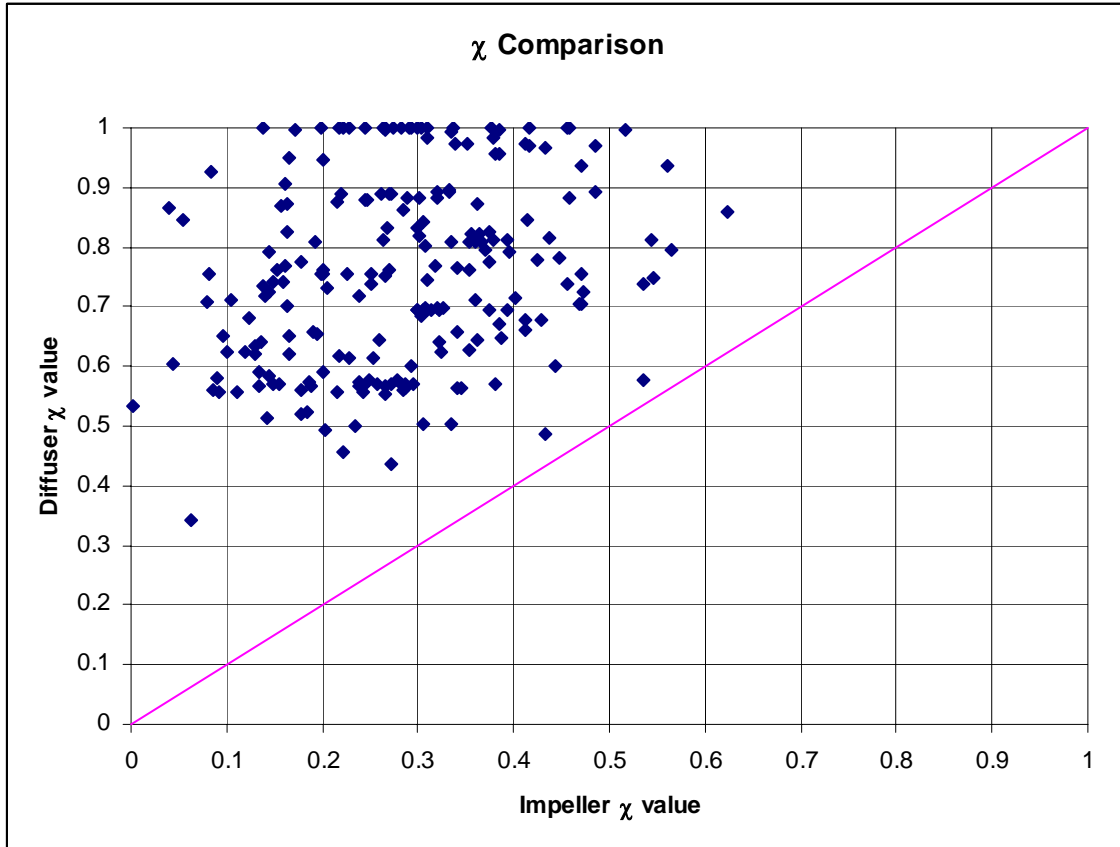
Figure 4-5. The cascade and channel diffuser χ_5 values calculated using the Bardina model plotted against the impeller χ_2 value.

Figure 4-5 illustrates the χ_5 values returned from the Bardina model. The χ_5 values are plotted against χ_2 (impeller) values; the diagonal line indicates that the χ value for the impeller and the diffuser would be equal. All of the values are physical and rational for the geometry of each respective case. As it can be seen, all of the χ_5 values are lower than the χ_2 values. There is not any conclusive evidence that indicates that this should be so for all diffuser cases. In fact, arguments can be made that would indicate that the diffuser value could be lower. This is an item that would require further study and traverse measurements at the impeller and diffuser exits to confirm any theories formulated.

Table 4-1. Results of the sensitivity study on χ_5. All variables were fixed except for χ_5 (varied from 0.75 to 0.95) and the change in the stage efficiency and pressure ratio were taken to determine the impact uncertainty in χ_5 produces in the total stage modeling.

Compressor Build #	Δ Stage Efficiency	Δ Stage Pressure Ratio
Build 1	0.790	0.526%
Build 2	0.865	0.558%
Build 3	1.118	0.718%
Build 4	0.138	0.065%
Build 5	0.808	0.519%
Build 6	0.693	0.462%
Build 7	0.603	0.386%
Build 8	0.787	0.519%
Build 9	2.604	0.967%
Build 10	2.763	1.245%
Average	1.117	0.596%

Because there is a lack of detailed traverse data to corroborate the values χ_5 received using the aforementioned method, a sensitivity study was performed. The sensitivity study was performed in COMPAL by holding all modeling inputs constant except for χ_5. The stage efficiency and pressure ratio were recorded across the entire speedline at two separate values of χ_5, 0.75 and 0.95, for 10 different compressor builds (two speedlines for each build for a total of 20 speedlines). This was done to determine how dependant the data match is on the χ_5 value used in diffuser modeling. The results to the study are shown in Table 4-1. There are three columns in the table; the first is a compressor build number, the second and third are the average change in the stage efficiency and stage pressure ratio across two speedlines as χ_5 changed from 0.75 to 0.95. The stage pressure ratio is presented as a percent of the actual value while the stage efficiency change is the difference in points of efficiency. The final row is an average of all the values for the 10 different compressor builds. For a change in χ_5 of 0.25, the prediction of stage efficiency varies on average by 1 point and the stage pressure ratio

less than 1%. These changes are not negligible but are relatively small for a rather large change in χ_5. An uncertainty in χ_5 of 0.25 is much larger than expected. However, even if such a large error in χ_5 exists, its influence on the stage efficiency and pressure ratio is not entirely unacceptable.

4.3   Channel Models

4.3.1 η_{a5} Modeling

The variables used in building a model for η_{a5} were normalized in the manner previously described. To do so required the standard deviation and the mean of the variable from the database. The final η_a model contained a total of 6 variables. Each variables name, mean, and standard deviation is listed in Table 4-2.

Some of the variables used may not be familiar and need to be defined. The inlet blade angle, α_{3b}, was taken with respect to the meridional plane. There is not as much variation in this variable as desired for modeling, as evidenced by the standard deviation, but the values are limited primarily because the designer does not want a great deal of incidence and blades for each build are typically designed to meet this requirement.

Table 4-2. The symbol, definition, mean and standard deviation for each variable used in the empirical equation for η_{a5} is presented.

Symbol	Variable Definition	Mean	Standard Deviation
$Cos(\alpha_{3b})$	Diffuser Inlet Blade Angle	0.345	0.052
AS_2	Impeller exit aspect ratio (Equation 4-23)	0.543	0.131
Ro_{CA}	Rossby Number(C,A) (Equation 4-25)	3.570	0.607
R_5/R_2	Diffuser Radius Ratio	2.160	0.384
AR_b	Area Ratio b (Equation 4-24)	2.755	0.624
L/W_{ex}	Diffuser Length to channel exit width ratio	5.928	2.424

The impeller exit aspect ratio, AS_2, Rossby Number (C, A), Ro_{CA}, and Area Ratio b, AR_b, are defined in the next three equations.

$$AS_2 = \frac{B_2}{W_2} \tag{4-23}$$

$$AR_b = \frac{A_2}{A_{th}} \tag{4-24}$$

$$Ro_{CA} = \frac{C_1 + C_{2m}}{2} \frac{60}{N * rcr_{rms}} \tag{4-25}$$

B_2, W_2, A_2, and A_{th} are the impeller exit height, impeller exit width, area at the exit of the impeller, and the area at the impeller throat respectively. In the above equations N is the rotational speed of the impeller, rcr_{rms} is the root-mean-square radius of curvature for the impeller, C_1 is the impeller inlet velocity with respect to a stationary reference frame, and C_{2m} is the velocity at the exit of the impeller after the primary and secondary flow mixing calculation has been performed, again with respect to the stationary reference frame. The other two variables in Table 4-2 are ratios as given in the table. They are the diffuser radius ratio, diffuser exit radius divided by the inlet radius value, and the diffuser length to width ratio, the linear length of the diffuser vane divided by the inlet channel width. All six variables are rational quantities one would expect, from a fundamental point of view, to have an impact on inlet effectiveness, or η_{a5}. The data modeling process yielded the following equation for η_{a5}:

$$\eta_{a5} = K_1 + K_2 \overline{\cos(\alpha_{3b})} - K_3 \overline{\cos(\alpha_{3b})}^2 - K_4 \overline{(AS_2)}\overline{(Ro_{CA})}$$

$$- K_5 \left(\overline{\frac{r_5}{r_2}}\right) - K_6 \left(\overline{\frac{r_5}{r_2}}\right)^2 + \overline{AR_b}\left[K_7\left(\overline{\frac{L}{W}}\right) - K_8 \overline{\cos(\alpha_{3b})}\right]$$

<div align="right">(4-26)</div>

The constants K_1 through K_5 used in this model are not necessarily the same as the ones used in any other model presented here, but are merely placeholders for the empirically derived constants.

The over bars in the equation are to signify that these variables have been normalized and are not the standard values of the non-dimensional variables indicated. The equation formulation exhibits several aspects of note. 1) The inlet blade angle terms appear to be the first two terms of a series expansion. 2) A similar type of expansion is evident for the diffuser radius ratio term. This is encouraging to see come out of empirical modeling. This may be taken as an indication of the level of information that has been gained from the database data reduction.

Figure 4-6 illustrates the performance of the model in predicting the η_{a5} value found through the data matching process. The ability of the η_{a5} model to predict the data is illustrated in the figure. Each marker represents a single speedline. The dots would fall on the diagonal line if the model exactly predicts the data value. As illustrated in the figure there are two clusters of data shown on the plot. Most of the data has a η_{a5} value of near 0.9. The fact that the information is all close to a single value made it difficult to build a solid empirical model.

Table 4-3. The statistical quantities used to determine model effectiveness for the channel.

Channel η_{a5}	
R^2	0.593835
MSE	0.001632
Standard Error	0.03323
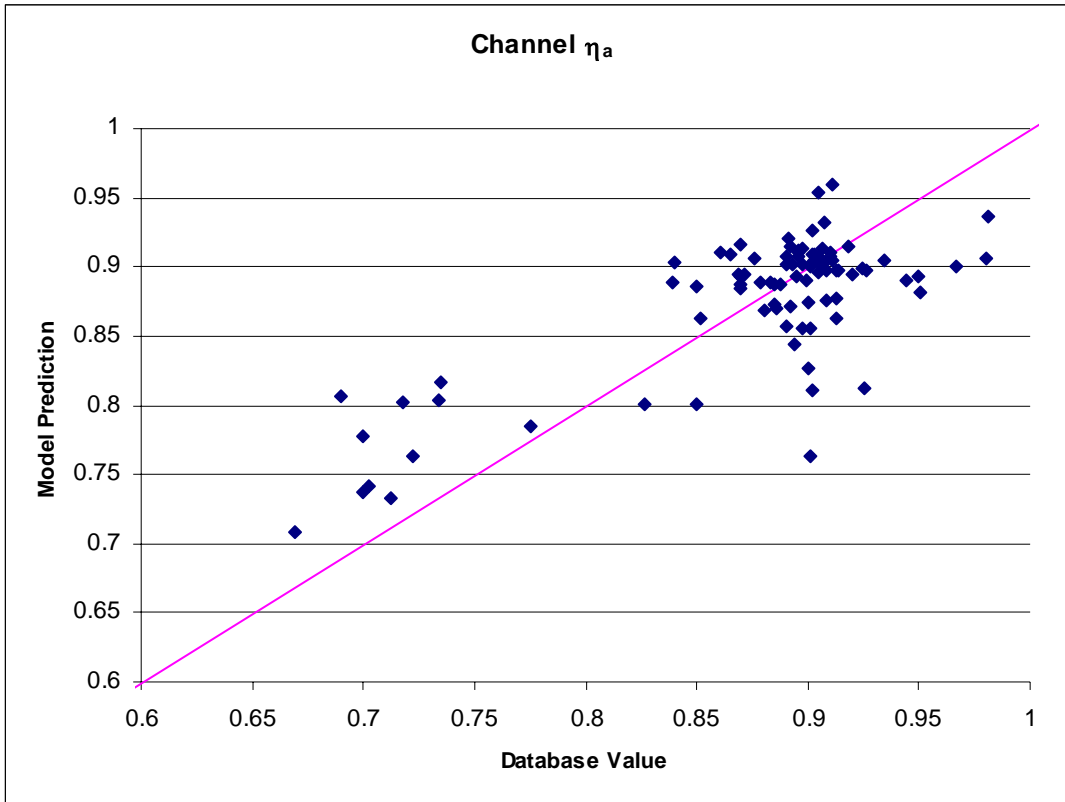
Figure 4-6. η_{a5} **obtained from Equation. 4-26 plotted vs. the database value of** η_{a5} **for the channel diffusers**

The model building for η_{a5} was somewhat successful but more difficult than expected. This quantity has turned out to be one of the most difficult terms to model, for the impeller [7] as well as the diffuser. The data that is regularly measured is static pressure at station locations and an inlet and exit temperature. It can be difficult to fully understand what flow physics may be involved in setting actual η_{a5} values without more

detailed traverses or boundary layer test data. The R^2 value reached in modeling η_{a5} is an indication of the lack of detailed traverse data.

4.3.2 η_{b5} Modeling

All variables used in modeling η_{b5} were normalized in the manner previously described. The final model developed for η_{b5} consisted of 6 variables. The name of each variable, in addition to their mean and standard deviation are listed in Table 4-4.

The following empirical model was made for η_{b5}:

$$\eta_{b5} = K_1 - K_2\left(\frac{\overline{Z_R}}{\overline{AR_{45}}}\right) - K_3\left(\frac{\overline{B_3}}{\overline{B_2}}\right)\left(\frac{\overline{L}}{\overline{W}}\right) + K_4\left[\overline{\cos(\alpha_{3b})}\right]^2 - K_5\left(\overline{Z_D}\right) \qquad \textbf{(4-27)}$$

Once again the over bar on the variables indicates that the variable has been normalized as described previously. The constants K_1 through K_5 used in this model are not necessarily the same as the ones used in any other model presented here, but are merely placeholders for the empirically derived constants.

The scaled variables make it difficult to examine the equation, as can typically be done to see the effect changing one variable would have on the predicted value. An illustration of the effect that scaling the variables has can be seen by looking at the variable Z_D, or diffuser vane number. As this value goes from 27 vanes to 28 vanes the contribution of the final term in the equation goes from a negative to a positive value. This term cannot be changed, however, without incurring change in other variables as well. The diffuser L/W and AR_{45} will also change having their own effect on the

equation—the effect is determined from the value in the design relative to the mean of the model building database.

Table 4-4. The symbol, definition, mean and standard deviation for each variable used in the η_{b5} empirical model for channel diffusers.

Symbol	Variable Definition	Mean	Standard Deviation
Z_R	Impeller Exit Blade Number	19.980	3.353
AR_{45}	Area Ratio Station 4- 5(excluding vane exit width)**	4.841	1.065
B_3/B_2	Vaneless Pinch	0.982	0.081
L/W_{ex}	Diffuser Length to channel exit width ratio	5.928	2.424
$Cos(\alpha_{3b})$	Diffuser Inlet Blade Angle	0.345	0.052
Z_D	Diffuser Blade Number	27.277	11.018

The physics captured by the variables used in the model for η_{b5} are more easily understood than many of those in the η_{a5} model, even for one relatively unfamiliar with radial compressor variables. The diffuser inlet blade angle and the diffuser length to width ratio have been previously described in the model for η_{a5}. The number of blades for both the impeller exit, Z_R, and the diffuser, Z_D, are easily understood and need no further definition. There are only two that need further defining: the vaneless pinch ratio, B_3/B_2, and the area ratio from stations 4 to 5, AR_{45}. B_3/B_2 is the ratio of passage heights at the inlet to the diffuser and the exit of the impeller. These heights are often not the same. In vaneless diffusers the vane height is often decreased after leaving the impeller to impede the onset of vaneless stall [4]. This was done in several of the builds contained in the database. The other variable of interest, AR_{45}, takes the form of the area at station 5,

---

* This area ratio is not the typical area ratio. Due to an error in the code output the area at station 5 neglected the exit blade width. The area at station 5 was simply $2\pi r_5^2$.

68

the diffuser exit, over the area at station 4 (the diffuser throat, or minimum area in the diffuser).

Table 4-5. The statistical quantities used to determine model effectiveness are listed in the table. The MSE, Standard Error, and R^2 values are at an encouraing levels .

Channel η_{b5}	
R^2	0.838525
MSE	0.002154
Standard Error	0.039678
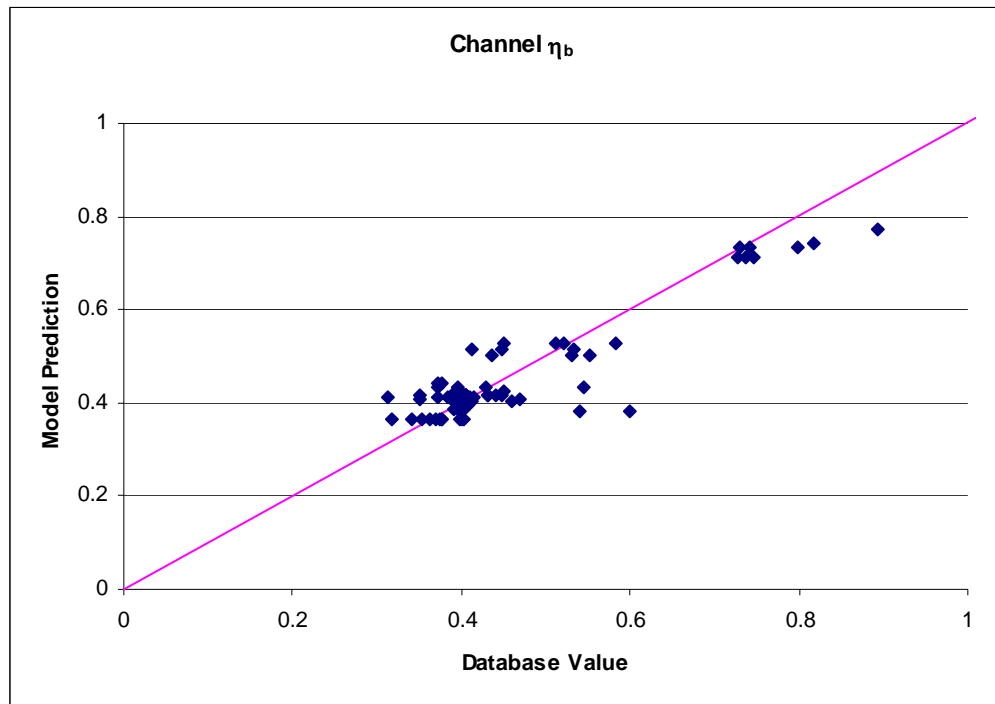
Figure 4-7. η_{b5} obtained from Equation. 4-27 plotted vs. the database value of η_{b5} for the channel diffusers

The effectiveness of the η_{b5} model was determined by the MSE value shown in Table 4-5. The MSE and the standard error are 0.00215 and 0.0397 respectively. These values give and indication of what kind of error to expect, on average, between the database value and the value predicted by the model. They indicate that the average error

expected is around 0.04, the standard error value and the square root of the MSE yield approximately the same value.

A graphical representation of the ability of the model to mach data values is shown in Figure 4-7. This shows the data reduction values of η_{b5} plotted against the empirical models prediction of the same. The markers would fall on the diagonal line if the model exactly predicts the data value. An Interesting observation can be made from the figure; at several locations there exists a horizontal line of dots. This horizontal line is an artifact of the model having only geometric variables and was not anticipated at the outset of model building. Without any fluid dynamic variables present in the model, the empirical model predicts the same η_{b5} value for multiple speedlines of the same compressor build. It is expected that when more data is added to the database, fluid dynamic dependencies will become prominent enough where they can pick up some of this variation.

4.3.3 δ_{5p} Modeling

The deviation of the primary flow from the blade at the diffuser exit for channel types of geometry were expected to be very small and this was confirmed by the results that were derived from Easy Control. In some cases the primary zone is negligibly small, corresponding to $\chi_5 = 1$. At this condition the value of δ_{5p} is identically zero—i.e. there is no primary zone and therefore no deviation. The results from Easy Control were generally small enough such that, for the final evaluation of the database, the value of δ_{5p} was fixed at zero. This value matched the output obtained from data reduction very well,

75% of the cases data showed deviation angles less than one degree and over 96% of all cases exhibited a deviation of less than 2 degrees.

4.4   Cascade Models

The modeling of the cascade diffusers was performed in a different manner than has been historically done. Many of the cascade diffuser modeling variables were chosen are more typical of channel diffusers. There is value to looking at the diffuser this way and much can be learned about the similarities and differences between the two types of diffusers.

4.4.1 η_{a5} Modeling

The empirical model built for η_{a5} was based on a total of 130 data points. Each data point corresponds to the maximum efficiency of each speedline. The variables output at the maximum efficiency point were normalized as discussed previously prior to use in empirical model building. The approach discussed before was employed and the final model is shown in Equation 4-28.

$$
\begin{aligned}
\eta_{a5} = {} & \mathrm{K}_1 - \overline{M_3}\left[\mathrm{K}_2 + \mathrm{K}_3\left(\overline{\frac{r_5}{r_2}}\right)\right] - \overline{\gamma_2}\left[\mathrm{K}_4 + \mathrm{K}_5(\overline{AR_b})\right] \\
& + \mathrm{K}_6\left(\overline{CP_{23}}\right)\left(\overline{\frac{Clr}{B_2}}\right) + \left(\overline{\frac{r_5}{r_2}}\right)\left[\mathrm{K}_7\overline{\cos(\alpha_{5b})} + \mathrm{K}_8\overline{\cos(\alpha_{3b})}\right] \\
& + \mathrm{K}_9\left(\overline{Ro_{CA}}\right)\left(\overline{E}\right) + \mathrm{K}_{10}\left(\overline{CPI_{23}}\right)\left(\overline{\frac{Z_D}{Z_R}}\right) + \mathrm{K}_{11}\left(\overline{CPI_{45}}\right)^2
\end{aligned}
\tag{4-28}
$$

The constants K_1 through K_{11} used in this model are not necessarily the same as the ones used in any other model presented here, but are merely place holders for the empirically derived constants. The above model is more complicated than the one created for the channel database with a total of 13 variables being used, the maximum number allowed for the database size. A list of the variables and values of mean and standard deviation for each is given in Table 4-6. The channel diffuser model (Equation 4-26) and Equation 4-28 share four common variables. These variables are the diffuser inlet blade angle, α_{3b}, diffuser radius ratio, r_5/r_2, Rossby Number, Ro_{CA}, and the area ratio, AR_b. It is encouraging to see a number of the same variables used in predicting η_{a5} for both types of vaned diffusers, indicating the capturing of similar physics between the two types of vaned diffusers. The inlet portion is quite similar between the two diffuser types and it is thus expected to find that there are similarities between the two models.

Table 4-6. The symbol, variable definition, mean and standard deviation for each variable used in the empirical equation for cascade η_{a5} is listed.

Symbol	Variable Definition	Mean	Standard Deviation
M_3	Mach Number at Diffuser Inlet	0.673	0.152
r_5/r_2	Diffuser Exit Radius/ Diffuser Inlet Radius	2.173	0.310
γ_2	Impeller Slip Factor	0.893	0.025
AR_b	Area Ratio b	2.204	0.628
CP_{23}	Pressure Recovery Coefficient 2-3	0.143	0.113
Clr/B_2	Tip Clearance Impeller Exit/Vane Height	0.052	0.010
$Cos(\alpha_{5b})$	Diffuser Exit Blade Angle	0.564	0.111
$Cos(\alpha_{3b})$	Diffuser Inlet Blade Angle	0.210	0.090
Ro_{CA}	Rossby Number(C,A)	4.172	1.063
E	Secondary Flow Area/Total Flow Area	0.500	0.152
CPI_{23}	Ideal Pressure Recovery 2-3 (Equation 1-2)	0.609	0.825
Z_D/Z_R	Diffuser Blade Number/Impeller Blade Number	0.703	0.211
CPI_{45}	Ideal Pressure Recovery 4-5 (Equation 1-5)	0.655	0.221

Some of the variables in Table 4-6 have not yet been defined such as the impeller slip factor, γ_2. This is a different way of treating deviation and describes the same phenomena. The term 'slip factor' comes from its application in relative velocity triangles to get the fluid flow angle correct at the impeller exit. Many different ways have been proposed for calculating this parameter. For this study it is calculated using the following relation

$$\gamma_2 = 1 - \frac{\sqrt{\cos\beta_{2b}}}{Z_R^{0.7}} \tag{4-29}$$

Another variable that has not been discussed is the vaneless space pressure recovery coefficient, CP_{23}. This is the classical definition of the pressure recovery over the inlet dynamic pressure

$$CP_{23} = \frac{P_3 - P_2}{\frac{1}{2}\rho C_2^2} \tag{4-30}$$

The ideal pressure recovery coefficients CPI_{23} and CPI_{45} are of the same form but are calculated using Equations 1-2 and 1-5 respectively.

The final variable that has not previously been defined is secondary flow area ratio, E. This quantity is evaluated at the impeller exit and is very similar to the calculation of χ_2. The difference is that E is an area ratio while χ_2 is a mass flow ratio and is defined

73

$$E = \left(\frac{A_{sec}}{A_{tot}} \right)_2 \tag{4-31}$$

where A_{sec} is the secondary flow area and A_{tot} is the total flow area all evaluated at the

impeller exit or station 2.

Table 4-7. MSE, Standard Error, and R^2 values for the η_{a5} cascade diffuser model.

Cascade η_{a5}	
R^2	0.537846
MSE	0.027864
Standard Error	0.167533
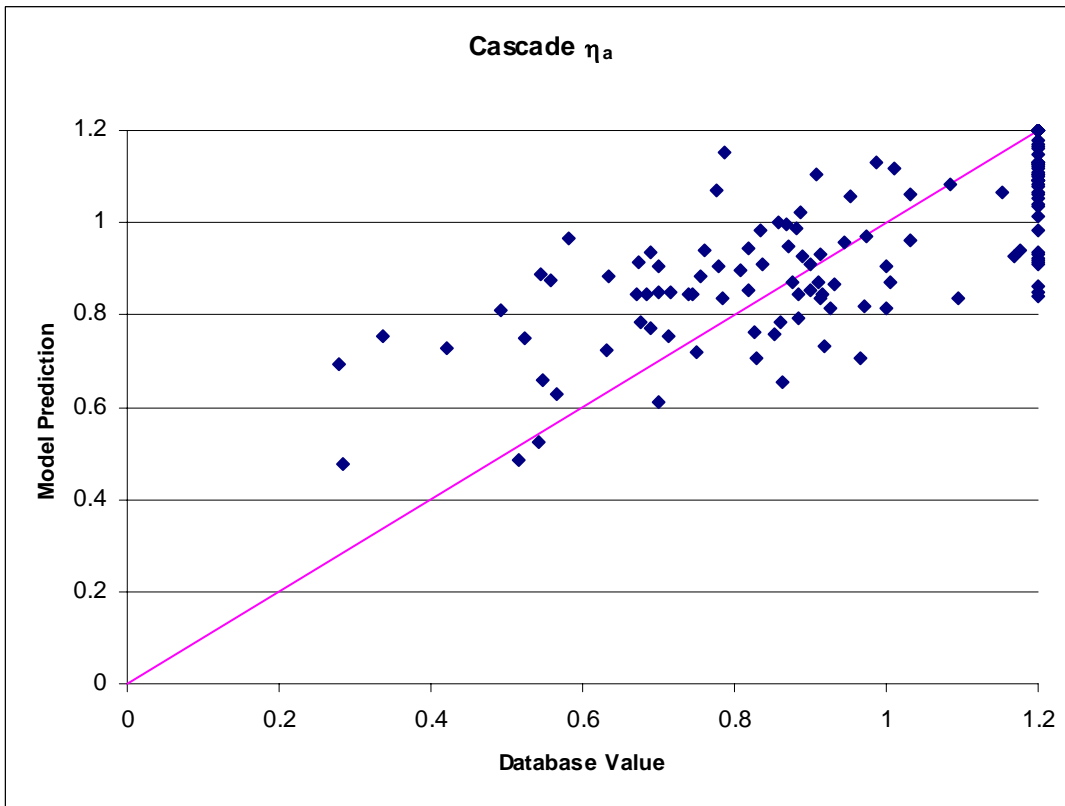
Figure 4-8. η_{a5} **obtained from Equation. 4-28 plotted vs. the database value of** η_{a5} **for the channel diffusers.**

74

Figure 4-8 illustrates graphically the performance of the model and Table 4-7 provides numerical summary of the model performance. Several items of note deserve attention. The numerical value of R^2 is very similar to that of the channel database ~6-7% lower. The MSE and standard error are much lower, however. This is understood as Figure 4-8 is viewed. There is much greater variation in the cascade models prediction of η_{a5} as compared to the database, than in the channel model.

A second item of note is the large collection of values on the right edge of Figure 4-8 where η_{a5}=1.2. The exact cause of this has not yet been determined due to a lack of data, although it is suspected that it is an artifact of insufficient data point density for the speedline being considered. When too few data points are taken along a speedline more uncertainty in determining η_{a5} exists and it is possible that Easy Control was unable to deduce the correct value of η_{a5}. These η_{a5} values of 1.2 would have severely impacted the model, making it impossible to predict reasonable results. In order to not bias the model they were left out of the model building set. The model was built only on the data which yielded η_{a5} values less than 1.2, comprising a total of 81 data points.

4.4.2 η_{b5} Modeling

Similar to the cascade η_{a5} model, the empirical model built for η_{b5} was also built with a total of 130 data points. Each data point is at the maximum efficiency of each speedline. The final model is shown in Equation 4-22.

$$\eta_{b5} = \frac{\overline{r_5}}{r_2}\Big[K_1 + K_2\big(\overline{\gamma_2}\big) - K_3\overline{\cos(\alpha_{5b})}\Big] - \overline{AR_{45}}\Big[K_4\overline{\cos(\delta_{2p})} + K_5\big(\overline{E}\big)\Big]$$

$$- K_6\left(\frac{\overline{B_3}}{B_2}\right)^2 + \overline{M_3}\Big[K_7 - K_8\overline{\cos(\delta_{2p})}\Big] + \overline{NS}\Big[K_9\big(\overline{CPI_{45}}\big) - K_{10}\overline{\cos(\alpha_{3b})}\Big] \qquad \textbf{(4-32)}$$

$$+ \frac{\overline{W_{ex}}}{r_5}\left[K_{11}\overline{\ln(\text{Re}_{23})} + K_{12}\left(\frac{\overline{B_3}}{B_2}\right)\right] + K_{13}\big(\overline{DR_{5I}}\big)\big(\overline{\gamma_2}\big) + K_{14}$$

The constants K_1 through K_{14} used in this model are not necessarily the same as the ones used in any other model presented here, but are merely place holder variables for the empirically derived constants. The above model is the most complicated of all created. A total of 13 variables were used, some multiple times in the equation. A list of the variables and their mean and standard deviation values are given in Table 4-8. There are very few common variables between the cascade and channel models for η_{b5}. The only variable common to both models are the diffuser radius ratio, r_5/r_2, and inlet blade angle, α_{3b}. It is believed that this is a result of the completely different geometry associated with the passage portion of the two different diffusers. There are some obvious differences between the two. Namely, the channel diffuser is long and straight while the cascade diffuser has a short turning passage portion. It is expected that there would be large differences between the two models.

The inclusion of the entire diffuser radius ratio, r_5/r_2, was somewhat a surprise. It was expected that the vaneless diffuser radius ratio, r_3/r_2, the ratio of the vaneless space prior to the vaned diffuser, would have played a more important role in the parameter modeling. This variable did not, however, appear to have a significant impact on the parameter modeling. It could be that this initial linear approach fails to pick up some non-linear affect this value may have.

Table 4-8. The symbol, variable definition, mean and standard deviation for each variable used in the empirical equation for cascade η_{b5} is listed.

Symbol	Variable Definition	Mean	Standard Deviation
r_5/r_2	Diffuser Radius Ratio	2.173	0.310
γ_2	Impeller Slip Factor	0.893	0.025
$Cos(\alpha_{5b})$	Diffuser Exit Blade Angle	0.564	0.111
AR_{45}	Area Ratio Station 4 to 5	2.166	1.387
$Cos(\delta_{2p})$	Impeller Exit Deviation--Primary Zone	0.997	0.001
E	Epsilon	0.500	0.152
B_3/B_2	Vaneless Pinch	0.885	0.026
M_3	Mach Number at Diffuser Inlet	0.673	0.152
NS	Stage Specific Speed	1.802	2.126
CPI_{45}	Ideal Pressure Recovery 4-5 (Equation 1-5)	0.655	0.221
$Cos(\alpha_{3b})$	Diffuser Inlet Blade Angle	0.210	0.090
W_{ex}/r_5	Diffuser Passage Exit Width/Exit Radius	0.292	0.056
$Ln(Re_{23})$	Natural log of the Vaneless Reynolds Number	12.190	0.295
DR_{5l}	Ideal Diffusion Ratio 4-5	2.119	2.401

An artifact of the type of modeling appears in the use of the terms AR_{45} as well as CPI_{45}. These are actually the same term in a different format (see equation 1-5 for $C_{pb,i}$). One could logically replace the ideal pressure recovery with a form of the area ratio; however, this was not done for this presentation.

Table 4-9. The statistical quantities used to determine model effectiveness of η_b for the cascade diffusers

Cascade η_{b5}	
R^2	0.802187
MSE	0.011557
Standard Error	0.088022

The modeling effectiveness quantities for the model are shown in Table 4-9 are R^2, MSE, and standard error. The MSE and standard error have values of 0.0116 and 0.0880

respectively. These are not as low as the values received for the channel model; in fact they are a little over double. This is visible when the model is shown in respect to the data as in Figure 4-9. There is also more variation in the data in the figure than there is in the channel data in Figure 4-7. Again, the data points would fall on the diagonal line if the model exactly predicts the data value. A larger variation is not unexpected with the cascade diffusers as the passage portion is not as highly designed for the purpose of pressure recovery [13]. The ability to match the values of η_{b5} is not as affected by the speedline data point density as they are in matching η_{a5}, although there are some lingering effects. This is because, as described earlier, η_{a5} largely controls the slope of the diffusion ratio curve while η_{b5} largely controls the level. The slope of the curve can be significantly changed by the addition of a point between choke and stall while the level does not change at all. There is some coupling involved between the two parameters and therefore changes in one do affect the other. This is evident from Equation 1-8. Overall the variables in the database showed more ability to account for the variation in the data.
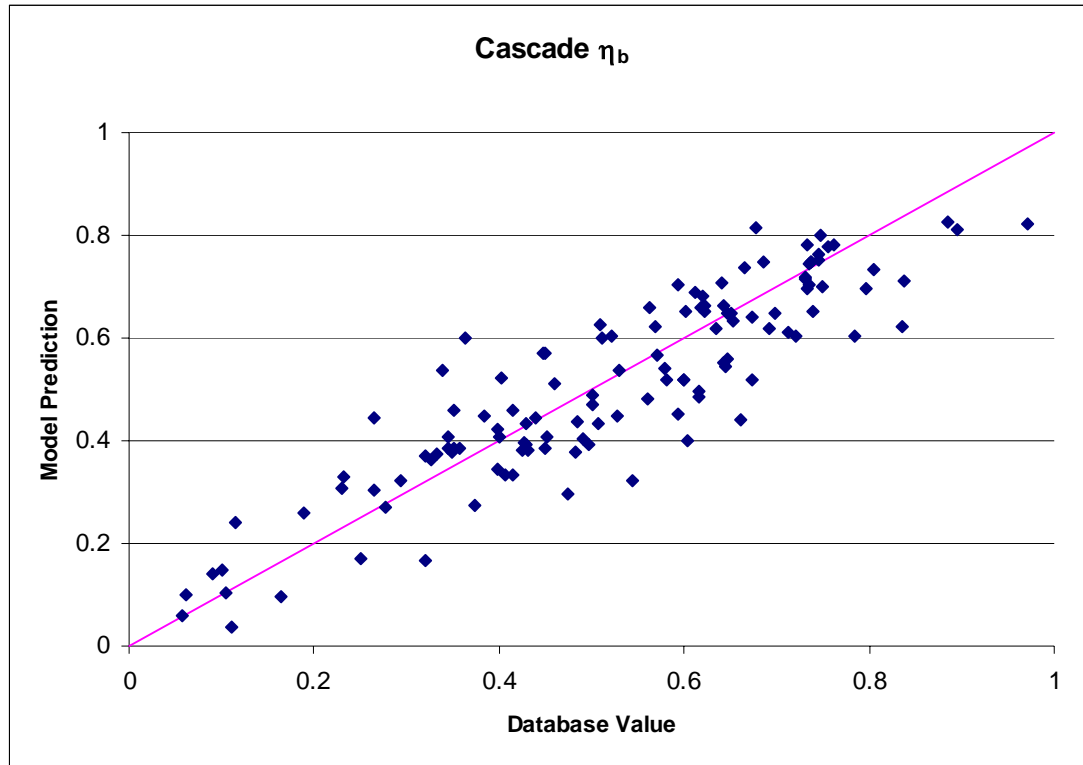
Figure 4-9. η_{b5} obtained from Equation. 4-32 plotted vs. the database value of η_{b5} for the channel diffusers.

4.4.3 δ_{5p} Modeling

Modeling of the deviation angle at the diffuser vane exit proved to be more challenging than initially anticipated. The data matching results returned from Easy Control for δ_{5p} were much like the results received for χ_5. The lack of any consistency in the values returned from the data matching made it evident that information outside of the assembled cascade database would have to be used to formulate an accurate and reliable model.

Upon some further searching with this new focus on cascade deviation angles, literature was found that proved to have a superior model for this given application. This model was created by Seymour Lieblein in 1960 [23]. This model takes the form:

$$\delta_{5p} = \delta_0 + \varphi\left(\frac{m_{\sigma=1}}{\sigma^b}\right) \qquad\qquad \textbf{(4-33)}$$

This equation has a number of new parameters that must be defined. In this equation δ_{5p} is the flow deviation, and δ_0 the zero-camber flow deviation angle or flow deviation when the blade is at zero camber. Camber is the asymmetry that exists between the top and bottom of the blade. This is illustrated in Figure 4-10 where two NACA blades are compared; the NACA 0506 (top) and NACA 6506 (bottom). The airfoil with zero camber (top) is symmetrical about the centerline while the bottom blade is the one used in the cascade database.
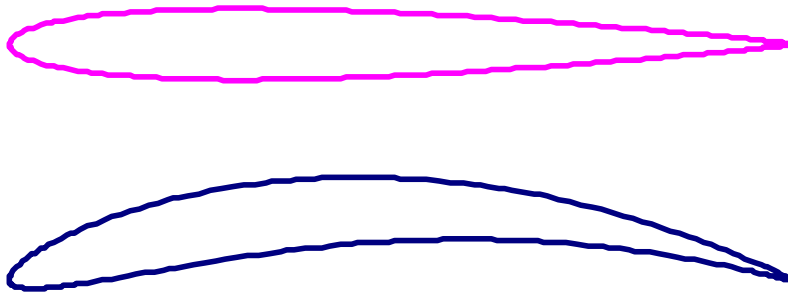
Figure 4-10. NACA 0506 (top) and NACA 6506 (bottom), the airfoil with zero camber (top) is symmetrical about the centerline.

There are still more terms in Equation 4-33 that need to be defined. φ is the blade turning angle or the difference between the inlet and exit blade angles and σ is the cascade solidity which is raised to the empirically determined exponent b. The cascade solidity is defined as the blade chord, or straight line distance from the tip of to the tail of

the blade, divided by the spacing between blades in the cascade. The exponent b was empirically determined by Lieblein. Figure 4-11 shows how the empirical exponent b varies with inlet flow angle, α.
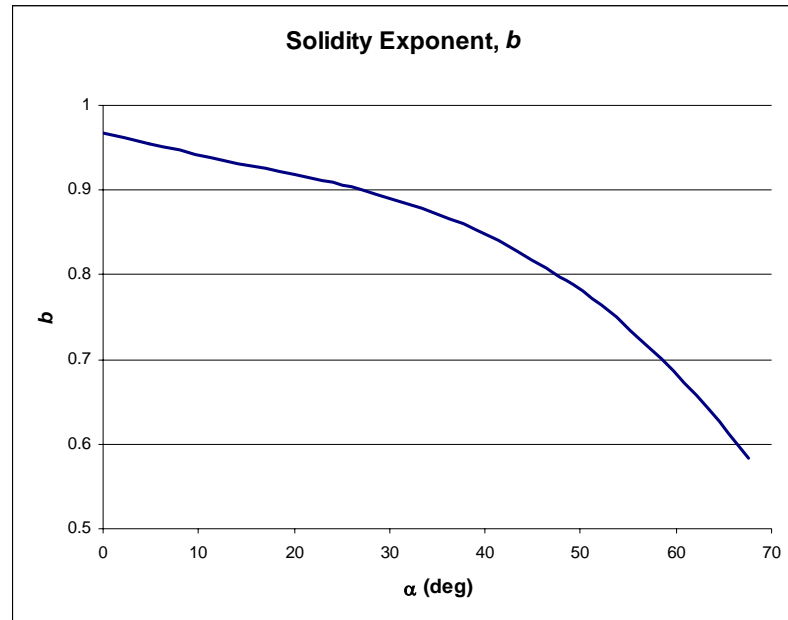
Figure 4-11. Solidity exponent b in deviation angle correlation vs. inlet air angle, α, from data for NACA 65-(A10) series airfoil [21].

The final term in Equation 4-33, $m_{\sigma=1}$, is more complicated to define. The deviation from an airfoil varies as the camber is increased. The term $m_{\sigma=1}$, is the slope of a line fit to the deviation change as the camber is increased for a cascade of solidity equal to 1. Figure 4-12 shows this slope term as a function of inlet flow angle, α.

A plot of the zero camber deviation, δ_0 as a function of inlet flow angle, α, and cascade solidity, σ, is illustrated in Figure 4-13. Figures 4-11—4-13 are presented by Lieblein and were obtained with a data acquisition program. With the inlet air angle, α, known from flow calculations in the vaneless diffuser, Figures 4-11 and 4-12 yield

81

unique values of the slope factor, $m_{\sigma=1}$, and the solidity exponent, b. The cascade solidity is used in conjunction with the inlet flow angle to determine a zero camber deviation for the blade shape. With these three things known the deviation can now be calculated.

Slope Term, $m_{\sigma=1}$
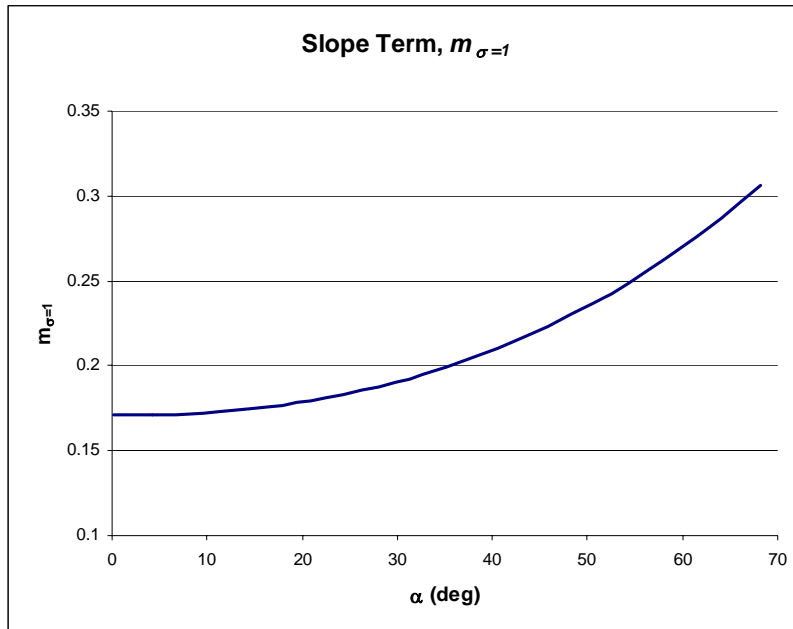
Figure 4-12. Values of slope factor, m, at $\sigma=1$ for determination of deviation angles of NACA 65-(A_{10}) series blades [21].

One thing has not been specified, however. This is at what point along a speedline to calculate the deviation. The deviation model is based on inlet flow angle, which varies for each point along a speedline. For the cases in the database the inlet flow angle varies, on average, 5 degrees across a speedline. Because of the small variation across the speedline, it was determined that little change would be observed by applying the model at different points along the speedline. To remain consistent with the speedline location of the other models, the maximum stage efficiency point was again used.

82
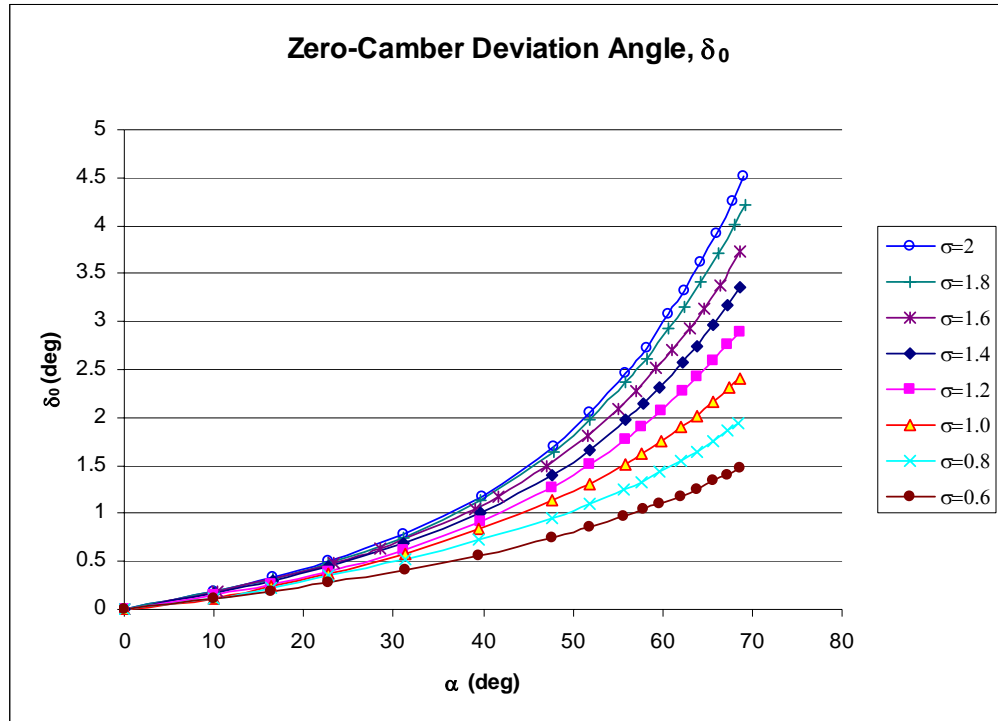
Figure 4-13. Zero-camber deviation angle, δ_0, as a function of inlet air angle, α, and solidity, σ, for NACA 65-(A10) series airfoil [21].

The zero-camber deviation is determined, in part, by the solidity of the cascade. The solidity is not always an integer for which a δ_0 value is easily determined. For this reason a linear interpolation routine was also included to interpolate to a zero-camber deviation that is accurate for any solidity of the given cascade. The code that was written to apply the Lieblein model is given in Appendix A.

4.5 Modeling Performance Evaluation

Overall validation for the database modeling was performed by applying the models to their respective databases and evaluating the predicted performance across the entire speedline. This was done by applying the empirical models in COMPAL using

analysis mode for each speedline in the database. It is understood that applying the models to the databases from which they were built is not a true indication of the performance of the models. However, the size of the databases necessitated that all of the data be used for model building. The models were applied to each speedline while holding the impeller values constant. This makes the impeller, as said in industry, frozen and gives a true indication of the impact of just the diffuser modeling.

The performance of the evaluation of the models was performed using the following steps: 1) the empirical models were used to calculate the TEIS and Two Zone input parameters, 2) these parameters were used in analysis mode to predict machine performance—they were the only inputs changed, all other modeling inputs were left at the optimal values determined by Easy Control, 3) the error between the data reduction and the analysis modes for key quantities were averaged across the entire speedline. It is this difference that is presented to give an indication of model performance along a speedline.

There are a few critical quantities that are representative for how well the diffuser modeling is performing—given that the impeller is frozen. One is the overall total-to-total stage efficiency, η_{tt}, described in Equation 3-1. The term total-to-total refers to the inlet and exit total quantities, rather than static, used in the calculation. Stage total pressure ratio, PR_{tt}, is also a good indication of modeling performance. This is a simple ratio of the calculated exit total pressure over the inlet total pressure. The final quantity examined is the diffusion ratio through the diffuser, DR_5, (Equation 1-7). The diffusion ratio gives an indication of how well the models for η_{a5} and η_{b5} perform. The other two indicators used, η_{tt} and PR_{tt}, yield an aggregate of the performance of all four models

84

combined. These three indicators provide characterization of how well the models are performing and capturing the variable dependencies.

4.5.1 Performance of Cascade Models

The models for η_{a5}, η_{b5}, χ_5, and δ_{5p} were applied to the cascade database in COMPAL as described above. There is a need for iteration on the solver in COMPAL since the η_{b5} model depends on the specific speed, *NS*. *NS* is a stage variable that requires the calculation in the diffuser to be complete prior to its calculation, thus iteration is necessary. The maximum number of iterations observed was four. Although the iteration time is consuming, it is acceptable since the performance gain is significant.

The overall diffuser match is quite good. This is illustrated in Figures 4-14-4-16 by using a histogram format. The number of cases is shown plotted against the average error across the speedline. The first, Figure 4-14, is the error in the total-to-total stage efficiency, η_{tt}, presented where the error is the difference between the analysis total-to-total stage efficiency and the data total-to-total stage efficiency where $\Delta\eta_{tt} = (\eta_{tt,Analysis} - \eta_{tt,Data})$. The models performed well for a majority of the cases. Over 70% of the speedlines in the database fall between under predicting by 2 points of efficiency and over predicting by 4 points of efficiency, on average across a speedline.

Although this performance is not as good as originally hoped, the limitations may be due to uncertainty in the automatic data reduction matching results for η_{a5} and η_{b5}. As discussed earlier, the low speedline data point density as well as insufficient station location measurements for many of the cascade diffuser cases made determining TEIS

and Two Zone input parameter values with high confidence impossible. These are undoubtedly the leading causes for not achieving original expectations.
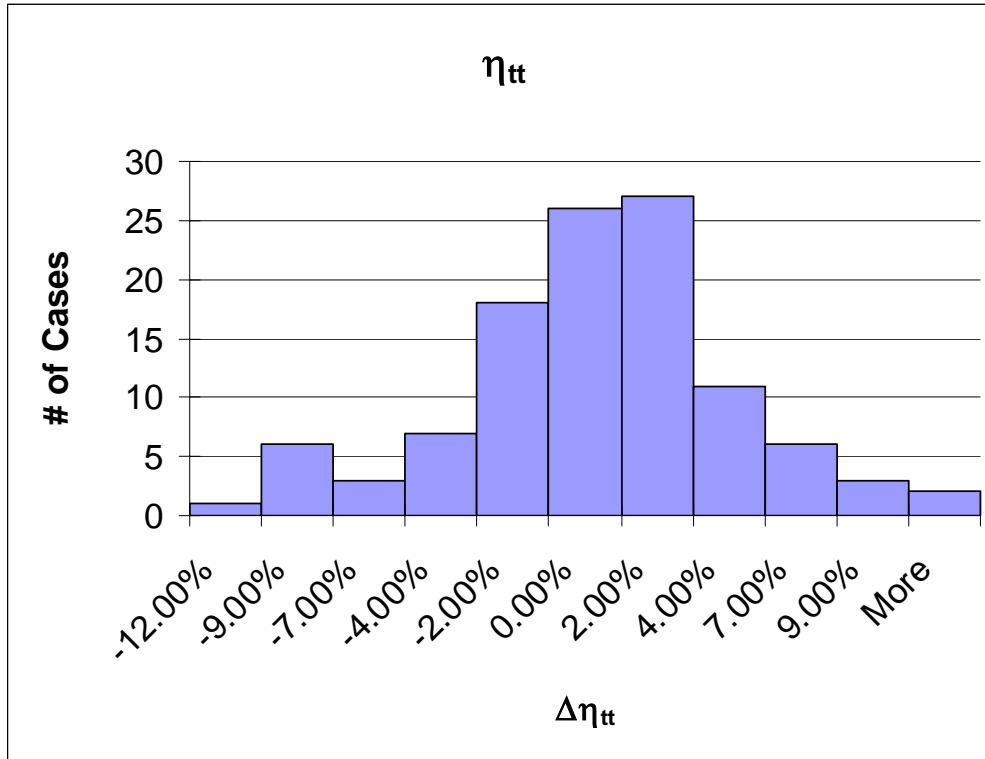
Figure 4-14. The stage efficiency error, averaged across a speedline, ($\eta_{tt,Analysis}$-$\eta_{tt,Data}$) is presented in a histogram format.

Figure 4-15 presents the average error in PR_{tt} in a similar format, with the only change being the manner in which the error is presented. It is presented in percent error where $\Delta PR_{tt}=(PR_{tt,Analysis}-PR_{tt,Data})/PR_{tt,Data}$. The average error is similar to that found for η_{tt}. Over 70% of the speedlines are between -2% and 4% error. The typical PR_{tt} for speedlines in the database has a magnitude between 1.7 and 3.0. This makes the average difference between the data reduction and analysis pressure ratios quite small.
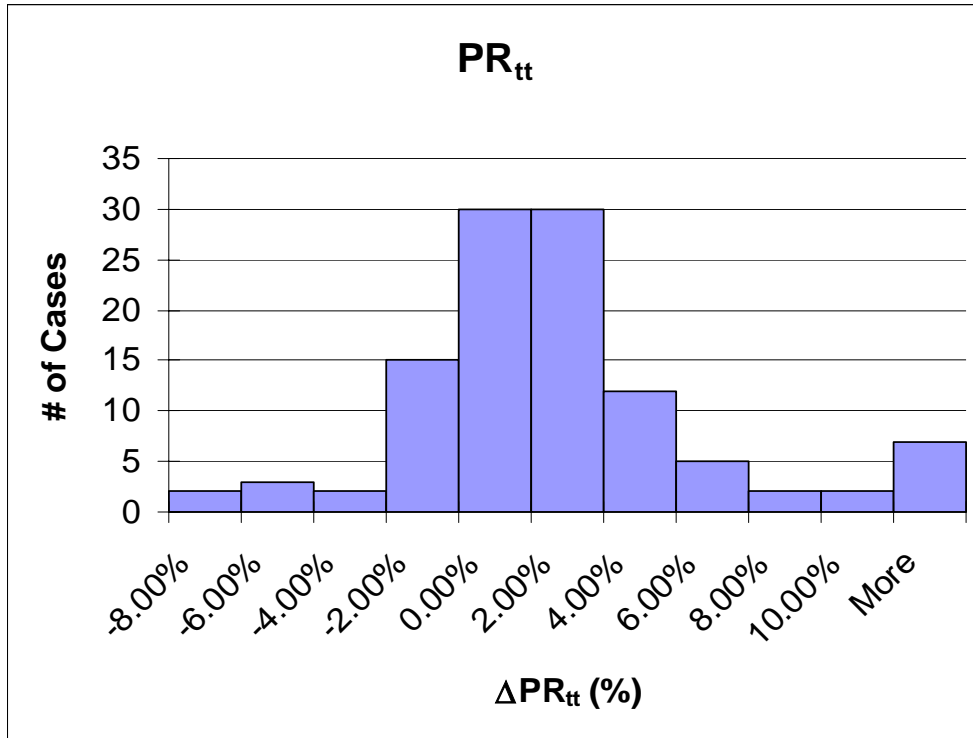
Figure 4-15. The error for the stage pressure ratio error, $\Delta PR_{tt}= (PR_{tt,Analysis}\text{-}PR_{tt,Data})/PR_{tt,Data})$, is presented in a histogram format. The error is averaged across each speedline.

Figure 4-16 shows a comparison of the diffuser diffusion ratio for analysis and data reduction. The error for DR_5 is calculated identically to the error for the plot of η_{tt}, $\Delta DR_5=(DR_{5,Analysis}\text{-}DR_{5, Data})$. The typical value of the DR_5 in this type of diffuser is about 1.3-1.5. The vast majority of the speedlines, 85%, lie in the range of ±0.1. This is the largest relative error that is found in the re-application of the models to the cascade database. The use of the DR_5 indicator is helpful in understanding where the modeling error is coming from because it is sampling the error of the models for η_{a5} and η_{b5} alone, χ_5, and δ_{5p} are not used in the calculation of the diffusion ratio. Matching the diffusion ratio is where the main concern in modeling lied at the outset. The error experienced is a product of the lack of measured static pressures at the inlet and exit of the diffuser vanes and the density of the data measurements on the speedlines. If there were measured static

pressures at stations 3 and 4 along with greater measurement density, superior models could likely be built.
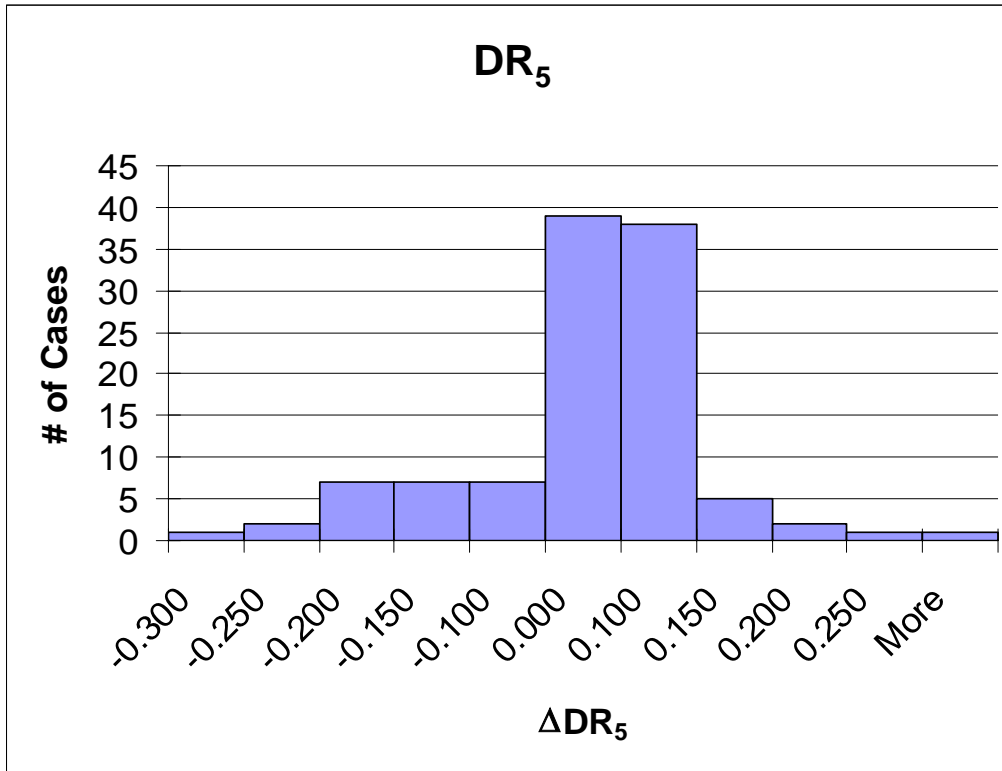
Figure 4-16. The diffusion ratio error, averaged across a speedline, $\Delta DR_5=(DR_{5,Analysis}-DR_{5,\ Data})$, is presented in a histogram format.

The models do appear to have a bias which lends to a small over prediction of the data, on average across a speedline. Upon seeing this there was some concern that the average of the model predictions was much greater the average of the data—in essence creating a bias in the models. This was explored and found to be untrue for both the η_{a5} and η_{b5} models. The difference between the average of the model prediction and the data was 0.005 for η_{a5} and 0.02 for η_{b5}. A change of this magnitude to the models—decrease

their prediction value by this difference in averages—would not have a noticeable effect on the data and model comparisons.

To gain a better feel of how the predictive models perform across a speedline, two examples are shown in Figures 4-17 and 4-18 for cascade diffuser builds. The impeller modeling has been frozen and just the diffuser modeling was considered. Each figure includes plots of stage efficiency, stage pressure ratio, vaned diffuser diffusion ratio, vaned diffuser loss coefficient, and vaned diffuser pressure recovery coefficient. The data is shown with a dashed line and the analysis is the solid line. The plots are representative of average examples of matching the data using the empirical models developed for cascade diffusers.
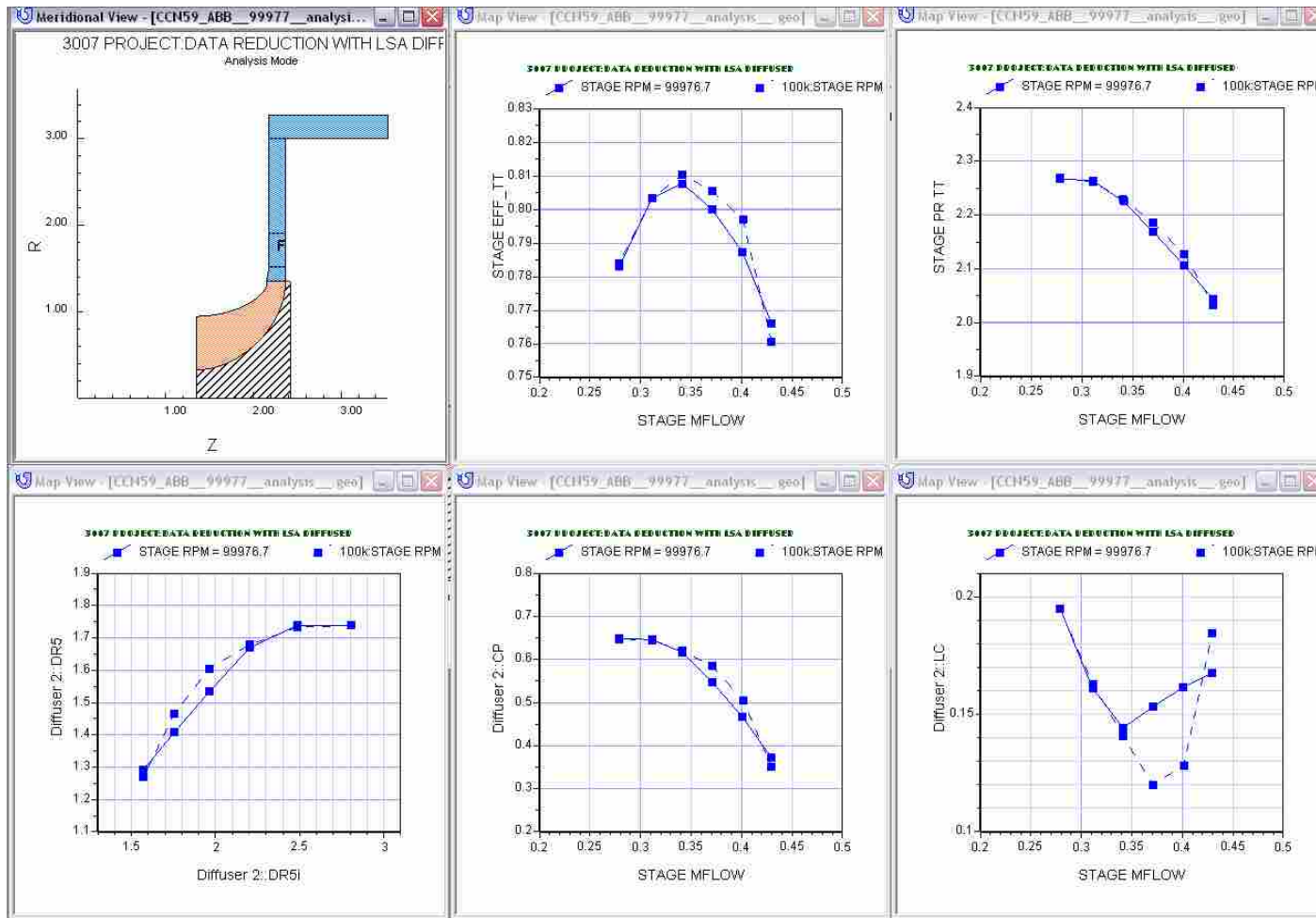
Figure 4-17. The diffuser data match in COMPAL is shown. The data is the dashed line the prediction using the developed models is the solid line. The top line from left to right: the stage efficiency vs. mass flow and pressure ratio vs. mass flow. Along the bottom from left to right: diffusion ratio vs. ideal diffusion ratio, diffuser pressure recovery coefficient vs. mass flow, and diffuser loss coefficient vs. mass flow.
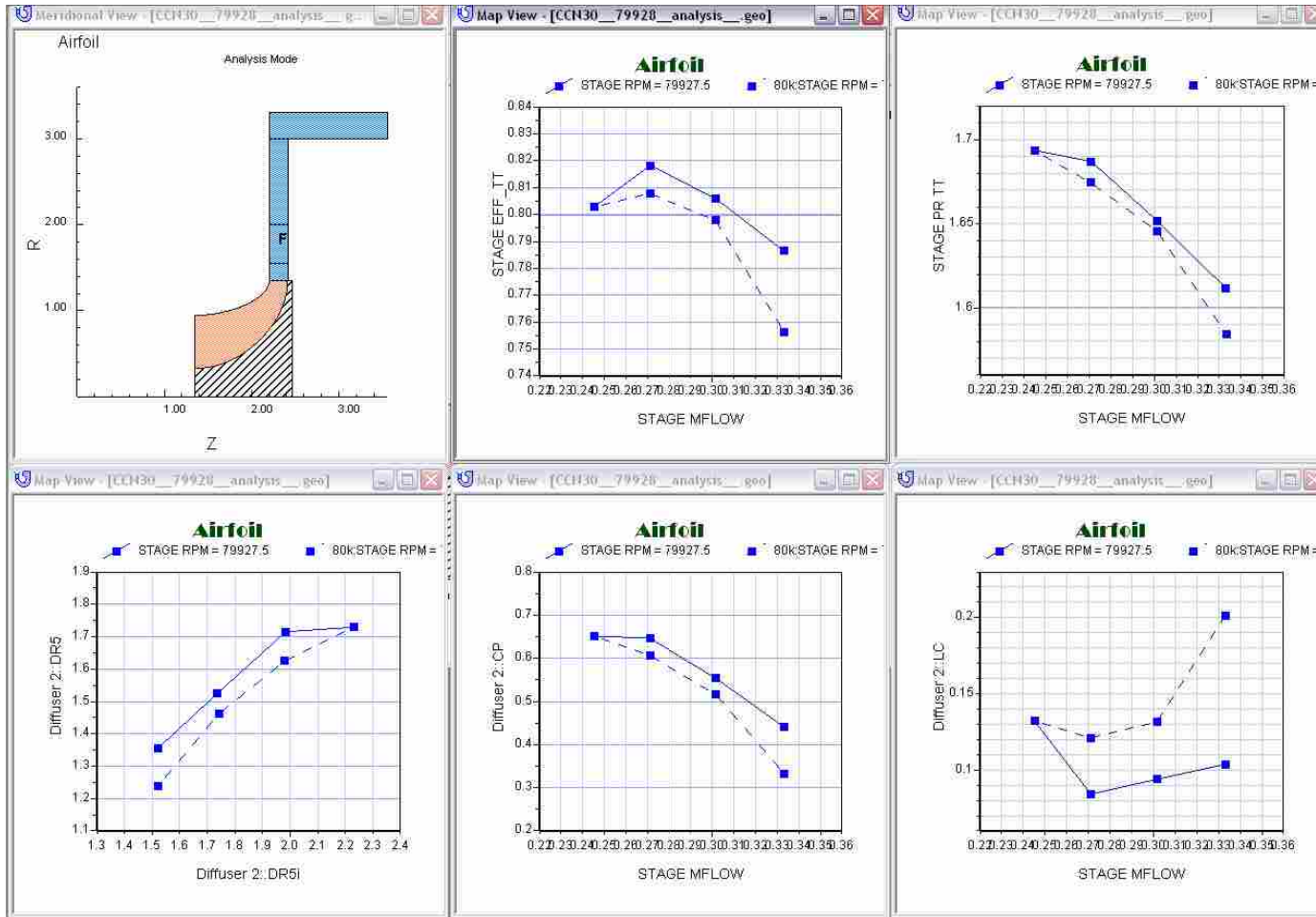
Figure 4-18. The diffuser data match in COMPAL is shown. The data is the dashed line the prediction using the developed models is the solid line. The top line from left to right: the stage efficiency vs. mass flow and pressure ratio vs. mass flow. Along the bottom from left to right: diffusion ratio vs. ideal diffusion ratio, diffuser pressure recovery coefficient vs. mass flow, and diffuser loss coefficient vs. mass flow

4.5.2   Channel Models Performance

The models for η_{a5}, η_{b5}, χ_5, and δ_{5p} were applied as well to the channel database through COMPAL in the same manner as outlined previously. Here there was no need to iterate on the solver in COMPAL, as required for the cascade database. This is due to the fact that no flow dependant variables are contained in the developed empirical models. The variables used were geometric or impeller based flow variables and did not change in COMPAL solver runs.
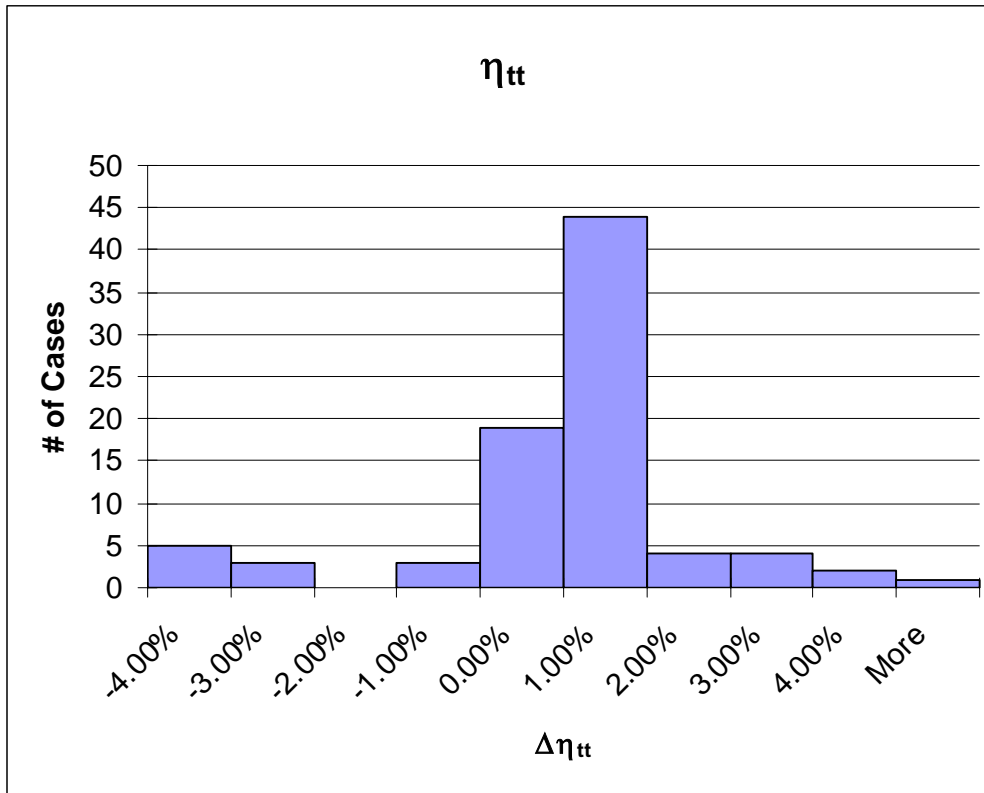
Figure 4-19. The stage efficiency error, averaged across a speedline, $\Delta\eta_{tt}=(\eta_{tt,Analysis}-\eta_{tt,Data})$, presented in a histogram format.

The overall diffuser match is excellent as can be seen in Figures 4-19-4-22. The figures follow an identical format to the ones previously presented. Figure 4-19 is the

92

error in the total-to-total stage efficiency, η_{tt}, presented where the error is the difference between the analysis total-to-total stage efficiency and the data total-to-total stage efficiency where $\Delta\eta_{tt}=(\eta_{tt,Analysis}-\eta_{tt,Data})$. The models performed well for a majority of the cases. Over 70% of the speedlines in the database fall within 2 efficiency points of the database value, on average across a speedline. This is an exceptional performance. It was the initial desire to receive this is kind of performance from the empirical models. The rest of the figures paint a similar picture of the models ability to match the data.
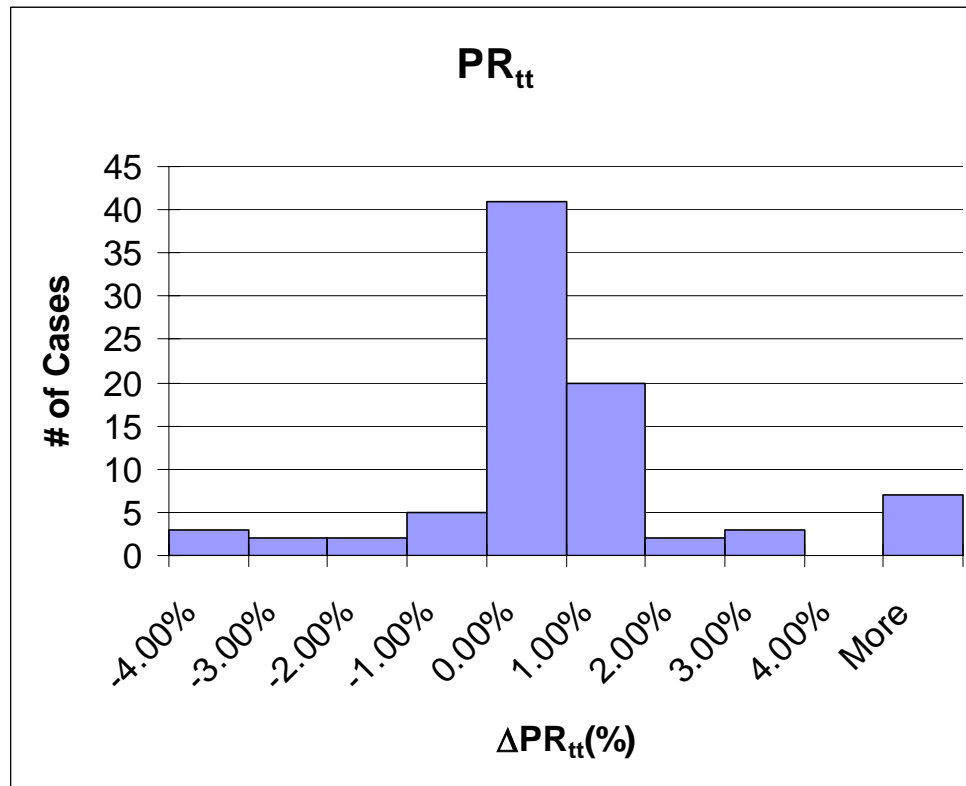
Figure 4-20. The stage pressure ratio error, averaged across a speedline, $\Delta PR_{tt}=(PR_{tt,Analysis}-PR_{tt,Data})/PR_{tt,Data})$, presented in a histogram format.

Figure 4-20 is presented in the same format as the pressure ratio plot shown earlier, the error calculation being $\Delta PR_{tt}=(PR_{tt,Analysis}-PR_{tt,Data})/PR_{tt,Data}$. The average error

is similar to that found for η_{tt}. Over 70% of the speedlines are between 0% and 2% error. The typical PR_{tt} for speedlines in the database has a magnitude between 1.7 and 3.6. This makes the average difference between the data reduction and analysis pressure ratios for the speedlines in the database very small. These two plots seem to indicate that implementation of the models yields good performance matching of the data.
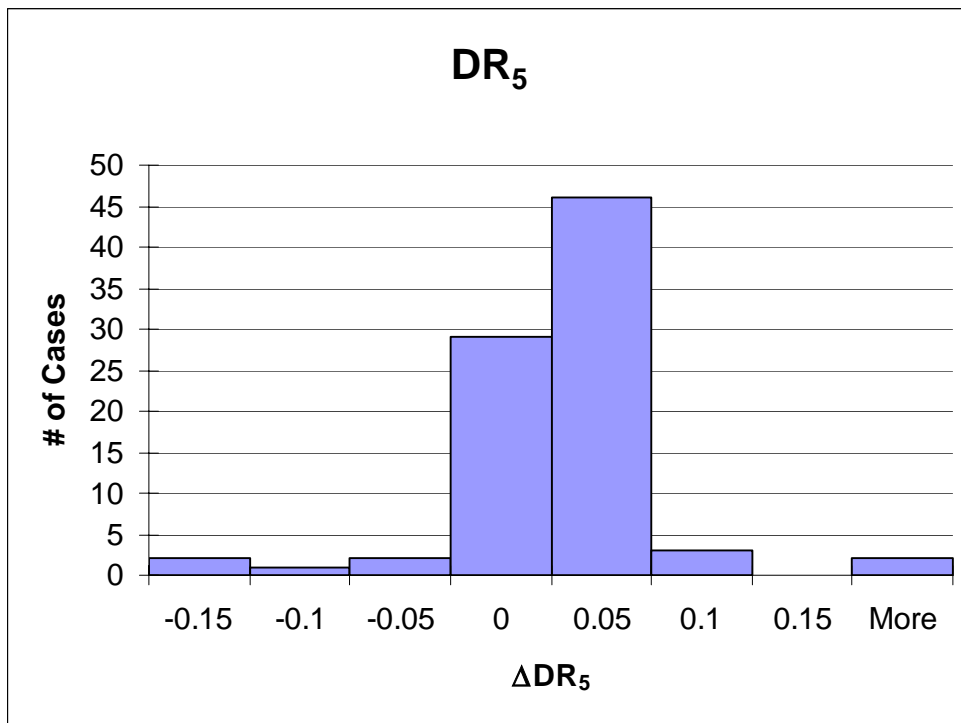
Figure 4-21. The diffusion ratio error, averaged across a speedline, $\Delta DR_5=(DR_{5,Analysis}-DR_{5,\ Data})$, presented in a histogram format. The error appears to be biased on the positive side.

The next figure, Figure 4-21 shows a comparison of the diffuser diffusion ratio between the analysis and data reduction modes. The error for DR_5 is calculated identically to the error for the plot of the diffusion ratio previously presented, $\Delta DR_5=(DR_{5,Analysis}-DR_{5,\ Data})$. The typical value of the DR_5 in this type of diffuser is about

1.4-1.8. The vast majority of the speedlines, well over 85%, lie in the range of 0 to 0.05. Evaluating the models for η_{a5} and η_{b5} from the diffusion ratio shows them to be performing very well.

There appears to be some a similar bias in the channel models as there were in the cascade models. Again the values of η_{a5} and η_{b5} were evaluated to determine if the average of the model predictions was much greater the average of the data. The difference between these averages was 0.03 for η_{a5} and 0.002 for η_{b5}. A change of this magnitude to the models would not have an appreciable effect on model calculations.

There is a fairly substantial difference in the channel and cascade models performance for predicting DR_5. The error for the cascade DR_5 modeling is nearly three times the error experienced in the channel modeling. This inability of the cascade models for η_{a5} and η_{b5} to predict the diffusion ratio like the channel models may well explain the difference in the ability to predict the stage η_{tt} and stage PR_{tt}. This seems to indicate that the models for χ_5 and δ_{5p} are not where most of the error lies in the cascade diffuser modeling. As stated earlier, this error in predicting η_{a5} and η_{b5} is a direct result of not having the data desired for model building. Had the desired data been acquired, the modeling performance of the cascade diffusers would, in all likeliness, be of a similar effectiveness.

Again, to gain a better feel of how the predictive models perform across a speedline, two examples are shown in Figures 4-22 and 4-23 for channel diffuser builds. The impeller modeling has been frozen and just the diffuser modeling was considered. Each figure includes plots of stage efficiency, stage pressure ratio, vaned diffuser diffusion ratio, vaned diffuser loss coefficient, and vaned diffuser pressure recovery

95

coefficient. The data is shown with a dashed line and the analysis is the solid line. The plots are representative of average examples of matching the data using the empirical models developed for channel diffusers.
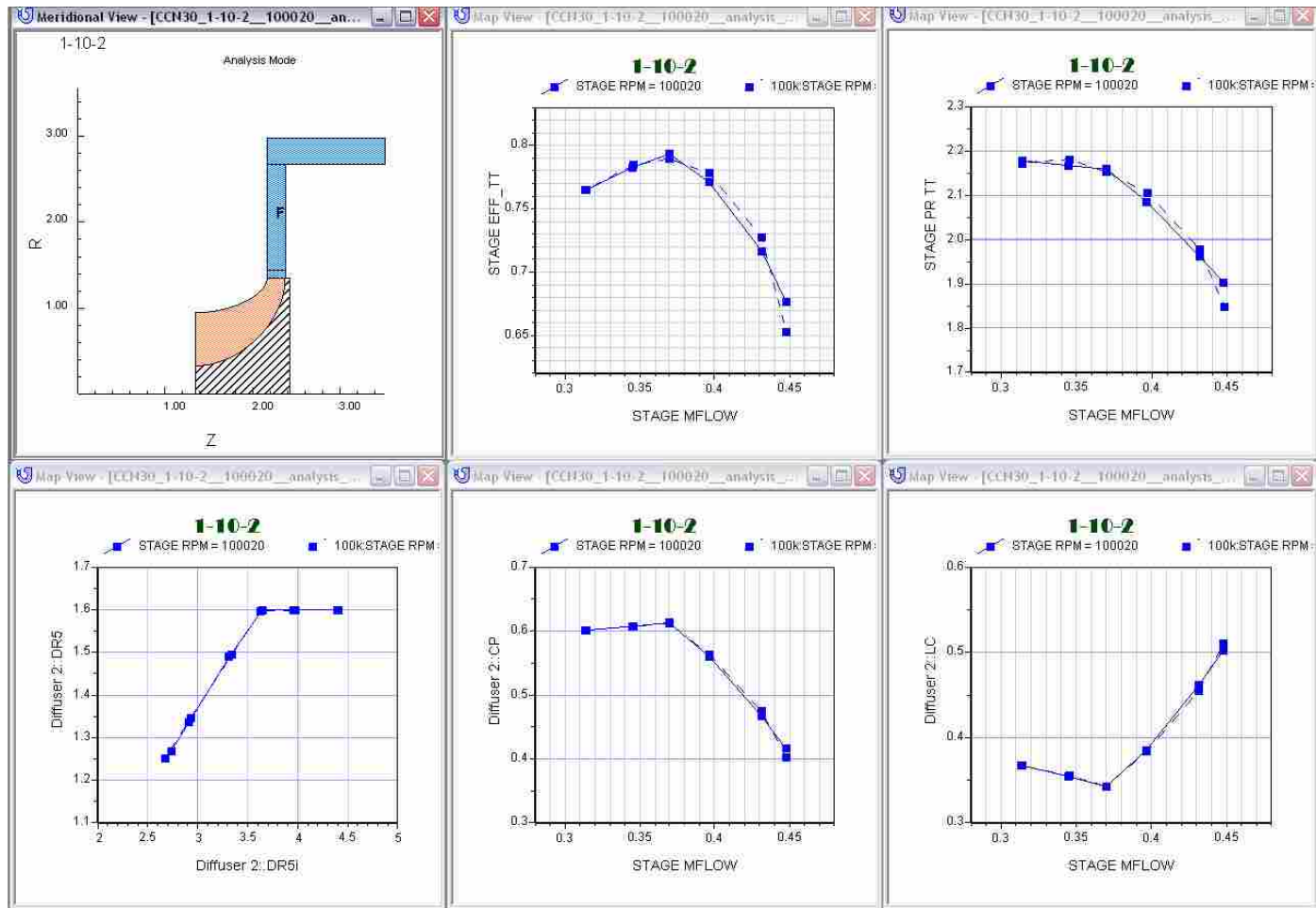
Figure 4-22. The diffuser data match in COMPAL is shown. The data is the dashed line the prediction using the developed models is the solid line. The top line from left to right: the stage efficiency vs. mass flow and pressure ratio vs. mass flow. Along the bottom from left to right: diffusion ratio vs. ideal diffusion ratio, diffuser pressure recovery coefficient vs. mass flow, and diffuser loss coefficient vs. mass flow
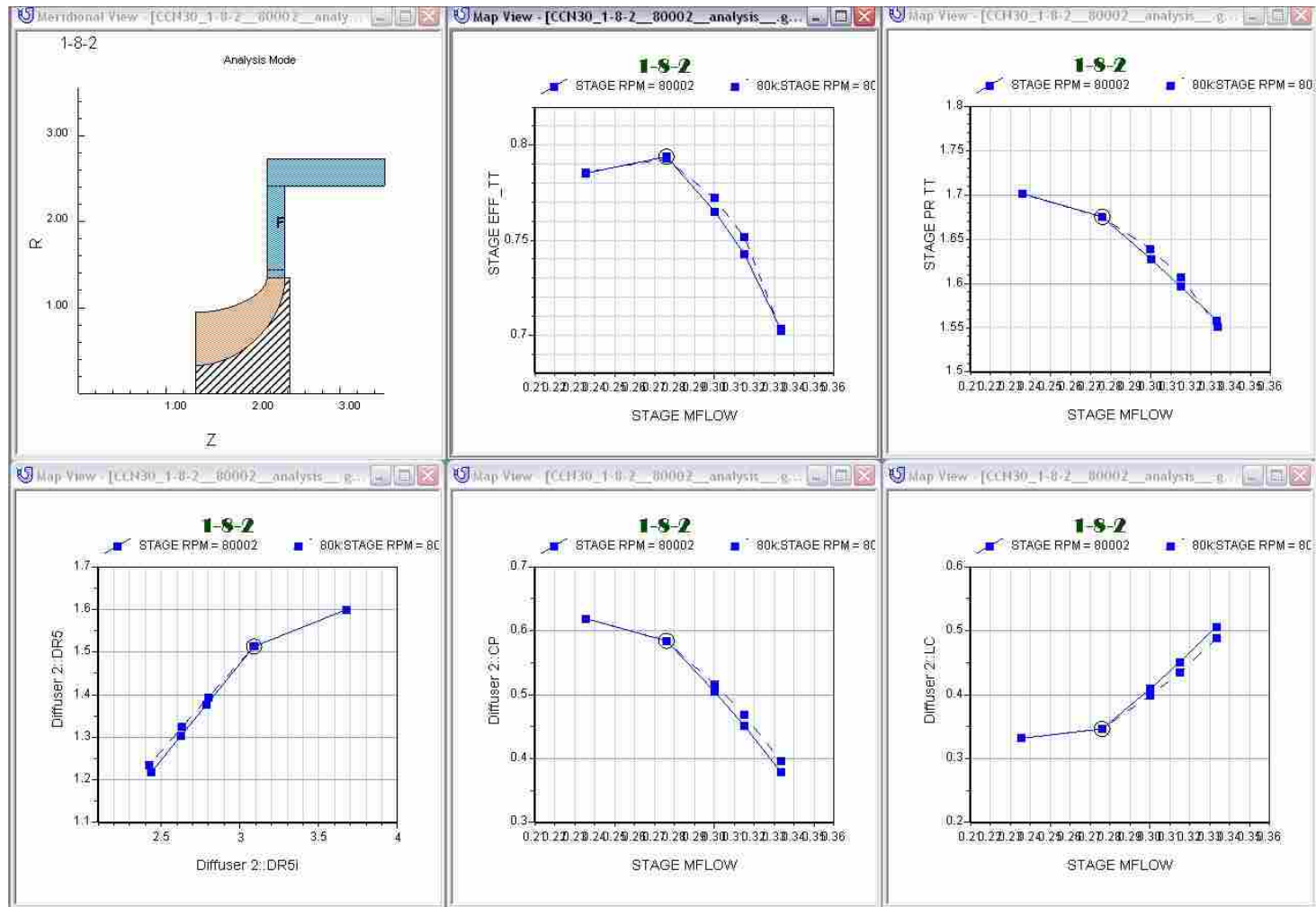
Figure 4-23. The diffuser data match in COMPAL is shown. The data is the dashed line the prediction using the developed models is the solid line. The top line from left to right: the stage efficiency vs. mass flow and pressure ratio vs. mass flow. Along the bottom from left to right: diffusion ratio vs. ideal diffusion ratio, diffuser pressure recovery coefficient vs. mass flow, and diffuser loss coefficient vs. mass flow

5 Conclusions and Recommendations

5.1 Conclusions

Empirical models for the TEIS and Two Zone model input parameters, η_{a5}, η_{b5}, χ_5, and δ_{5p}, for two different types of vaned diffusers, channel and cascade, were presented in this thesis. The centrifugal compressor experimental data used in the model building was obtained from Concepts NREC, an industry sponsor. Each dataset provided was evaluated for quality and reliability and only the data deemed reliable were used in the model building databases. This narrowed the model building databases considerably; however, it also increased the confidence in the deduced values of η_{a5}, and η_{b5}. The empirical models presented were built solely on this higher quality data.

Seven models were proposed for use in predicting the TEIS and Two Zone model input parameters η_{a5}, η_{b5}, χ_5, and δ_{5p}. Models for η_{a5}, η_{b5} and δ_{5p} were specific to the vaned diffuser, channel or cascade, present in the compressor builds in the database while the model for χ_5 is common to both diffuser types. The models were applied to the databases from which they were built to gain an indication of modeling performance. It was determined that the models performed well; with the channel models yielding better performance than the models for the cascade diffusers. This discrepancy between the performances of the two types of diffuser models underscore the importance of acquiring

99

sufficient data to be able to determine the physics occurring in each element of the compressor stage. This includes a greater data point density on each speedline taken as well as more measurement locations for each stage tested (level 1 quality data). There is still much physical behavior that occurs in turbomachinery that is not yet well understood. Without high quality data at a sufficient data point density, advances in compressor modeling will slow or perhaps stall.

These are the first models ever built for the TEIS and Two Zone model inputs applied to channel and cascade diffusers. As such they will become a benchmark for future studies. The work with these models is not complete, however; there is much work that still needs to be done. This was but an initial attempt at modeling the TEIS and Two Zone input parameters and iteration will need to be done with this model building process to ensure the fidelity of the models. The databases were not of a size that data could be withheld from the model building to be used later for validating the models. Instead the models performance was evaluated by applying all of the models, simultaneously, to the database from which they were built. The determination of the effectiveness of the combined modeling is based on the average error across the entire speedline. The models proved to be effective and a contributing step to employing such models for use in future compressor design.

After a proper validation, the developed empirical models could then be used to predict the four input parameters, η_{a5}, η_{b5}, χ_5, and δ_{5p}, needed to close the system of equations formed by the TEIS and Two Zone models. The designer would then, by varying geometric design variables, change the values of η_{a5}, η_{b5}, χ_5, and δ_{5p} that are predicted by the empirical equations, these values would be automatically updated when

design choice quantities are changed in the program. The empirical equations could also be included in an optimization loop with the COMPAL code to meet new design and challenging design requirements.

5.2 Recommendations

As previously stated, this is the first attempt to create empirical models for the TEIS and Two Zone input parameters. And like most initial research, future improvements are expected. It is recommended that in future work:

1) More experimental data is gathered, more cases at a greater data point density on each speedline, to validate the models on cases which are not in the empirical model building databases. Changes may need to be made to ensure the models have general applicability. The evaluation of the models on datasets outside of the model building database would be a true indication of the models expected performance in design.

2) In the real scenario, the diffuser input models need to be used in conjunction with impeller models. The tests that were preformed for this thesis were done with a frozen impeller. Additional change is expected to the impeller modeling input parameters when a vaned diffuser is utilized downstream. Impeller performance is affected by the presence of diffuser vanes [17]—especially when the vanes are in close proximity to the impeller such as is the case for channel diffusers. The changes to the impeller models may come in the form of an additional "diffuser factor" which is active only when vaned diffusers are present.

3) Additional study needs to be devoted to developing a greater understanding of η_{a5} for cascade and channel diffusers. This would involve data of a very high quality (level 1a) that include traverses of the flow field prior to entry into the vaned diffuser passage. With this data the physics could be better understood and much could be gained that would improve diffuser design. This data could also be used to eliminate some of the uncertainty in the deduced values of η_{a5} and η_{b5} for the cascade diffusers and increase the performance of the models built. The modeling for the cascade diffusers could also be repeated with the more classical variables and perhaps would yield improved results.

6 References

1 Dixon, S.L., *Fluid Mechanics and Thermodynamics of Turbomachinery, Fourth Ed.*, Butterworth-Heinemann, Boston, 1998.

2 Japikse D, Baines N. C., *Introduction to Turbomachinery,* Concepts ETI, Inc., Norwich, VT, and Oxford University Press, Oxford, England, 1994.

3 Nasa website: http://www.grc.nasa.gov/WWW/5810/facilities/CE18/CC3.jpg

4 Japikse, D., *Centrifugal Compressor Design and Performance*, Concepts ETI, Inc., Wilder VT, USA, 1996.

5 Japikse, D., Personal Communication, March 7, 2003.

6 Fox, R., McDonald, A., Pritchard, P., *Introduction to Fluid Mechanics, Sixth Ed.*, John Wiley and Sons, Inc., Hoboken, NJ, 2006.

7 Pelton, R. J., to be published

8 Japikse, D., "Assessment of Single- and Two-Zone Modeling of Centrifugal Compressors, Studies in Component Performance: Part 3," ASME Paper No. 85-GT-73, 1985.

9 Whitfield, A., Baines, N. C., *Design of Radial Turbomachines,* Longman Scientific & Technical, John Wiley & Sons, Inc., New York, 1990.

10 Eckardt, D., "Instantaneous Measurements in the Jet-Wake Discharge Flow of a Centrifugal Compressor Impeller," Journal of Engineering for Power. July 1975. pp. 337-345.

11 Dean, R. C., Senoo, Y., "Rotating Wakes in Vaneless Diffusers," Journal of Basic Engineering. September 1960. pp. 563-574.

12 Dubitsky, O., Japikse, D., *Vaneless Diffuser Advanced Model*, ASME Turbo Expo paper number GT2005-68130, June 2005

13 Japikse, D., Personal Communication, November 8, 2005.

14 Neter, J., Wasserman, W., Kutner, M. *Applied Linear Regression Models,* Richard D. Irwin, Inc., Homewood, Illinois 60430, 1983.

15 Hocking, R. *Methods and Applications of Linear Models*, Second Ed. John Wiley & Sons Inc., Hoboken, New Jersey 07030, 2003

16 Kleinbaum, D., Kupper, L., Muller, K., Nizam, A. *Applied Regression Analysis and Other Multivariable Methods*. Brooks/Cole Publishing Co., Pacific Grove, CA 93950, 1998.

17 Ziegler, K., Gallus, H., Niehuis, R. "A Study on Impeller-Diffuser Interaction—Part I: Influence on the Performance," Journal of Turbomachinery Vol. 125: 173-182. 2003.

18 Ziegler, K., Gallus, H., Niehuis, R. "A Study on Impeller-Diffuser Interaction—Part II: Detailed Flow Analysis," Journal of Turbomachinery Vol. 125: 183-192. 2003.

19 Japikse, D., *Turbomachinery Diffuser Design Technology*, Concepts ETI, Inc., Wilder VT, USA, 1984.

20 Bardina, J., Kline, S., Ferziger, J. "Computation of Straight Diffusers at Low Mach Number Incorporating an Improved Correlation for Turbulent Detachment and Reattachment," Department of Mechanical Engineering, Stanford University, 1982.

21 Coles, D., "The Law of the Wake in the Turbulent Boundary Layer," *Journal of Fluid Mechanics*, Vol. 1, 1956, pp. 191-226.

22 Bradshaw, P. S Ferris, D. H., Atwell, N. P., "Calculation of Boundary Layer Development Using the Turbulent Energy Equation," *Journal of Fluid Mech*., Vol. 28, Part 3, 1967, pp 593-616.

23 Lieblein, S. "Incidence and Deviation-Angle Correlations for Compressor Cascades," *Journal of Basic Engineering*, September 1960, pp. 575-587

Appendix A.   Coded Models

The code used in conjunction with COMPAL was written in Python.   This code utilized an OLE (Object Linking and Embedding) link that is provided in COMPAL. The calculations follow this format: The COMPAL solver was first utilized with initial guesses for the TEIS and Two Zone input parameters. The outputs of the analysis run are fed into the attached code via the OLE link. The coded models are then used to generate new inputs for the TEIS and Two Zone models. The solver is re-run with the new inputs. This is repeated until the models converge to a single solution. The model convergence process typically involved four solver runs and was repeated for each compressor case.

```
################################################################################
# Python objects for OLE interface with PUMPAL/COMPAL
#
#    Contents:        MsecM5Correlation Chi model—made form the Bardina code.
#                     Calculations -   where calculations for the Chi model are performed.
#                     rkm44 -   Runge Kutta routine for Chi model.
#                     ETAaModel  -  ETAa model for channel diffusers.
#                     ETAbModel  -  ETAb model for channel diffusers.
#                     DeltaModel   -  Lieblein model for cascade deviation.
#                     ETAaCascadeModel  -  ETAa model for cascade diffusers.
#                     ETAbCascadeModel  -  ETAb model for cascade diffusers.
#
#        Author:    Jamin Bitter
#        Date:      9/12/2006
################################################################################

import units
from math import cos,sin,radians,atan,log

def MsecM5Correlation(resultsTable):
   """UserFunction   MsecM5 FOIL Diffuser   """
```

```python
##    from Calculations import*
##    from  rmk44 import*
  global AK2, AR, WN, THETA, RST1, B, X1W1, ANW1, CP, CF, H, YP1, WPN, XN0, F0, T0, UN0,pi
  pi=3.14159265359
  Rin = resultsTable["Diffuser[2]Rin"][0]
  unitName = resultsTable.GetUnits("Diffuser[2]Rin")
  Rin = units.ConvertToSI(Rin, unitName)
  Rex = resultsTable["Diffuser[2]Rex"][0]
  unitName = resultsTable.GetUnits("Diffuser[2]Rex")
  Rex = units.ConvertToSI(Rex, unitName)
  Wth = resultsTable["Diffuser[2]Win"][0]
  unitName = resultsTable.GetUnits("Diffuser[2]Win")
  Wth = units.ConvertToSI(Wth, unitName)
  Wex = resultsTable["Diffuser[2]Wex"][0]
  unitName = resultsTable.GetUnits("Diffuser[2]Wex")
  Wex = units.ConvertToSI(Wex, unitName)
  alphab_in = resultsTable["Diffuser[2]ALPHABin"][0]
  Bin = resultsTable["Diffuser[2]Bin"][0]
  unitName = resultsTable.GetUnits("Diffuser[2]Bin")
  Bin = units.ConvertToSI(Bin, unitName)
  Visc = resultsTable["ILVISC"][0]
  unitName = resultsTable.GetUnits("ILVISC")
  Visc = units.ConvertToSI(Visc, unitName)
  RHO = resultsTable["Diffuser[1]RHOex"][0]
  unitName = resultsTable.GetUnits("Diffuser[1]RHOex")
  RHO = units.ConvertToSI(RHO, unitName)
  CPin = resultsTable["Diffuser[1]CP"][0]
  ZD = resultsTable["Diffuser[2]Number Blades"][0]
    L_eff = (Rex-Rin)/cos(radians(alphab_in)) - 2*Rin*sin(2*pi/ZD)*sin(radians(90-alphab_in))
  """effective length = (length - E)--- (compressor book pg3-59)"""
  if (CPin < -0.668):                       #Blck4 calculations
    Blck4 = 0.02466
  elif (-0.668 <= CPin <= 0.2):
    Blck4 = 0.07344*CPin**2 + 0.09831*CPin + 0.05744
  else:
    Blck4 = 1.125*CPin**2 - 0.35*CPin + 0.105


  delta = Blck4*Wth*4                       #boundary layer thickness
  delta_star_eq = Blck4*Bin*Wth/(2*Bin+2*Wth-4*delta) #equivalent displacement thickness
  """
  This is a duplication of Bardina's code, translated from the original FORTRAN.
  """
  XN0=0
  F0=0
  #%%%%%%%%INPUTS%%%%%%%%%%%%%%%
  #TWOTHETA=7;                        #2*theta diffuser divergence angle
  Y=[0,0,0]
  DSTAR1=delta_star_eq               #effective inlet delta_star--displacement thickness
  DELTA1=DSTAR1*8                      #effective inlet boundary layer thickness
  ANU=Visc/RHO                     #kinematic viscosity
  N=L_eff                       #Effective Diffuser length
  W1=Wth                         #Throat width
  X1=0                          #compressor book E--inlet region before the throat
  b=Bin                         #vane height
  Wex=Wex                          #diffuser exit width
  X2=0                          #Exit length after Wex--like an exit X1
```

```
    TWOTHETA=180/pi*(4*atan((Wex-W1)/(2*N)))    #Calculated diffuser divergence angle
    #%%%%%%%%%%%%%%%%%%%%%%%%%%%%%
    RST1 =W1*DSTAR1/ANU
    B = 2*DSTAR1/W1
    Y[2] = DSTAR1/DELTA1
    X1W1 = X1/W1
    X2W1 = X1/W1
    ANW1 = N/W1
    ABSERR=1.0e-5
    AK2=1.5894898556
    Y[1]=B
    THETA=pi*TWOTHETA/360
    AR = 1+2*ANW1*sin(THETA)/cos(THETA)
    XN=-X1W1
    YP=[0,0,0]
    i=1
    Calculations(XN,Y,YP)
    while (XN-0.5)<=(ANW1+X2W1):
        #chi_2d=2*Wex*(delta-delta1)/(2*Wex*(delta-delta1)+(Wex-2*delta)*(b-2*delta))
        #Epsilon=1-(Wex-2*delta)*(b-2*delta)/(b*Wex)
        #Epsilon_2d=2*delta/Wex
        XOUT=XN+1
        delta=Y[1]*Wex*0.95
        delta1=Y[2]*delta
        chi_3d=(delta-delta1)*(2*b+2*Wex-4*delta)/((delta-delta1)*(2*b+2*Wex-4*delta)+(Wex-
2*delta)*(b-2*delta))
        if(chi_3d>1):
            chi_3d=1

        rkm44(XN,XOUT,Y,ABSERR,YP)
        XN=XN+1
        if (chi_3d==1):
            break


    return chi_3d

def Calculations(XN,Y,YP):
    from math import cos, sin, exp, sqrt, log
    #[Y,YP,SH,CP,CF,H,WN]=Calculations(XN,Y,YP,ANW1,THETA,B,RST1,AK2,X1W1)
    global AK2, AR, WN, THETA, RST1, B, X1W1, ANW1, CP, CF, H, YP1, WPN, XN0, F0, T0, UN0
    #%%%%%%%%%***********************
    #% Calculations
    #%%%%%%%%%%%%GEOMETRY%%%%%%%%%%%%%%
    if (XN>ANW1/(cos(THETA))):
        WN=AR
        WPN=0
    elif (XN>0):
        WN=THETA*(2*XN+1/(sin(THETA)))
        WPN=2*THETA
        if (WN>AR):
            WN=AR
            WPN=0

    else:
        WN=1
```

```python
    WPN=0

#%%%%%%%%%%%%CONTINUITY
UN=(1-2*B)/(1-2*Y[1])/WN
CP = 1-UN**2
RST=RST1*UN*WN*Y[1]/B
#%%%%SKIN FRICTION CORRELATIONS AND SHAPE FACTOR%%%%%
VT=0.44*(abs(1-2*Y[2]))**0.885*(Y[2]/RST)**0.115
if (Y[2]>0.50):
    VT=-VT

SH=1.5*Y[2]+(2*AK2-3)*VT+(3.5-2*AK2)*VT**2/Y[2]
C2=0.115*((2*AK2-3)*VT+(7-4*AK2)*VT**2/Y[2])
C1=1.5-(3.5-2*AK2)*VT**2/Y[2]**2+(0.115-2*Y[2])/Y[2]*((2*AK2-3)+(7-
4*AK2)*VT/Y[2])*(0.3+0.4*Y[2])/RST**0.115

#%%%%%%%%BOUNDARY LAYER PARAMETERS
CF=2*0.41*0.41*VT*abs(VT)
H=1/(1-SH)
#%%%%%%%%%ETA=Y/DELTA
C=0.24
if (Y[2]>0.50):
    C=1.3*Y[2]-0.4

if (VT>=(5.3212*Y[2]-3.117086*C)):
    ET=0.25
else:
    DEL=1
    ET=atan(sqrt(2*Y[2]/C-1))/pi-0.006*(1/Y[2]-2)/Y[2]
    while abs(DEL) >= 0.0001:
        F=VT*log(ET)-2*(Y[2]-VT)*(cos(pi*ET/2))**2+C
        DEL=-F/(VT/ET+pi*(Y[2]-VT)*sin(pi*ET))
        ET=ET+DEL



#%%%%%%MATRIX COEFFICIENTS%%%%%%%%%%%%%%%%%%%%%%%%%%%%

X1=0
if ((WPN>0) & (Y[2]<0.5) & (THETA>0.12)):
    X1=0.0060/WN/Y[1]

A11=(C2+1-SH)/Y[1]/(1-2*Y[1])+(2-SH+X1/Y[2])/(0.5-Y[1])
A21=1/(1-2*Y[1])
A22=Y[1]/Y[2]/(1-Y[2])
B1=0.41*0.41*VT*abs(VT)/WN/Y[1]+WPN*(2-SH+X1/Y[2])/WN
#%%%%%%%%%%%%%%%SHEAR AND LAG EQUATIONS
TEQ=0.0168*Y[2]*(VT/ET+pi*(Y[2]-VT)*sin(pi*ET))
TEQ=TEQ/(1+9*ET**6)
if (XN==-X1W1):
    T0=TEQ
    UN0=1

if (WPN==0):
    if (XN==0):
        XN0=0
```

```
      F0=0

   T=TEQ*Y[2]*abs(XN-XN0)/(80*WN*Y[1]+abs(XN-XN0)*Y[2])
   T=T+(T0+abs(XN-XN0)*F0/80)/(1+abs(XN-XN0)*Y[2]/80/WN/Y[1])*(UN0/UN)**2
   B2=10*T*Y[2]/WN/(1-Y[2]);
   YP[1]=(B2*C1-B1*A22)/(C1*A21-A11*A22)
elif (Y[2]>0.48):
    TEQ=0.13*TEQ/0.168
    if (WPN==0):
      TEQ=TEQ*(1-Y[2])/Y[2]

    T=TEQ
    B2=10*T*Y[2]/WN/(1-Y[2])
    YP[1]=(B2*C1-B1*A22)/(C1*A21-A11*A22)
else:
   YP0=1;
   T1=TEQ
   j=1
   while (abs(YP0-YP[1])>0.00001):
     BETA=WN*Y[1]*(2*YP[1]/(1-2*Y[1])-WPN/WN)/15/0.41/0.41/VT/VT
     if (BETA>0):
       BETA=0

     if (BETA<-30):
       BETA=-30

     T=T1*(0.013+0.0038*exp(BETA))/0.0168
     T=TEQ*Y[2]*abs(XN-XN0)/(80*WN*Y[1]+abs(XN-XN0)*Y[2])
     T=T+(T0+abs(XN-XN0)*F0/80)/(1+abs(XN-XN0)*Y[2]/80/WN/Y[1])*(UN0/UN)**2
     if ((Y[2]<0.5)&(Y[1]>Y[2]/2)):
       T=0

     B2=10*T*Y[2]/WN/(1-Y[2])
     YP0=YP[1]
     YP[1]=(B2*C1-B1*A22)/(C1*A21-A11*A22)
     j=j+1


XN0=XN
UN0=UN
T0=T
F0=Y[2]*(TEQ-T)/WN/Y[1]
YP[2]=(B2*A11-B1*A21)/(C1*A21-A11*A22)
#%%%%%%%%%%LIMITS ON ENTRAINMENT%%%%%%%%%

if (Y[2]<0.42265) or (WPN==0):
   YP1=YP[1]
else:
   if (YP[2]>0):
     if(YP[1]<(WPN*(1-Y[1])/2/WN)):
       YP1=YP[1]
     else:
       YP[1]=WPN*(1-2*Y[1])/WN/2
       YP[2]=(A11*YP[1]-B1)/C1
       T0=(A21*YP[1]-A22*YP[2])*WN*(1-Y[2])/10/Y[2]
```

```
            YP1=YP[1]


        else:
            YP[2]=0
            YP[1]=B1/A11
            T0=A21*YP[1]*WN*(1-Y[2])/10/Y[2]


    return (Y,YP,SH,WN)


def rkm44(XN,XOUT,Y,ABSERR,YP):
    global AK2, AR, WN, THETA, RST1, B, X1W1, ANW1, CP, CF, H, YP1, WPN, XN0, F0, T0, UN0
    ABE=0
    Q= (XOUT-XN)/256
    YO=[0,0,0]
    Y1=[0,0,0]
    FE=[0,0,0,0,0,0,0,0,0,0,0]
    while not(XN==XOUT):
        YO[1]=Y[1]
        YO[2]=Y[2]
        XO=XN;
        if ((ABE/ABSERR) >1.2):
                DX=0.5*DX

        if ((ABE/ABSERR) >0.5):
                DX=2*DX

        if (ABE==0):
                DX=Q

        if((XN+DX)>XOUT):
                DX=(XOUT-DX)

        Calculations(XN,Y,YP)
        FE[1]=DX*YP[1]
        FE[2]=DX*YP[2]
        Y[1]=YO[1]+FE[1]/3
        Y[2]=YO[2]+FE[2]/3
        XN=XO+DX/3
        Calculations(XN,Y,YP)
        FE[3]=DX*YP[1]
        FE[4]=DX*YP[2]
        Y[1]=YO[1]+(FE[1]+FE[3])/6
        Y[2]=YO[2]+(FE[2]+FE[4])/6
        Calculations(XN,Y,YP)
        FE[5]=DX*YP[1]
        FE[6]=DX*YP[2]
        Y[1]=YO[1]+(FE[1]+3*FE[5])/8
        Y[2]=YO[2]+(FE[2]+3*FE[6])/8
        XN=XO+DX/2
        Calculations(XN,Y,YP)
        FE[7]=DX*YP[1]
        FE[8]=DX*YP[2]
        Y[1]=YO[1]+(FE[1]-3*FE[5]+FE[7])/2
        Y[2]=YO[2]+(FE[2]-3*FE[6]+FE[8])/2
```

110

```
        Y1[1]=Y[1]
        Y1[2]=Y[2]
        XN=XO+DX
        Calculations(XN,Y,YP)
        FE[9]=DX*YP[1]
        FE[10]=DX*YP[2]
        Y[1]=YO[1]+(FE[1]+4*FE[7]+FE[9])/6
        Y[2]=YO[2]+(FE[2]+4*FE[8]+FE[10])/6
        ABE=max(abs(Y[2]-Y1[2]),abs(Y[1]-Y1[1]))


return (XN,Y,YP)
```

```python
def ETAa_Channel_Model(resultsTable, index):
    #get parameter inputs
    AlphaBin = resultsTable["Diffuser[2]ALPHABin"][index]
    LWRatio = resultsTable["Diffuser[2]LW_Ratio"][index]
    AS2 = resultsTable["AS2"][index]
    ARb = resultsTable["ARb"][index]
    r5 = resultsTable["Diffuser[2]Rex"][index]
    r2 = resultsTable["R2"][index]
    RossCA = resultsTable["Rossby Number (C,A)"][index]
    unitName = resultsTable.GetUnits("Diffuser[1]Rin")
    r2 = units.ConvertToSI(r2, unitName)
    r5 = units.ConvertToSI(r5, unitName)
    AlphaBin=cos(radians(AlphaBin))
    R5_R2=r5/r2
    #normalixe the variables
    R5_R2=(R5_R2-2.15995787)/0.38363724
    AlphaBin=(AlphaBin-0.345226106)/0.052497993
    RossCA=(RossCA-3.570142308)/0.606808011
    AS2=(AS2-0.543139867)/0.130751581
    ARb=(ARb-2.755071178)/0.624422152
    LWRatio=(LWRatio-5.928224796)/2.423644183
    #Perform calculation
    ETAa5 = K1 - K2*AS2*RossCA + K3  AlphaBin-K4*AlphaBin**2 -K5*R5_R2-K6*R5_R2**2 -
K7*AlphaBin*ARb +K8*ARb*LWRatio

    return ETAa5
```

```python
def ETAb_Channel_Model(resultsTable, index):
    #get parameter inputs
    AlphaBin = resultsTable["Diffuser[2]ALPHABin"][index]
    LWRatio = resultsTable["Diffuser[2]LW_Ratio"][index]
    AR45 = resultsTable["Diffuser[2]AR45"][index]
    ZR = resultsTable["ZR"][index]
    Bex = resultsTable["Diffuser[1]Bex"][index]
    Bin = resultsTable["Diffuser[1]Bin"][index]
    ZD = resultsTable["Diffuser[2]Number Blades"][index]
    unitName = resultsTable.GetUnits("Diffuser[1]Bin")
    Bin = units.ConvertToSI(Bin, unitName)
    Bex = units.ConvertToSI(Bex, unitName)
    AlphaBin=cos(radians(AlphaBin))
    AR45=1/AR45
    Bex_Bin=Bex/Bin
    #normalixe the variables
    AlphaBin=(AlphaBin-0.345226106)/0.052497993
    LWRatio=(LWRatio-5.928224796)/2.423644183
    AR45=(AR45-0.007390968)/0.001914087
    ZR=(ZR-19.98019802)/3.352551858
    ZD=(ZD-27.27722772)/11.01827465
    Bex_Bin=(Bex_Bin-0.981506151)/0.080867376
    #Perform calculation
    ETAb5 = K1 -K2*ZR*AR45 +K3*AlphaBin**2 -K4*ZD -K5*Bex_Bin*LWRatio
    return ETAb5
```

```python
def DeltaModel_Cascade(resultsTable):
    b3_in = resultsTable["Diffuser[2]ALPHABin"][0]
    b3_ex = resultsTable["Diffuser[2]ALPHABex"][0]
    r3 = resultsTable["Diffuser[2]Rin"][0]
    r5= resultsTable["Diffuser[2]Rex"][0]
    ZD = resultsTable["Diffuser[2]Number Blades"][0]
    beta3 = resultsTable["Diffuser[2]ALPHAin"]
    unitName = resultsTable.GetUnits("Diffuser[2]ALPHABin")
    b3_in = units.ConvertToSI(b3_in, unitName)
    b3_ex = units.ConvertToSI(b3_ex, unitName)
    r3 = units.ConvertToSI(r3, unitName)
    r5 = units.ConvertToSI(r5, unitName)
    beta3 = sum(beta3)/len(beta3)
    #calculations
    bl_turn = b3_in - b3_ex
    STAG_angle =((b3_in + b3_ex) / 2)
    chord = (r5 - r3)/(sin(radians(90 - STAG_angle)))
    solidity  = chord * ZD / (3.14159265359 * (r3 + r5))
    if (2.0>solidity>=1.8):
        dp1   =   2.10765E-07*beta3**4   -   1.03184E-05*beta3**3   +   0.000426810*beta3**2   +
0.015588918*beta3
        dp2   =   1.27353E-07*beta3**4   -   1.20919E-05*beta3**3   +   0.000648995*beta3**2   +
0.006404357*beta3
        sol1 = 2.0
        sol2 = 1.8
    elif (1.8>solidity>=1.4):
        dp1   =   1.27353E-07*beta3**4   -   1.20919E-05*beta3**3   +   0.000648995*beta3**2   +
0.006404357*beta3
        dp2   =   1.45927E-07*beta3**4   -   8.44923E-06*beta3**3   +   0.000424739*beta3**2   +
0.012520409*beta3
        sol1 = 1.8
        sol2 = 1.4
    elif (1.4>solidity>=1.2):
        dp1   =   1.45927E-07*beta3**4   -   8.44923E-06*beta3**3   +   0.000424739*beta3**2   +
0.012520409*beta3
        dp2   =   4.40777E-08*beta3**4   +   2.07627E-06*beta3**3   +   4.93577E-05*beta3**2   +
0.014834111*beta3
        sol1 = 1.4
        sol2 = 1.2
    elif (1.2>solidity>=1.0):
        dp1   =   4.40777E-08*beta3**4   +   2.07627E-06*beta3**3   +   4.93577E-05*beta3**2   +
0.014834111*beta3
        dp2   =   1.27353E-07*beta3**4   -   1.20919E-05*beta3**3   +   0.000648995*beta3**2   +
0.006404357*beta3
        sol1 = 1.2
        sol2 = 1.0
    elif (1.0>solidity>=0.8):
        dp1   =   1.27353E-07*beta3**4   -   1.20919E-05*beta3**3   +   0.000648995*beta3**2   +
0.006404357*beta3
        dp2   =   1.12176E-07*beta3**4   -   1.11076E-05*beta3**3   +   0.000540571*beta3**2   +
0.007396954*beta3
        sol1 = 1.0
        sol2 = 0.8
    else:
        dp1   =   1.12176E-07*beta3**4   -   1.11076E-05*beta3**3   +   0.000540571*beta3**2   +
0.007396954*beta3
```

```
    dp2   =   4.68004E-08*beta3**4   -   3.29977E-06*beta3**3   +   0.000189986*beta3**2   +
0.008869015*beta3
    sol1 = 0.8
    sol2 = 0.6

delta0 = (solidity - sol2) / (sol1 - sol2) * (dp1 - dp2) + dp2
b = -1.48909E-06*beta3**3 + 6.21700E-05*beta3**2 - 0.003117669*beta3 + 0.968167495
m =  1.73635E-07*beta3**3 + 1.74127E-05*beta3**2 - 1.68042E-05*beta3 + 0.170874299
delta5p = delta0 + bl_turn * (m / (solidity ** b))
return delta5p
```

```python
def ETAaCascadeModel(resultsTable, index):
    #get parameter inputs
    AlphaBin = resultsTable["Diffuser[2]ALPHABin"][index]
    AlphaBex = resultsTable["Diffuser[2]ALPHABex"][index]
    RossCA = resultsTable["Rossby Number (C,A)"][index]
    Mach3 = resultsTable["Diffuser[2]Mach_IN"][index]
    CP24I = resultsTable["Diffuser[2]Diffuser CpAideal"][index]
    CP45I = resultsTable["Diffuser[2]Diffuser CpBideal"][index]
    VnlsCP = resultsTable["Diffuser[1]CP"][index]
    SIG2 = resultsTable["Solidity"][index]
    ZR = resultsTable["ZR"][index]
    R5 = resultsTable["R5"][index]
    R2 = resultsTable["R2"][index]
    ARb = resultsTable["ARb"][index]
    Clr_B2 = resultsTable["Clr/B2"][index]
    E = resultsTable["E"][index]
    ZD = resultsTable["Diffuser[2]Number Blades"][index]
    unitName = resultsTable.GetUnits("R2")
    R5 = units.ConvertToSI(R5, unitName)
    R2 = units.ConvertToSI(R2, unitName)
    AlphaBin=cos(radians(AlphaBin))
    AlphaBex=cos(radians(AlphaBex))
    R5_R2=R5/R2
    ZD_ZR=ZD/ZR
    #normalixe the variables
    AlphaBin=(AlphaBin-0.210194812)/0.090445705
    AlphaBex=(AlphaBex-0.564203765)/0.110816251
    RossCA=(RossCA-4.17195316)/1.062581394
    Mach3=(Mach3-0.672667269)/0.151830822
    CP24I=(CP24I+0.609317655)/0.824600944
    CP45I=(CP45I-0.654617508)/0.220526493
    SIG2=(SIG2-0.892557629)/0.024626053
    ZD_ZR=(ZD_ZR-0.703165584)/0.210542314
    ZD=(ZD-12.2421875)/1.897972784
    R5_R2=(R5_R2-2.173496845)/0.309753051
    ARb=(ARb-2.20357083)/0.627938567
    Clr_B2=(Clr_B2-0.051953709)/0.009667044
    E=(E-0.499873291)/0.152188538
    VnlsCP=(VnlsCP-0.143216516)/0.112820278
    #Perform calculation
    ETAa5 = K1 -K2*Mach3 -K3*Mach3*R5_R2 -K4*ARb*SIG2+K5*AlphaBex*R5_R2 -K6*SIG2
+K7*ZD-K8*VnlsCP*Clr_B2+K9*AlphaBin*R5_R2+K10*CP45I**2+K11*RossCA*E
+K12*CP24I*ZD_ZR
    return ETAa5
```

```python
def ETAbCascadeModel(resultsTable, index):
    #get parameter inputs
    AlphaBin = resultsTable["Diffuser[2]ALPHABin"][index]
    AlphaBex = resultsTable["Diffuser[2]ALPHABex"][index]
    SIG2 = resultsTable["SIG2"][index]
    R5 = resultsTable["R5"][index]
    R3 = resultsTable["Diffuser[2]Rin"][index]
    R4 = resultsTable["Diffuser[2]Rex"][index]
    R2 = resultsTable["R2"][index]
    ARb = resultsTable["ARb"][index]
    B3 = resultsTable["Diffuser[1]Bex"][index]
    B2 = resultsTable["B2"][index]
    Wex = resultsTable["Diffuser[2]Wex"][index]
    Mach3 = resultsTable["Diffuser[2]Mach_IN"][index]
    VnlsRe = resultsTable["Diffuser[1]Reynolds"][index]
    DR5i = resultsTable["Diffuser[2]Diffuser DR5i"][index]
    CP45I = resultsTable["Diffuser[2]Diffuser CpBideal"][index]
    AR45 = resultsTable["Diffuser[2]AR45"][index]
    E = resultsTable["E"][index]
    DeltaP = resultsTable["DELTAP"][index]
    DR2I = resultsTable["DR2I"][index]
    NS = resultsTable["Specific Speed(NS)"][index]
    unitName = resultsTable.GetUnits("R2")
    R5 = units.ConvertToSI(R5, unitName)
    R4 = units.ConvertToSI(R4, unitName)
    R3 = units.ConvertToSI(R3, unitName)
    R2 = units.ConvertToSI(R2, unitName)
    B3 = units.ConvertToSI(B3, unitName)
    B2 = units.ConvertToSI(B2, unitName)
    Wex = units.ConvertToSI(Wex, unitName)
    DeltaP=cos(radians(DeltaP))
    AlphaBin=cos(radians(AlphaBin))
    AlphaBex=cos(radians(AlphaBex))
    R5_R2=R5/R2
    R5_R3=R5/R3
    B3_B2=B3/B2
    Wex_Rex=Wex/R4
    VnlsRe=log(VnlsRe)
    #normalixe the variables
    DR2I=(DR2I-2.030462716)/0.74994732
    AlphaBin=(AlphaBin-0.210194812)/0.090445705
    AlphaBex=(AlphaBex-0.564203765)/0.110816251
    Mach3 = (Mach3 -0.672667269)/0.151830822
    Wex_Rex = (Wex_Rex -0.292145856)/0.056113298
    DeltaP = (DeltaP -0.997189921)/0.001378716
    SIG2 = (SIG2 -0.892557629)/0.024626053
    AR45 = (AR45 -44.79332891)/20.69762863
    B3_B2 = (B3_B2 -0.885084148)/0.026271895
    R5_R2 = (R5_R2 -2.173496845)/0.309753051
    R5_R3 = (R5_R3 -1.419851864)/0.391256532
    ARb = (ARb -2.20357083)/0.627938567
    E = (E -0.499873291)/0.152188538
    VnlsRe =( VnlsRe -12.1904453)/0.294892606
    DR5i = (DR5i -2.119296922)/2.401065052
    NS=(NS-1.801774925)/2.125803656
    #Perform calculation
```

```
#original model
ETAb5  =  K1+K2*R5_R2  +K3*SIG2*R5_R2  +K4*CP45I*NS  -K5*B3_B2**2+K6*DR5i*SIG2  -
K7*NS*AlphaBin -K8*AR45*E +K9*B3_B2*Wex_Rex+K10*VnlsRe*Wex_Rex +K11*Mach3*DeltaP -
K12*AlphaBex*R5_R3 +K13*Mach3 -K14*DeltaP*AR45
    return ETAb5
```